

UC Riverside

UC Riverside Electronic Theses and Dissertations

Title

Synthesis of Small Molecule Candidate Insulin Mimics by the Claisen Rearrangement

Permalink

<https://escholarship.org/uc/item/4tf6m10c>

Author

Nalbandian, Jenifer N.

Publication Date

2013

Peer reviewed|Thesis/dissertation

UNIVERSITY OF CALIFORNIA
RIVERSIDE

Synthesis of Small Molecule Candidate Insulin Mimics
by the Claisen Rearrangement

A Dissertation submitted in partial satisfaction
of the requirements for the degree of

Doctor of Philosophy

in

Chemistry

by

Jenifer Natée Nalbandian

August 2013

Dissertation Committee:

Dr. Michael C. Pirrung, Chairperson

Dr. Michael J. Marsella

Dr. Richard J. Hooley

Copyright by
Jenifer Natée Nalbandian
2013

The Dissertation of Jenifer Natée Nalbandian is approved:

Committee Chairperson

University of California, Riverside

Acknowledgements

First, I would like to thank God for calling me to be a chemist and for choosing to love and use foolish things like me to shame the wise. All I do is by Your grace and for Your glory. Through all the storms and trials of grad school, You have been my Comforter and Deliverer. Even when I was faithless, You remained faithful, patiently revealing Your character to me. I thank Christ Jesus my Lord, who has given me strength, that He considered me trustworthy and faithful, appointing me to His service. Through You, I have a hope and a future.

I would like to also thank my husband for being there for me through all of the victories, failures, and freak-outs of my graduate career. You have been my best friend, boyfriend, fiancé, husband, chef, leader, personal assistant, chauffeur, garbage collector, counselor, graphic designer, protector, nurse, walking buddy, pastor, handyman, mover, massage therapist, computer programmer, deliveryman, partner, co-host, supporter, and more. I truly would not have made it through grad school without you by my side. I love you so much and I cannot wait to see what God has planned for us after grad school.

Thank you to my family for always believing that God had great things in store for me. Mom and Dad, you were there for every science fair, test, project, presentation, and paper that led to this point. Every time I wanted to quit, you both were there, encouraging me, loving me, and reminding me who I am in Christ. I would not be where I am today without your love, prayers, and money (hahaha). To my younger siblings, Nathan, Madelynne, Ethan, and Elijah: you four are my favorite people in the whole world and I would do anything for you. Thank you for all the Thanksgivings and

Christmases where I was able to forget about the stress of school and just have a great time, hanging out with my hilarious siblings. Thank you to my Nalbandian family for loving and accepting me. I am thankful God allowed me to marry into such a great family.

Thank you to my best friends, Mattie and Melissa, for putting up with having a best friend that did not have time to call or visit often. Thank you to my Vegas friends, Erin, Erin, Tanya, and Hayley for always making me laugh whenever we get together. Thank you to my Pepperdine friends, especially Jan Bello and Malia, for those great dinners we had where we laughed, complained, and reminisced. Thank you to Tiffany and Theresa for the fun times we had while working together in the lab. Thank you to Nisana and Renee for the breakfasts, lunches, and dinners. Hanging out with you ladies was always the highlight of my day. Thank you to Angie for allowing me to force you to move in with me and for always being so hilarious. Thank you to Dr. Debbie Smith for being my friend. Having a Spirit-filled woman of God with a PhD as my friend has been a real blessing. Thank you to my family at The Rock for loving me and Michael and helping us grow into the people we are today.

Finally, thank you to Prof. Pirrung for your support and guidance. Thank you to the past and present members of the Pirrung group for your help with everything, especially with getting my reactions to work, figuring out the problem sets, changing the gas cylinders, refilling the acetone dispenser, doing the inventories. You all made the time I spent in lab so much more interesting. Also, fellowship support from NIH (GM086130) is greatly appreciated.

Copyright Acknowledgement

The text and figures in Chapter 4, in part or in full, are a reprint of the material as it appears in *Tetrahedron Lett.* **2013**, *54*, 3752-3754, with permission from Elsevier. The co-author, Prof. Michael C. Pirrung, listed in that publication directed and supervised the research, which forms the basis for this chapter.

Dedication

This dissertation is dedicated to Jesus Christ, “For in Him all things were created: things in Heaven and on earth, visible and invisible...all things have been created through Him and for Him.” Colossians 1:16

This dissertation is also dedicated to my husband, Michael, for his support, patience, and love.

ABSTRACT OF THE DISSERTATION

Synthesis of Small Molecule Candidate Insulin Mimics
By the Claisen Rearrangement

by

Jenifer Natée Nalbandian

Doctor of Philosophy, Graduate Program in Chemistry
University of California, Riverside, August 2013
Dr. Michael C. Pirrung, Chairperson

The aim of this dissertation is the discovery of novel small molecule insulin mimics. Natural product demethylasterriquinone B1 (DAQ B1) is an orally active insulin mimic, but this small molecule contains a quinone moiety that hindered further development of this drug class. The Pirrung lab has successfully replaced the offensive quinone with a pyrone ring derived from the natural product kojic acid, while maintaining the promising biological activity of DAQ B1.

The first part of the dissertation describes work toward the synthesis of a diverse library of potential activators of the insulin receptor, indolylkojates. Past work in the Pirrung lab developed a synthetic route to candidate kojate-based insulin mimics that relies on the Claisen rearrangement as a key step. This route employs iodoanilines as a starting point in a Sonogashira reaction with an *O*-propargylated kojate to make the target indolylkojates, but the use of iodoanilines is limited by the low commercial availability of iodoarenes. In the present study, various functionalized arenes were examined as replacements for iodoaniline, but all failed to be productive coupling partners with our

functionalized kojate. Finally, success was achieved through the use of a benzyloxy-substituted iodoaniline.

The second part discloses results from the examination of our indolykijate target compounds for signs of axial chirality. We hypothesized that a large group in the 4-position of the indole would provide sufficient steric bulk that rotation about the indole-kijate bond would be restricted. The synthesis of a (4-bromo)indolykijate disproved this theory, as chiral chromatography failed to indicate the presence of discreet atropisomers.

The third part details work done to develop a catalyst that would allow the Claisen rearrangement step to be conducted at lower temperatures than those typically required under thermal conditions (160-190 °C). Literature surrounding the catalyzed Claisen rearrangement of *O*-allyl kojates is scarce, but, using catalysts known to efficiently mediate the rearrangement of (allyloxy)acrylates and allyl aryl ethers, a catalyst screen was developed. Lewis acid Zn(OTf)₂ was determined to be the best catalyst for the rearrangement of *O*-allyl kojates at low temperatures, with the best yield arising from the use of *trans*-cinnamyl kojate as the substrate.

Table of Contents

Acknowledgments.....	iv
Dedication.....	vii
Abstract.....	viii
Table of Contents.....	x
List of Figures.....	xiii
List of Schemes.....	xv
List of Tables.....	xx
List of Abbreviations.....	xxi
Chapter 1: Introduction.....	1
1.1 Diabetes Overview.....	1
1.2 Insulin.....	2
1.3 Diabetes: Causes and Symptoms.....	8
1.4 Diabetes Treatments.....	10
1.5 The First Orally-Active Insulin Mimic: DAQ B1.....	14
1.6 Total Syntheses and SAR Studies of DAQ B1 by Other Groups.....	19
1.7 Total Syntheses and SAR Studies of DAQ B1 by the Pirrung Group.....	23
1.8 Derivatives of DAQ B1: Synthesis and Biological Activity.....	30
1.9 Quinone Replacements.....	35
1.10 Kojate-Based Compounds Synthesized by Stille Coupling.....	37
1.11 Kojate Library Synthesis by the Claisen Rearrangement.....	39
1.12 Other Known Small Molecule Insulin Mimics.....	44

1.13 Conclusion	47
Chapter 2: Synthesis of a Library of Candidate Insulin Mimics	49
2.1 Introduction.....	49
2.2 Pyridone Synthesis.....	49
2.3 Coupling of <i>o</i> -Halonitrobenzene and Alkyne	58
2.4 Coupling of 2-Aminoaryl Triflate and Alkyne	64
2.5 Synthesis of <i>tert</i> -Butyl 2-(Benzyloxy)-6-iodophenylcarbamate.....	70
2.6 Synthesis of Claisen Rearrangement Precursors.....	75
2.7 Claisen Rearrangement of 7-Benzyloxyindole Kojic Acid Derivatives	78
2.8 Conclusion	79
Chapter 3: Examination of Biaryl Bond Of Prospective Kojate-Based Insulin Mimics by Chiral HPLC	81
3.1 Atropisomerism.....	81
3.2 Synthesis of a 4-Bromoindolylkojate Derivative.....	84
3.3 Analysis by Chiral HPLC	96
3.4 Synthesis of a 4-Bromoindolyl Pyridone Derivative	98
3.5 Conclusion	99
Chapter 4: Catalytic Claisen Rearrangements of <i>O</i> -Allyl Kojates	100
4.1 Introduction.....	100
4.2 Literature Examples of Catalytic Claisen Rearrangements of (Allyloxy)acrylates and Allyl Aryl Ethers	105
4.3 Attempted Catalytic Claisen Rearrangement of an Indolylkojate	111
4.4 Preliminary Results from the Catalytic Claisen Rearrangements of <i>O</i> -Prenyl Kojates	113

4.5 Catalyst Screen.....	117
4.6 Synthesis of Other <i>O</i> -Allyl Kojates	123
4.7 Reaction Scope.....	127
4.8 Conclusion	132
Chapter 5: Experimental Details	134
References.....	165

List of Figures

Figure 1.1 Peptide sequence of insulin	2
Figure 1.2 The release of insulin from a β -cell.....	4
Figure 1.3 Insulin receptor with bound substrate.....	5
Figure 1.4 Domains of the insulin receptor	6
Figure 1.5 Insulin chains A and B (denoted InsA and InsB) bound to IR. The apo α CT helix is shown in yellow while the α CT helix in the presence of bound insulin is shown in purple	7
Figure 1.6 Orally active Type 2 diabetes treatments	11
Figure 1.7 Natural products from Merck's small molecule IR activator screen.....	14
Figure 1.8 Insulin receptor tyrosine kinase (IRTK) activity at various concentrations of DAQ B1 (solid circles) and hinulliquone (open circles).....	15
Figure 1.9 Tyrosine kinase (TK) activation in CHO.IR, CHO.IGFIR, CHO.EGFR, and CHO.PDGFR cells at various concentrations of DAQ B1	16
Figure 1.10 IRTK activity of cells with various concentrations of insulin in the presence and absence of DAQ B1	17
Figure 1.11 DAQ B1 analogs for SAR study by Merck.....	22
Figure 1.12 Aryl substitutions made to the quinone ring of DAQ B1 leading to the identification of "compound 2	23
Figure 1.13 Methylated indoles and asterriquinones for the methyl scan study.....	28
Figure 1.14 Regions of interaction between DAQ B1 and IR, as determined by methyl scanning experiment	29
Figure 1.15 DAQ B1 derivatives for the study of IR dimerization induced by DAQ B1	30
Figure 1.16 Potent IR-activators from library screen	32
Figure 1.17 Different types of quinines	34
Figure 1.18 7-substituted mono-indolybenzoquinones active as insulin mimics	34

Figure 1.19 Quinone-containing drugs on the market	35
Figure 1.20 Early candidates for quinone replacements	36
Figure 1.21 Kojic acid.....	37
Figure 1.22 Synthetic small molecule insulin mimics	45
Figure 1.23 Naturally-occurring insulin mimics.....	47
Figure 2.1 <i>tert</i> -Butyl 2-(Benzyloxy)-6-iodophenylcarbamate 101	71
Figure 3.1 Example of atropisomerism in a biologically active biaryl compound	82
Figure 3.2 Potentially atropisomeric indolylokojate derivative	83
Figure 3.3 Atropisomeric monoindolyldichlorobenzoquinones	84
Figure 3.4 HPLC chromatogram of 63	85
Figure 3.5 Model kojate system for chirality study	85
Figure 3.6 Example of TLC analysis of 127 and 128 , eluting with 25% hexanes in EtOAc and stained with vanillin. From left to right, 128 , mixed spot, 127	96
Figure 3.7 HPLC chromatogram of 127	97
Figure 4.1 <i>O</i> -allyl kojates vs. (allyloxy)acrylates, both depicted as complexed to a metal catalyst	105
Figure 4.2 Guanidinium catalysts	107
Figure 4.3 Proposed model of guanidinium catalyst binding	108
Figure 4.4 BOX ligand synthesized by Dr. Zou	114
Figure 4.5 Kinetic rate plot for the Zn(OTf) ₂ -catalyzed Claisen rearrangement of 144 ..	122
Figure 4.6 Kinetic rate plot for the uncatalyzed Claisen rearrangement of 144	123

List of Schemes

Scheme 1.1 First total synthesis of DAQ B1	20
Scheme 1.2 Total synthesis of DAQ B1 by Tatsuta's group	20
Scheme 1.3 First total synthesis of DAQ B1 completed by the Pirrung group	24
Scheme 1.4 Second total synthesis of DAQ B1 reported by the Pirrung group	25
Scheme 1.5 Concise synthesis of DAQ B1 by the Pirrung group	26
Scheme 1.6 Preparation of kojate derivatives by Stille coupling	38
Scheme 1.7 Generic Claisen rearrangement of (indole)methyl kojates	40
Scheme 1.8 Test reaction for the Claisen protocol	41
Scheme 1.9 Sonogashira-cyclization-Claisen sequence	42
Scheme 1.10 Claisen Rearrangement protocol using a Boc-protected indole	43
Scheme 1.11 Synthesis of an indolylkojate library	44
Scheme 2.1 Early report of an exchange reaction using kojic acid	50
Scheme 2.2 Proposed reaction mechanism for the pyrone to pyridone exchange reaction	51
Scheme 2.3 Proposed mechanism for the exchange reaction of pyrone 55	51
Scheme 2.4 Exchange reaction for the synthesis of <i>N</i> -butyl- and <i>N</i> -allylpyridones	52
Scheme 2.5 Failed exchange reactions	53
Scheme 2.6 <i>N</i> -isopropylpyridone synthesis in EtOH.	53
Scheme 2.7 Teitei's reported pyrone to pyridone exchange reaction and condensation cascade	55
Scheme 2.8 Exchange reaction/condensation attempt with 55	55
Scheme 2.9 Failed exchange reactions with hydroxyl- and methoxylamine	56

Scheme 2.10 Tsuruoka's reported <i>N</i> -hydroxypyridone synthesis	56
Scheme 2.11 Failed application of the Tsuruoka synthesis	56
Scheme 2.12 Manipulations of <i>N</i> -hydroxypyridone 85	57
Scheme 2.13 Select examples of Yoakim's S _N Ar protocol	59
Scheme 2.14 Failed S _N Ar between 55 and <i>o</i> -fluoronitrobenzene	60
Scheme 2.15 Optimization of model system for S _N Ar reaction	61
Scheme 2.16 S _N Ar reaction catalyzed by phosphazene base	62
Scheme 2.17 Failed phosphazene base-catalyzed cross coupling	62
Scheme 2.18 Attempted Sonogashira cross-coupling reactions of <i>o</i> -bromonitrobenzene and 55	63
Scheme 2.19 Literature transformations of 2-aminophenol	65
Scheme 2.20 Synthesis of aryl triflate 96	65
Scheme 2.21 Rate acceleration of the alkynylation of catechol ditriflate by the addition of <i>n</i> Bu ₄ NI	66
Scheme 2.22 Sonogashira coupling of 2-amidoaryl triflate 97 and phenylacetylene	67
Scheme 2.23 Dai's proposed palladium cycle	68
Scheme 2.24 Sonogashira coupling of 55 and 96 in the presence of <i>n</i> Bu ₄ NI	69
Scheme 2.25 Unexpected <i>O</i> -Boc product formation	71
Scheme 2.26 Room temperature rearrangement of 102	72
Scheme 2.27 Proposed mechanism for <i>O</i> → <i>N</i> Boc transfer	73
Scheme 2.28 Microwave-assisted rearrangement of 102	73
Scheme 2.29 Literature example of the selective, solvent-free <i>N</i> -Boc protection of ethanolamine	74
Scheme 2.30 Syntheses of 104 using conventional heating	75

Scheme 2.31 Synthesis of Sonogashira substrate 101	75
Scheme 2.32 Production of 106 by Sonogashira coupling	76
Scheme 2.33 Two-step protocol to yield (indole)methyl kojate 107	77
Scheme 2.34 Songashira-indole cyclization procedure for the synthesis of pyridone-based derivatives	78
Scheme 2.35 One-pot Claisen rearrangement and deprotection to obtain indolylkojate 111	79
Scheme 3.1 Aldol/dehydration reaction	86
Scheme 3.2 Indole-cyclization of 117	87
Scheme 3.3 Failed mesyl protection reactions	88
Scheme 3.4 Successful protection of indole with <i>p</i> TsCl	89
Scheme 3.5 Examples of the utility of Hui's novel tosyl protection protocol	90
Scheme 3.6 Optimization of the indole protection step	91
Scheme 3.7 DIBAL-mediated ester reduction	91
Scheme 3.8 Optimized ester reduction in the presence of LAH	92
Scheme 3.9 Methyl ester reduction, mediated by LiBH ₄	93
Scheme 3.10 Synthesis of kojate derivative 125	93
Scheme 3.11 Incomplete Claisen rearrangement and deprotection	94
Scheme 3.12 Methods for the synthesis of 128	95
Scheme 3.13 Claisen rearrangement of 128	96
Scheme 3.14 Pyrone-to-pyridone exchange reactions	98
Scheme 4.1 Crucial Claisen rearrangement in the synthesis of prospective kojate-based insulin mimics	101
Scheme 4.2 Wender's thermal Claisen rearrangement	101

Scheme 4.3 Claisen rearrangement of an <i>O</i> -allyl kojate, catalyzed by Zn(OTf) ₂ -PyBOX	102
Scheme 4.4 Bode's enantioselective NHC-catalyzed Claisen rearrangement	103
Scheme 4.5 Yb(OTf) ₃ -catalyzed Claisen rearrangements of allyl and crotyl aryl ethers	106
Scheme 4.6 Cu(OTf) ₂ - and Yb(OTf) ₃ -catalyzed Claisen rearrangements of (allyloxy)acrylates	106
Scheme 4.7 Rate enhancement in the presence of Ph ₂ GuanBARF	107
Scheme 4.8 Enantioselective Claisen rearrangements catalyzed by 139	108
Scheme 4.9 Gold (I) catalyst for the rearrangement of allyl aryl ethers	110
Scheme 4.10 BF ₃ •OEt ₂ -catalyzed Claisen rearrangement for the synthesis of demethylsuberosin	110
Scheme 4.11 Europium(III)-catalyzed Claisen rearrangement	110
Scheme 4.12 Attempted Ph ₂ GuanBARF-catalyzed Claisen rearrangement	113
Scheme 4.13 Unsuccessful Claisen rearrangements in the presence of (PPh ₃)AuOTf... ..	113
Scheme 4.14 Facile synthesis of 142	114
Scheme 4.15 Methods for the synthesis of <i>O</i> -prenyl kojate 144	116
Scheme 4.16 Possible explanation for consistent moderate yields in the Zn(OTf) ₂ -catalyzed rearrangement of <i>O</i> -prenyl kojate 144	121
Scheme 4.17 Evidence of a competing elimination reaction pathway	121
Scheme 4.18 Facile synthesis of 151 and 152	124
Scheme 4.19 Unsuccessful synthesis of 153	124
Scheme 4.20 Alternative route for the synthesis of 153	124
Scheme 4.21 Synthesis of <i>trans</i> -substituted allylic kojates	125
Scheme 4.22 Literature synthesis of <i>cis</i> -crotyl bromide	125

Scheme 4.23 Attempted coupling of kojic acid and <i>cis</i> -crotyl bromide.....	126
Scheme 4.24 Fruitless attempts to methylate 55	126
Scheme 4.25 Efficient protocol for the formation of 158	127
Scheme 4.26 Initial THP removal in the synthesis of 157	127
Scheme 4.27 Indolylkojate used to examine the scope of the Zn(OTf) ₂ -catalyzed reaction	131
Scheme 4.28 Establishment of the superiority of Zn(OTf) ₂ as catalyst	132

List of Tables

Table 1.1	Indoles used in the combinatorial synthesis of an asterriquinone library	31
Table 1.2	Indolylquinones in the combinatorial synthesis of an asterriquinone library	32
Table 2.1	Unsuccessful Sonogashira coupling of 55 and 96	70
Table 3.1	Optimization of the Aldol reaction	87
Table 4.1	Pd(II)-catalyzed Claisen rearrangements of (allyloxy)acrylates	109
Table 4.2	Metal triflates as catalysts for the Claisen rearrangement of 53	112
Table 4.3	Microwave-assisted catalytic Claisen rearrangements	115
Table 4.4	Catalyst Screen	118
Table 4.5	Catalyzed Claisen rearrangement of various <i>O</i> -allyl kojates, conducted with Zn(OTf) ₂ (10 mol%)	128

List of Abbreviations

aq	Aqueous
Boc	<i>tert</i> -Butoxycarbonyl
Bn	Benzyl
BOX	Bis(oxazoline)
Bu	Butyl
Bz	Benzoyl
CHO	Chinese hamster ovary
DAQ	Demethylasterriquinone
DCE	1,2-Dichloroethane
DDQ	2,3-Dichloro-5,6-dicyano-1,4-benzoquinone
DIBAL	Diisobutylaluminum hydride
DIPEA	Diisopropylethylamine
DMAP	4-Dimethylaminopyridine
DMF	<i>N, N</i> -Dimethylformamide
EC ₅₀	Half-maximal effective concentration
EGFR	Epidermal growth factor receptor
EtOAc	Ethyl acetate
EtOH	Ethanol
equiv	Equivalent(s)
FGFR	Fibroblast growth factor receptor
GAPDH	Glyceraldehyde 3-phosphate dehydrogenase

GC	Gas chromatography
GLUT	Glucose transporter
GSK	Glycogen synthase kinase
HPLC	High-performance liquid chromatography
HMDS	Hexamethyldisilazide
IGFIR	Insulin-like growth factor receptor
<i>i</i> Pr	Isopropyl
IR	Insulin receptor
IR	Infrared
IRR	IR-related receptor
IRS	Insulin receptor substrate
LAH	Lithium aluminum hydride
LDA	Lithium diisopropylamide
LCMS	Liquid chromatography/mass spectrometry
MeOH	Methanol
MHC	Major histocompatibility complex
Ms	Methanesulfonyl
NHC	<i>N</i> -heterocyclic carbene
NMR	Nuclear Magnetic Resonance
PDGFR	Platelet-derived growth factor receptor
PKB/Akt	Protein kinase B
PI3K	Phosphatidylinositol 3-kinase

PIP ₂	Phosphatidylinositol 4,5-bisphosphate
PIP ₃	Phosphatidylinositol 3,4,5-trisphosphate
PMB	<i>p</i> -Methoxybenzyl
ROS	Reactive oxygen species
SAR	Structure-activity relationship
TBAF	Tetrabutylammonium fluoride
TBS	<i>tert</i> -Butyldimethylsilyl
TEBA	Triethylbenzylammonium chloride
Tf	Trifluoromethanesulfonyl
THF	Tetrahydrofuran
THP	Tetrahydropyran
TK	Tyrosine kinase
TLC	Thin-layer chromatography
TMS	Trimethylsilyl
Ts	<i>p</i> -Toluenesulfonyl

Chapter 1. Introduction

1.1 Diabetes Overview

Diabetes mellitus, or simply diabetes, is the broad term used to classify various diseases that cause elevated levels of glucose in the blood, due to the body's inability to produce and/or properly utilize insulin, the peptide hormone. The two main classes of diabetes are Type 1 and Type 2 diabetes. Type 1 diabetes is identified by the body's total inability to produce insulin. Typically, patients diagnosed with Type 1 diabetes are children or young adults, prompting this class of the disease to formerly be called "juvenile diabetes." The more common Type 2 diabetes is caused by an insufficient production of insulin or a resistance to the effects of endogenous insulin. Type 2 accounts for 95% of the national cases of diabetes, usually affecting obese adults. While Type 1 symptoms typically begin suddenly, Type 2 has a more gradual onset. According to the 2011 National Diabetes Fact Sheet, it is estimated that there are over 25 million individuals in the United States that suffer from diabetes. This large number, which accounts for approximately 8% of the population, includes almost 19 million Americans that have been diagnosed and 7 million that remain undiagnosed. The disease is becoming increasingly widespread in this nation, as evidenced by the 1.9 million newly diagnosed cases of diabetes in 2010 alone. In 2012, diabetes patients cost the U.S. \$176 billion in direct medical costs, as well as \$69 billion in reduced productivity, which equals an astounding \$245 billion in total costs due to this pervasive ailment.

1.2 Insulin

Insulin consists of two peptide chains, chain A and chain B, which are comprised of 21 and 30 amino acids, respectively (Figure 1.1). In 1955, Fred Sanger deduced the peptide sequence of insulin, simultaneously proving that peptides exist as single compounds with a defined amino acid sequence.¹ This discovery earned Sanger the Nobel Prize in Chemistry in 1958. Insulin exists as three α -helices, due to the constraints of disulfide bonds. Chain A has an internal disulfide bond (A6-A11) and chains A and B are linked to one another by two disulfide bonds (A7-B7 and A20-B19). Shin and coworkers studied the role of each disulfide bond of insulin, with respect to the structure, activity, and stability of insulin.² This study was accomplished through the synthesis of three mutants that each lacked one disulfide bond. They found that all three disulfide bonds are integral for the binding of insulin to its receptor and that bond A20-B19 was responsible for proper protein folding.

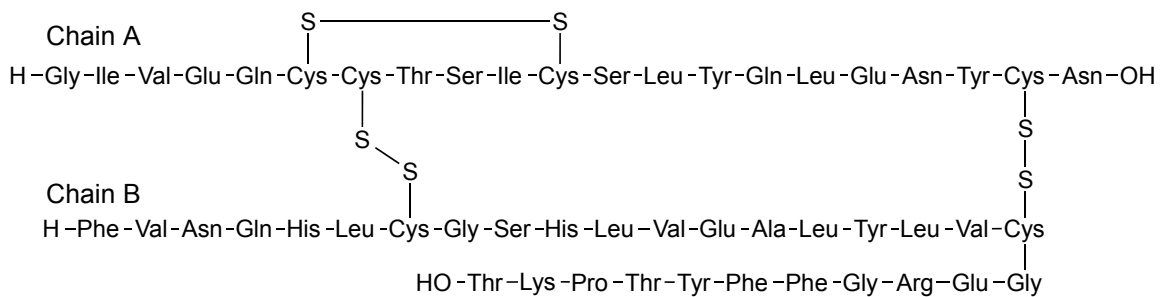


Figure 1.1 Peptide sequence of insulin.

In the body, β -cells, found in the islets of Langerhans of the pancreas, are responsible for the production, storage, and release of insulin. Insulin release is triggered

by the presence of glucose in the bloodstream following a meal. Glucose is shuttled into β -cells by the Glucose Transporter 2 (GLUT2) transmembrane protein (Figure 1.2). Within the cell, glucose is phosphorylated by glucokinase, a process that initiates glycolysis and respiration, resulting in an increase in the ratio of ATP:ADP. The increased concentration of ATP causes the ATP-sensitive potassium channel to close, effectively sequestering positively-charged potassium ions within the cell. This build-up of positive charge induces a depolarization of the cell membrane that triggers the opening of the calcium channels to transport calcium ions into the cell. The sudden increase in the calcium concentration incites the diffusion of vesicles filled with insulin from the β -cell into the blood, by exocytosis. Once the initial stores of insulin are exhausted, a second, more protracted phase of insulin production and secretion is initiated by the β -cell to keep up with the heightened blood glucose levels. Once the blood glucose concentration declines to normal fasting levels of less than 5.5 mM,³ the release of insulin from β -cells is arrested.

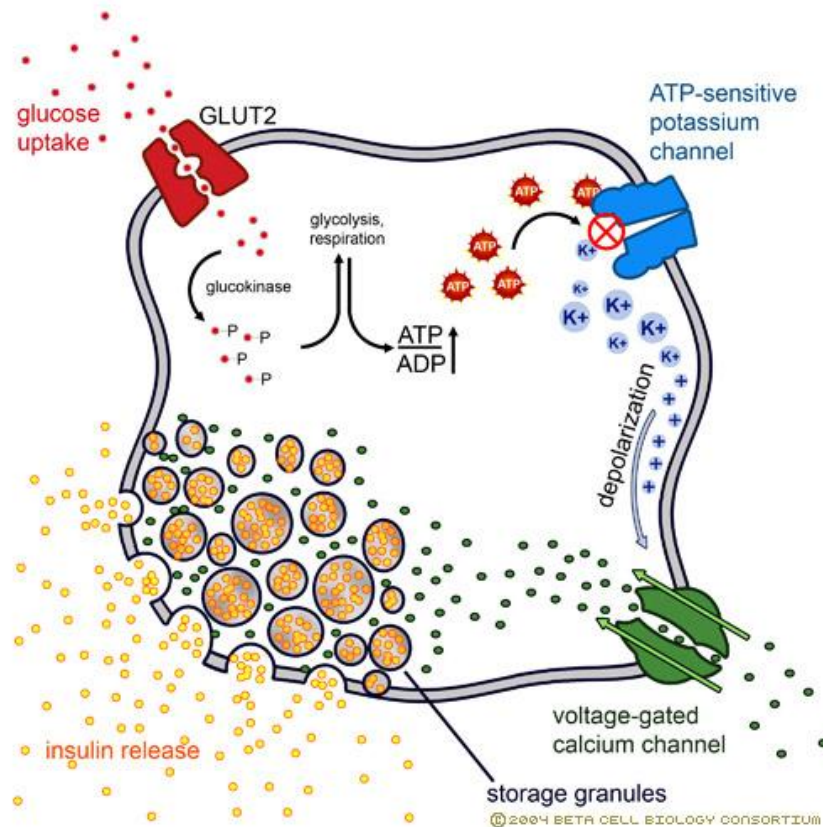


Figure 1.2 The release of insulin from a β -cell.
 © 2004 Beta Cell Biology Consortium.⁴

In the bloodstream, circulating insulin binds to the insulin receptor (IR), a transmembrane tyrosine kinase receptor, typically located on the surface of muscle or fat cells (myocytes and adipocytes, respectively). Structurally, the receptor is a homodimer of two $\alpha\beta$ subunits (Figure 1.3). The two extracellular α subunits, linked to one another by a disulfide bond, each contain a binding site for insulin. The α subunits are each connected to one transmembrane β subunit also through disulfide bonds. The peptide chain that makes up one of the α subunits is 723 amino acid residues long, while one of the β chains is 620 residues long. The β subunits contain tyrosine kinase domains that can

phosphorylate tyrosine residues of other proteins or even of the receptor itself, when ligand is bound.

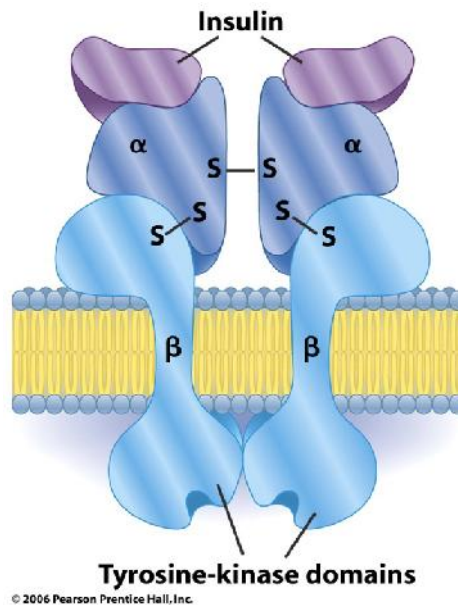


Figure 1.3 Insulin receptor with bound substrate.
© 2006 Pearson Prentice Hall, Inc.⁵

Recently, Menting and colleagues have reported the first 3-dimensional view of insulin bound to its receptor, by obtaining the crystal structures of insulin bound to four simplified versions of the extracellular regions of the insulin receptor.⁶ The ectodomain of the receptor (extracellular region) consists of six domains: the first and second leucine-rich-repeat domains (L1 and L2); the cysteine-rich domain (CR); and the first, second, and third fibronectin type III domains (FnIII-1, FnIII-2, and FnIII-3) (Figure 1.4). The other domains include the insert (ID), transmembrane (TM), juxtamembrane (JM), and tyrosine kinase (TK) regions. The insert domain of the α chain ($ID\alpha$), contained within

the FnIII-2 α , concludes with the C-terminal end of the α chain (α CT segment), which consists of residues 704-719. The β -sheets of L1 and the α CT segment were previously believed to be the primary region of contact for bound insulin,⁷ but Menting's work indicated that the L1 domain and α CT region are in contact with one another, while insulin interacts mainly with the α CT segment.⁶ Menting was also able to prove that a conformational change occurs in IR at the α CT segment in the presence of insulin (Figure 1.5). The α -helix of α CT is bound to L1 in the absence of ligand (apo), but, upon insulin binding, the α CT segment is relocated so that it can interact with both L1 and insulin.^{6,8} Menting's studies determined that His710 and Phe714 of the α CT segment were essential for binding to insulin.⁶ The binding of insulin to IR ultimately leads to a conformational change in the receptor as a whole, though, to date, there is not much known about this transformation process.

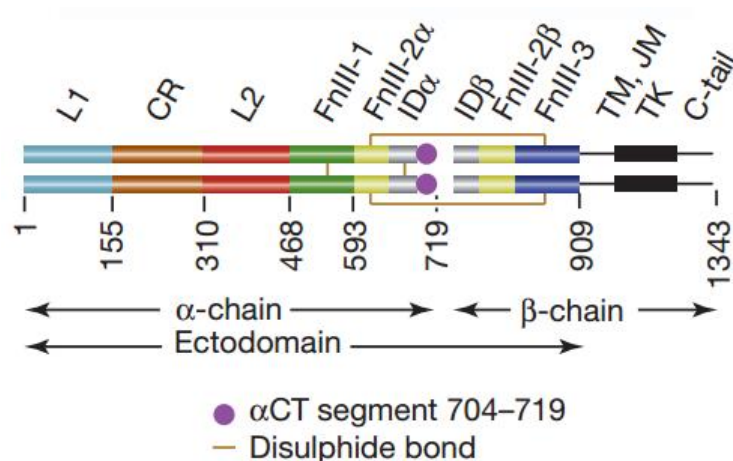


Figure 1.4 Domains of the insulin receptor.
Image copied from Menting, J. G. et al. *Nature* **2013**, 493, 241-245.

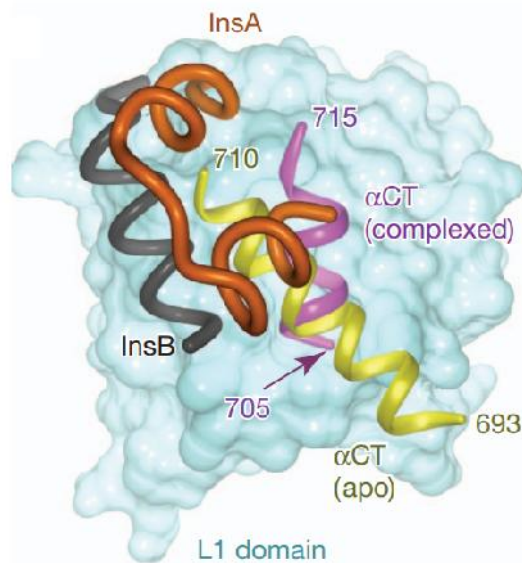


Figure 1.5 Insulin chains A and B (denoted InsA and InsB) bound to IR. The apo α CT helix is shown in yellow while the α CT helix in the presence of bound insulin is shown in purple.

Image copied from Menting, J. G. et al. *Nature* **2013**, 493, 241-245.

It is believed that the conformational change of the receptor is responsible for the autophosphorylation of the tyrosine kinase domains that ensues following ligand binding. Activation of the receptor causes the tyrosine kinase of one $\alpha\beta$ subunit to phosphorylate activation loop residues Tyr1158, Tyr1162, and Tyr1163 of the other $\alpha\beta$ subunit. Autophosphorylation of IR initiates phosphorylation of tyrosine residues of the insulin receptor substrates (IRS 1-4), Shc, and Gab 1 proteins within the cell. The phosphorylated IRS proteins bind to phosphatidylinositol 3-kinase (PI3K), which phosphorylates phosphatidylinositol 4,5-bisphosphate (PIP₂) to yield phosphatidylinositol 3,4,5-trisphosphate (PIP₃). The serine/threonine-specific protein kinase B (PKB, also known as Akt) is activated by PIP₃, which is thereby enabled to induce the movement of intracellular vesicles containing GLUT4. By a process of exocytosis, GLUT4 is

positioned in the cell membrane, where it transports glucose from the blood stream into the cell. In only a few minutes from initial insulin activation, the concentration of GLUT4 in the cell membrane increases 5- to 30-fold, leading to a 10- to 30-fold increase in glucose removal from the bloodstream.⁹

Within myocytes, glucose is taken into the cell and used for energy. Conversely, in adipocytes, glucose is stored in the form of glycogen for future energy needs. Protein kinase B inhibits the activity of glycogen synthase kinase 3 (GSK-3) by phosphorylation. Deactivating GSK-3 inhibits phosphorylation of glycogen synthase, which frees this protein to convert glucose into glycogen. In all, insulin is instrumental in both the removal of glucose from the blood stream and also the storage of glucose in the cell for future use.

1.3 Diabetes: Causes and Symptoms

The proper production and use of insulin by the body are the central issues of diabetes. Type 1 diabetes is a condition where the body's immune system attacks the β -cells of the pancreas. This chronic autoimmune disorder may go unnoticed for years until approximately 80% of the body's β cells are obliterated,¹⁰ causing an insulin deficiency that is evidenced by high blood glucose levels. As a point of reference, the mass of β cells in a normal human pancreas totals roughly 1-2 g.¹¹ It is commonly believed that T lymphocytes are responsible for the mass destruction of β cells, though evidence has recently surfaced implicating B lymphocytes as well.¹⁰ Though the specific cause of Type 1 diabetes remain unclear, it is generally accepted that autoimmune diseases are caused by a combination of genetic and environmental factors.¹² Major histocompatibility

complex (MHC) class II genes have been linked to a predisposition for Type 1 diabetes, as these genes regulate the body's immune responses.¹⁰ Various enteroviruses, including echoviruses and coxsackie viruses, have been identified as likely environmental triggers of Type 1 diabetes.¹³

Type 2 diabetes arises from a developed resistance to the effects of insulin in conjunction with an impaired ability to produce additional insulin to compensate for this insulin resistance. The combination of poor diet and exercise to the point of obesity is generally accepted as the major cause of Type 2 diabetes,¹⁴ though genetics has also been found to play a role.¹⁵ Insulin resistance can arise due to a reduced number of insulin receptors present on the cell membrane, which hinders the cell's ability to transport glucose into the cell. As blood glucose levels remain elevated, β cells must adapt and increase in mass in order to produce and excrete enough insulin to remedy the situation. In non-diabetic obese individuals, their mass of β cells is enlarged to compensate for increased food intake. Conversely, obese Type 2 diabetics have been shown to be characterized by a reduced β cell mass, as the body fails to adjust to the increased need for insulin.¹⁶ Other potential issues attributed to a loss of insulin sensitivity include a depletion in the number of insulin receptors present on the cell surface,¹⁷ defective tyrosine kinase activity in IR, and downstream problems that lead to a decline in the number of GLUT4 transporters that end up situated in the membrane,¹⁸ though the origin of these issues remains a puzzle.

Type 1 and 2 diabetics share some common symptoms, including glucose found in the urine (glycosuria), fatigue or unconsciousness, increased hunger and thirst, and

impaired vision. A symptom specific to Type 2 diabetics is numbness or pain in the extremities, while Type 1 is often marked by sudden weight loss. In the long-term, often with or without treatment, diabetics are prone to complications, such as loss of eyesight and/or hearing, amputations, skin infections, nerve and kidney damage, cardiovascular disease, and even death.

1.4 Diabetes Treatments

Due to the body's degenerative ability to produce insulin, the treatment for Type 1 diabetes patients is daily insulin injections, coupled with proper diet and exercise. When diagnosed with Type 2 diabetes, an individual will be advised to make a drastic lifestyle change that includes exercise, dietary changes, and weight loss. In addition to these behavioral modifications, patients are often prescribed insulin-sensitizing medications. These orally-active drugs, namely the biguanide metformin and thiazolidinediones pioglitazone and rosiglitazone (Figure 1.6), improve the cell's utilization of glucose by reducing the body's developed resistance to insulin.¹⁹ Another drug class often prescribed is that of insulin secretagogues. This class can be divided into sulfonylurea drugs, such as glyburide, glimepiride, and glipizide, and non-sulfonylurea drugs, such as repaglinide and nateglinide. These secretagogues act by causing the ATP-sensitive potassium channel to close, which has the overall effect of stimulating β cell secretion of insulin.²⁰ Alpha-glucosidase inhibitors help patients achieve normal blood sugar levels by inhibiting the enzyme responsible for breaking down disaccharides to yield glucose. Drugs belonging to this class- acarbose, miglitol, and voglibose- curtail spikes in blood glucose levels

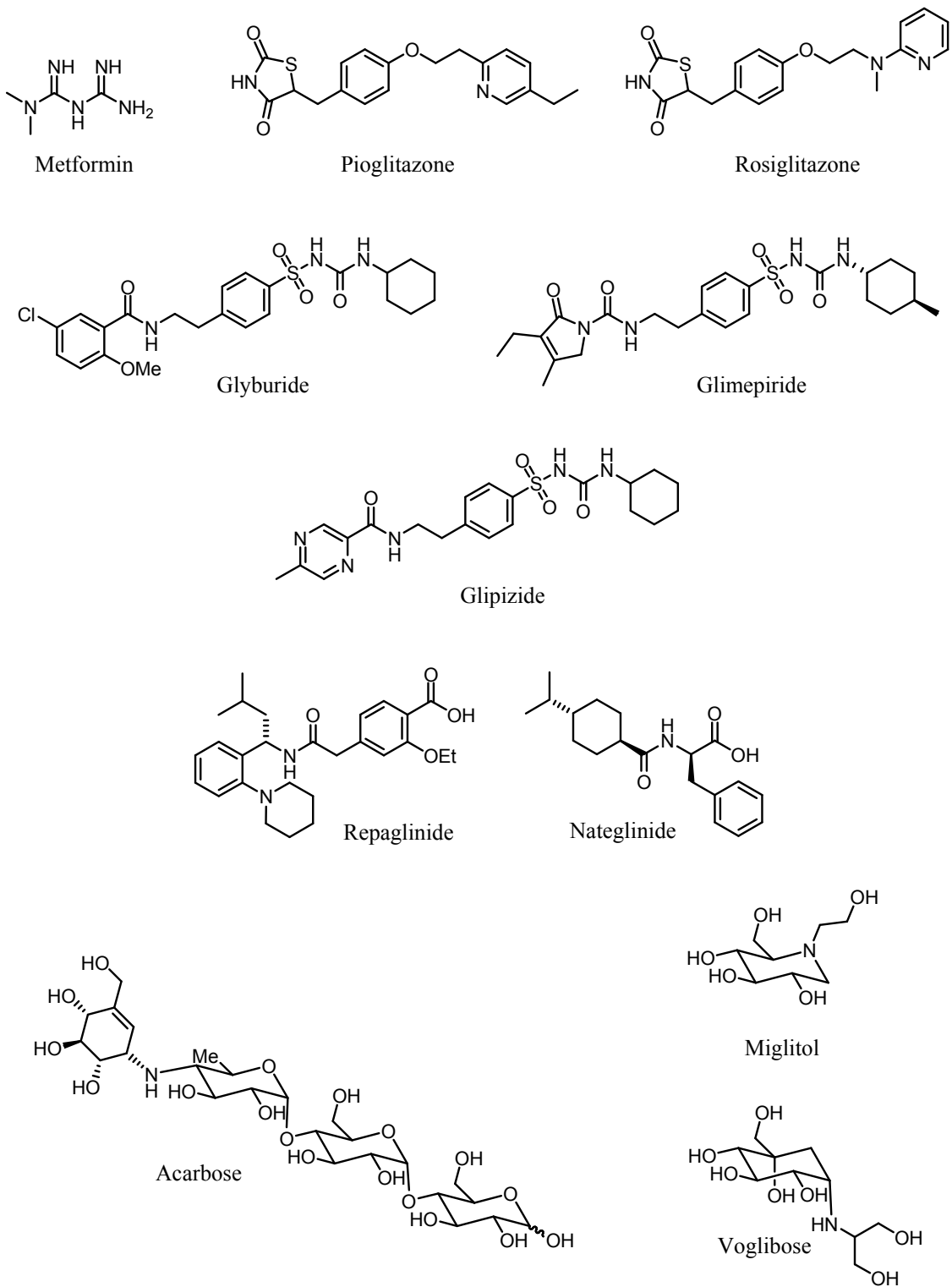


Figure 1.6 Orally active Type 2 diabetes treatments.

following a meal.¹⁹ Insulin injections can also be used as a treatment measure, either as a solitary option or in tandem with one of the oral medications mentioned above.

In 1922, Frederick Banting and Charles Best became the first scientists to successfully extract and purify insulin, a breakthrough in diabetes research that earned them a Nobel Prize in Medicine in 1923. Derived from the pancreatic secretions of dogs, the first injection of purified insulin administered to 14-year old diabetic Leonard Thompson proved to be a monumental success, with the boy's blood glucose decreasing from 0.520% to 0.120% within the span of a day.²¹ Prior to this first insulin injection, a diabetes diagnosis meant that the individual only had 3 years or less left to live.²² Later commercialization of this treatment by Eli Lilly ensured that countless diabetics would be able to live longer, healthier lives.

Since 1922, various peptide-based insulin analogs have been developed with diverse durations of activity, compared to that of insulin.²³ The rapid-acting analogs (insulin lispro, insulin aspart, and insulin glulisine) have slightly modified peptide sequences compared to that of insulin, leading to faster absorption and improved glycemic regulation. The mode of action of the long-acting analogs, insulin glargine and insulin detemir, involves precipitation or albumin binding at the site of injection and self-association that leads to a prolonged release of these insulin analogs into the bloodstream.

Insulin and insulin analogs (*vide supra*) have the drawback that they are all delivered by means of injections. Chronic treatments that involve frequent injections raise numerous concerns, including needle sterility and anxiety or fear concerning needles that could lead to patient non-compliance and/or the development of additional health issues.

The therapeutic use of insulin also carries with it problems surrounding storage. As a protein, care must be taken to store insulin at the proper temperature; insulin must be refrigerated, as it has a shelf-life of only one month when stored at room temperature. One remedy for the matter of frequent injections has been the advancements made in the realm of insulin pumps. Originally the size of a back pack, they are now discreet enough to go virtually unnoticed.²³ The computer-controlled system consists of a reservoir of a rapid-acting insulin analog that is pumped through a needle implanted in the abdomen, delivering a steady, low-dose of analog throughout the day. Though the insulin pump has been found to improve the quality of life for diabetics, this treatment still suffers from its reliance on needles and a peptide hormone that is unstable in the long-term.

Many individuals with Type 2 diabetes are able to avoid the difficulties inherent to the use of a protein to treat a chronic disorder, by merely controlling their glucose levels through diet, exercise, and the use of an orally-active diabetes medication (Figure 1.6). Unfortunately for Type 1 diabetics, their survival remains dependent on the administration of doses of insulin. None of the small molecule oral treatments currently in use for Type 2 diabetics act upon IR, mimicking the activity of insulin. The discovery of a small molecule insulin mimic would offer immense relief to those who would be able to exchange their painful daily injections for the ease of a pill. Additionally, the manufacturing costs for the synthesis and distribution of a small molecule would be much lower compared to the current costs associated with the use of insulin. Reduced manufacturing costs could translate into reduced costs for the patient. Furthermore, treatment costs would be lessened, as syringes and needles become obsolete in the lives

of diabetics. Cost of treatment is significant for many diabetes patients, as researchers have found that lower income regions have a higher incidence of diabetes.²⁴

1.5 The First Orally-Active Insulin Mimic: DAQ B1

In 1999, researchers at Merck reported the identification of natural product demethylasterriquinone B1 (DAQ B1, also known as L-783,281) (Figure 1.7), isolated from the *Pseudomassaria* sp. fungus of Congo.²⁵ Metabolite DAQ B1 was screened among 50,000 samples of natural products and synthetic compounds and was found to be an activator of IR in Chinese hamster ovary cells that overexpress the human IR (CHO.IR). Incubation of the cells with a concentration of 3-6 μM DAQ B1 induced a response in the tyrosine kinase domain of IR that was half that of the maximal activity of insulin (Figure 1.8). Furthermore, a concentration of 10-20 μM DAQ B1 was sufficient to stimulate tyrosine kinase activity of IR with activity similar to that of insulin.²⁶ In the same assay, a constitutional isomer of DAQ B1, natural product hinulliquinone (Figure 1.7), was found to be about 100 times less active (Figure 1.8), a preliminary indication of the selectivity of DAQ B1 for IR.

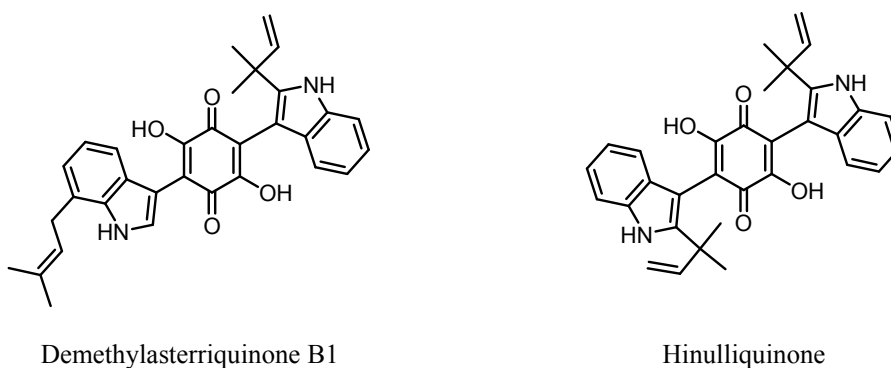


Figure 1.7 Natural products from Merck's small molecule IR activator screen.

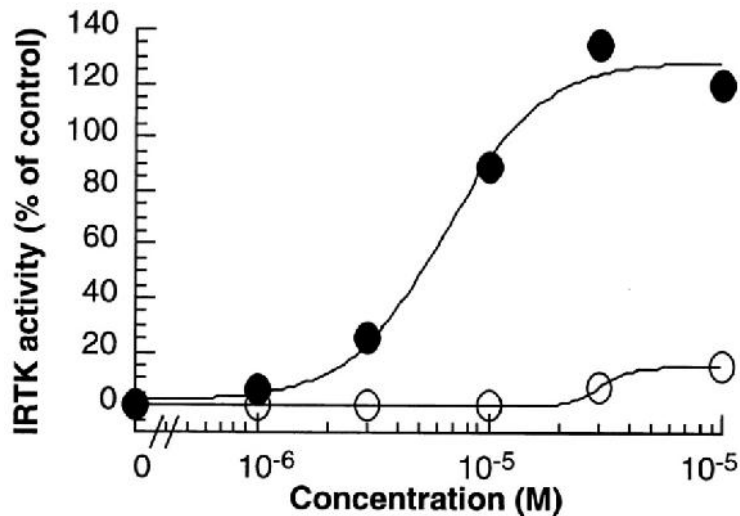


Figure 1.8 Insulin receptor tyrosine kinase (IRTK) activity at various concentrations of DAQ B1 (solid circles) and hinulliquione (open circles).
Image copied from Zhang, B. et al. *Science* **1999**, 284, 974-977.

The selectivity of DAQ B1 for IR was further demonstrated in a tyrosyl phosphorylation assay where DAQ B1 was incubated in the presence of CHO cells overexpressing receptors that are known to be homologous to IR (Figure 1.9).^{25,26} Concentrations of greater than 30 μM were required to see weak activation of the tyrosine kinase domains of the insulin-like growth factor receptor and epidermal growth factor receptor (CHO.IGFIR and CHO.EGFR, respectively). Cells overexpressing platelet-derived growth factor receptor (CHO.PDGFR) were not activated by DAQ B1, even at concentrations as high as 100 μM . This data indicates that the ability of DAQ B1 to induce tyrosine phosphorylation is limited to the insulin receptor at low concentrations.

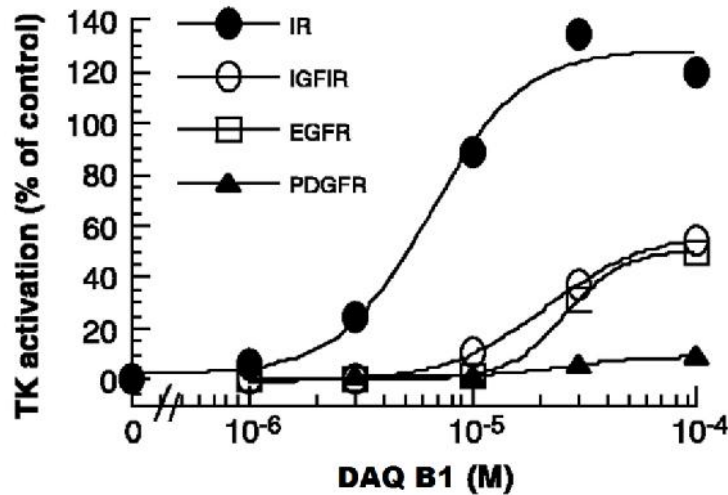


Figure 1.9 Tyrosine kinase (TK) activation in CHO.IR, CHO.IGFIR, CHO.EGFR, and CHO.PDGFR cells at various concentrations of DAQ B1. Image copied from Zhang, B. et al. *Science* **1999**, 284, 974-977.

Cells treated with insulin in the presence of DAQ B1 (0.6-2 μ M), exhibited a drastic increase in receptor activation when compared to cells treated with insulin alone (Figure 1.10). This finding suggests that DAQ B1 could be used as an insulin sensitizer as well. In addition to stimulating tyrosine phosphorylation in IR, DAQ B1 was also found to activate various downstream events leading up to and including the induction of glucose uptake in rat adipocytes and myocytes. In vivo, oral administration of DAQ B1 led to a significant improvement in hyperglycemia of *db/db* and *ob/ob* mice, models of type 2 diabetes. Another study indicated that intracerebroventricular injections of DAQ B1 reduced food intake and body weight in rats in a dose-dependent manner,²⁷ whereas it is known that the therapeutic use of insulin stimulates weight gain by means of adipogenesis, the process by which preadipocytes differentiate into adipocytes. This places the administration of DAQ B1 in sharp contrast to the use of insulin injections, as

DAQ B1 not only reduces blood glucose levels, but also has the capacity to improve insulin sensitivity through weight loss.

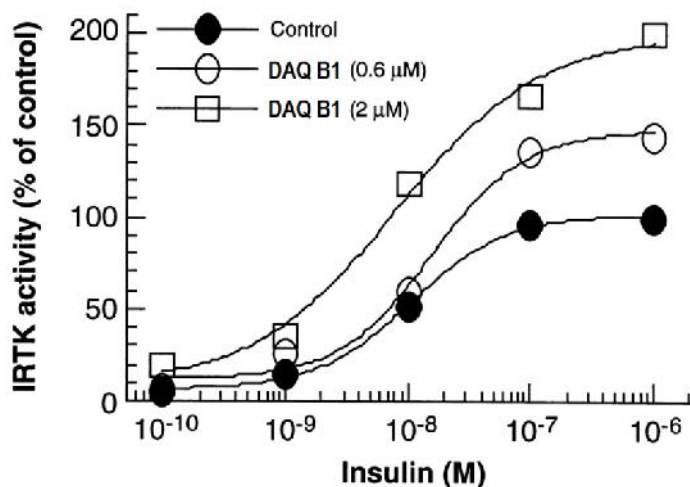


Figure 1.10 IRTK activity of cells with various concentrations of insulin in the presence and absence of DAQ B1.

Image copied from Zhang, B. et al. *Science* **1999**, 284, 974-977.

The Merck group also did preliminary work to study the mode of action of DAQ B1. Several pieces of evidence pointed to the site of DAQ B1 interaction being the intracellular tyrosine kinase region of IR, instead of the extracellular α subunit that is involved in insulin binding to the receptor. First, DAQ B1 did not act as a competing ligand, displacing radiolabeled insulin from IR, and it did not decrease insulin's affinity for the receptor. In experiments with cells overexpressing chimeric receptors consisting of the intracellular domain of IR fused with the extracellular domain of the nonhomologous IR-related receptor (CHO.IRR/IR), insulin was unable to activate the tyrosine kinase domain, as expected, yet DAQ B1 maintained its activity. In a cell-based

assay using recombinant IR to compare the activity of hinulliquinone and DAQ B1, only DAQ B1 was found to stimulate tyrosine kinase activity of the receptor. An additional piece of evidence was the fact that when IR intracellular domain was incubated with DAQ B1, a modified pattern of partial proteolysis was observed. All of the aforementioned results demonstrate that DAQ B1 likely interacts with the tyrosine kinase domain of the receptor, causing the required conformational change that leads to receptor autophosphorylation and eventual glucose uptake by the cell.

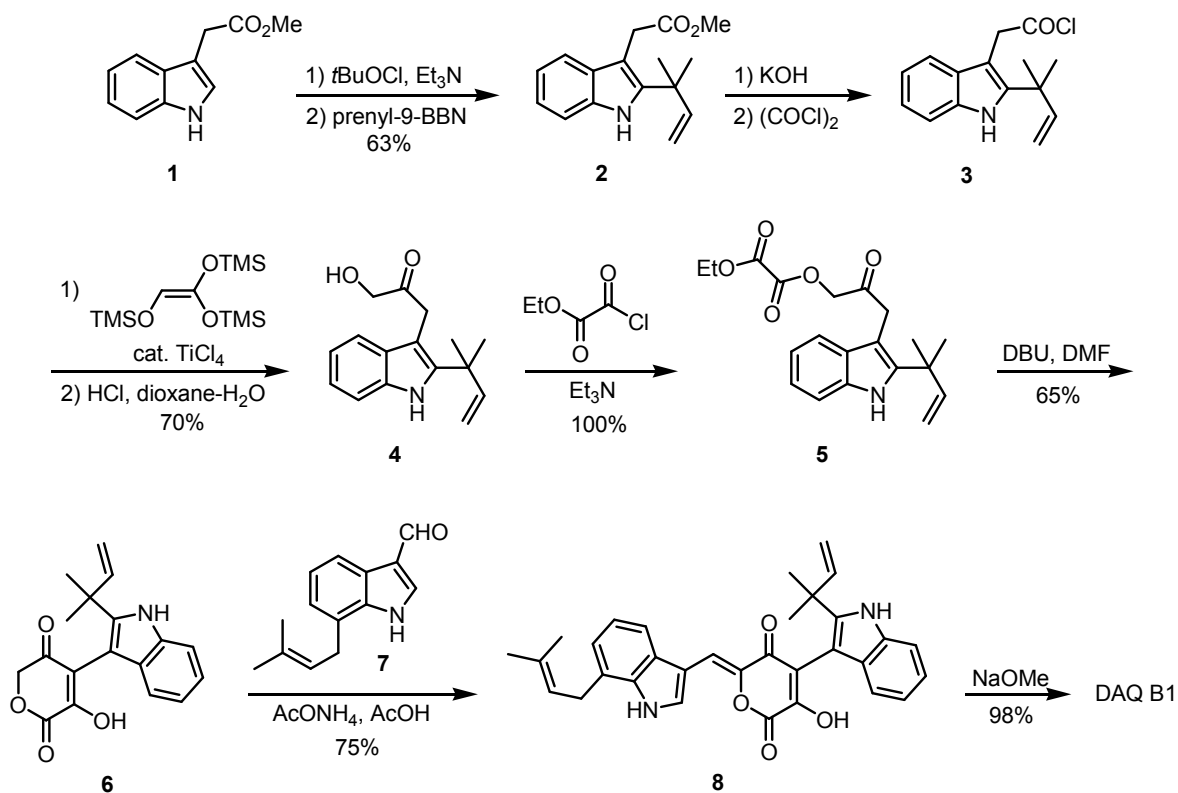
The downstream protein targets of DAQ B1 have been a point of interest for the Pirrung group. Phosphorylation of IRS-1 protein was detected in the presence of DAQ B1 *in vitro*.²⁸ Furthermore, DAQ B1 was shown to selectively induce phosphorylation of PKB/Akt. In a phage display cloning experiment, glyceraldehyde 3-phosphate dehydrogenase (GAPDH) was identified as another protein target of DAQ B1.²⁹ In the absence of agonists, such as DAQ B1, GAPDH is believed to exist as a tetramer in order to act as a phosphatase of PIP₃. It is postulated that DAQ B1 inhibits tetramerization of GAPDH, which allows PIP₃ to remain phosphorylated and activate PKB/Akt.

This novel orally active insulin mimic was found to also affect signaling upstream from the insulin receptor. Activation of IR by DAQ B1 has been shown to induce insulin gene expression, thereby stimulating the synthesis of insulin.³⁰ When isolated β cells were treated with DAQ B1 in the presence of glucose, the intracellular concentration of calcium was found to increase by 178% compared to basal levels, leading to the secretion of insulin.³¹ This finding demonstrates that DAQ B1 is active both as an insulin secretagogue and as an insulin mimic.

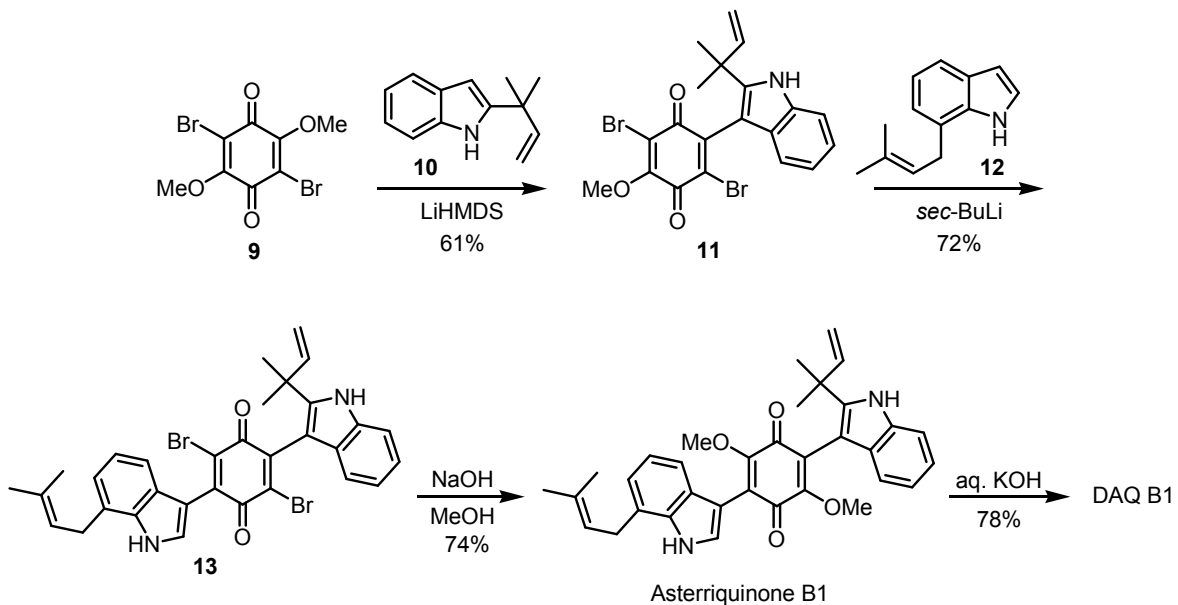
1.6 Total Syntheses and SAR Studies of DAQ B1 by Other Groups

Soon after their discovery of the biological benefits of DAQ B1, scientists at Merck completed the first total synthesis of this orally-active natural product (Scheme 1.1).³² To begin, methyl 3-indolylacetate **1** was converted to a chloroindolenine by reaction with *tert*-butyl hypochlorite. Treatment of this intermediate with prenyl-9-BBN yielded 2,3-disubstituted indole **2**. Ester **2** was then saponified and converted to acid chloride **3**. Compound **3** was converted to α -hydroxy ketone **4**, which was acylated with ethyl oxalyl chloride and cyclized to afford pyrandione intermediate **6**. The second required indole **7**, synthesized from 7-prenyl indole, was condensed with **6** to obtain **8**. In the presence of sodium methoxide, compound **8** rearranged to generate DAQ B1 in a total of 10 steps and 19% overall yield.

Tatsuta and coworkers completed an alternate total synthesis with the use of three building blocks (Scheme 1.2)³³ instead of the two used in the Merck total synthesis.³² Lithiation of 2-isoprenylindole **10** followed by treatment with dibromodimethoxyquinone **9** led selectively to the formation of monosubstituted quinone **11**. The second indole, 7-prenylindole **12** was also lithiated and the resulting anion reacted with **11** to generate bis-indolyldibromoasterriquinone **13**. Initial attempts at hydrolyzing this intermediate to directly obtain DAQ B1 proved inefficient, with the desired product being isolated in only 30% yield. Alternatively, the dimethoxyquinone, asterriquinone B1, was obtained by treatment of **13** with NaOH in MeOH in a high yielding reaction (74%). Finally, DAQ B1 was isolated following treatment of asterriquinone B1 with KOH in 78% yield.



Scheme 1.1 First total synthesis of DAQ B1.



Scheme 1.2 Total synthesis of DAQ B1 by Tatsuta's group.

With the exciting biological activity of DAQ B1, an understanding of the structure-activity relationship (SAR) of this natural product became necessary. To do this, Merck synthesized and tested the activity of numerous DAQ B1 analogs (Figure 1.11).³⁴ The first systematic modifications they made concerned the quinone core, exchanging the two hydroxyl groups of DAQ B1 for methoxy groups, amines, and triflates (compounds **14**). Biological activity associated with these changes indicated that both the 2- and 4-hydroxy groups were required for insulin mimetic activity. Attempts at activating IR using N-methylated analogs **15** were unsuccessful in comparison to DAQ B1. The final modification was to the prenyl groups to obtain analogs **16**. Again, none of these variations led to the identification of a lead compound with activity superior to that of DAQ B1, though the activity of most of these analogs was similar to that of DAQ B1.

Further modifications were made to DAQ B1 with the aim of improving the potency of the insulin mimic.³⁵ The indole moieties of DAQ B1 were substituted for other aromatic rings and then the resulting dihydroxyasterriquinones **17** were tested in an IRTK activation assay (Figure 1.12). Of the compounds tested, “compound 2,” as it was designated by Merck, emerged as a potent insulin mimetic. “Compound 2” results from the exchange of both of DAQ B1’s substituted indoles for an N-methylated indole and a simple phenyl ring. Not only was “compound 2” highly potent, with an EC₅₀ of 300 nM compared to 5.0 μM for DAQ B1, but it was also highly selective for IR, with no stimulation of the tyrosine kinase activity of IGFIR, EGFR, or PDGFR at concentrations as high as 30 μM. A structurally similar dihydroxyquinone with a free indole nitrogen had the same potency as “compound 2,” but showed no specificity for IR. Oral dosing of

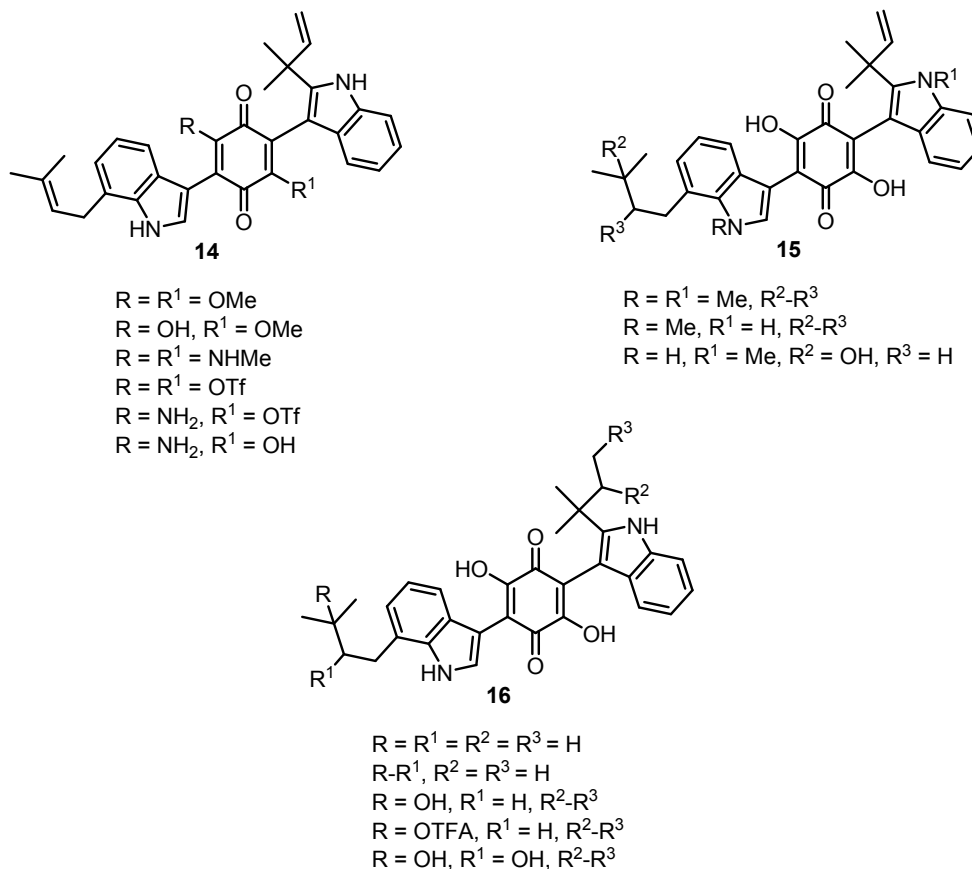


Figure 1.11 DAQ B1 analogs for SAR study by Merck.

“compound 2” to *db/db* mice decreased blood glucose levels in a dose-dependent manner. In the absence of sufficient insulin levels, “compound 2” was able to improve the uptake of glucose in vivo, suggesting that this compound has activity as an insulin sensitizer as well.³⁶ Further study of this small molecule, which like DAQ B1 activates Akt/PKB, revealed “compound 2” had the ability to decrease body weight in obese mice.³⁷

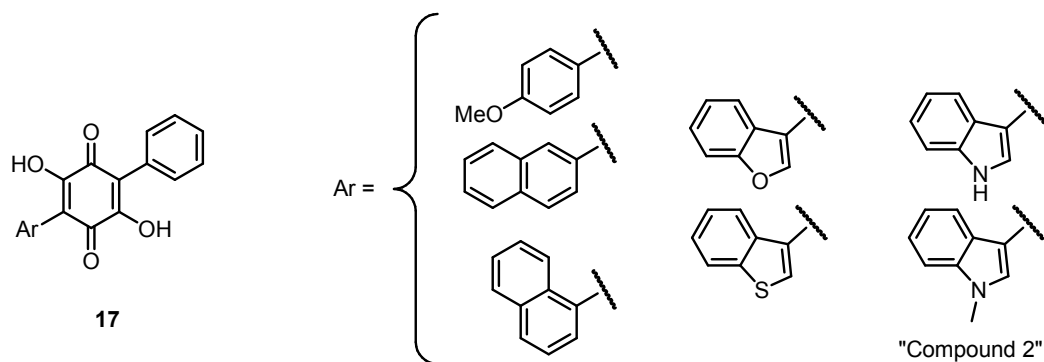
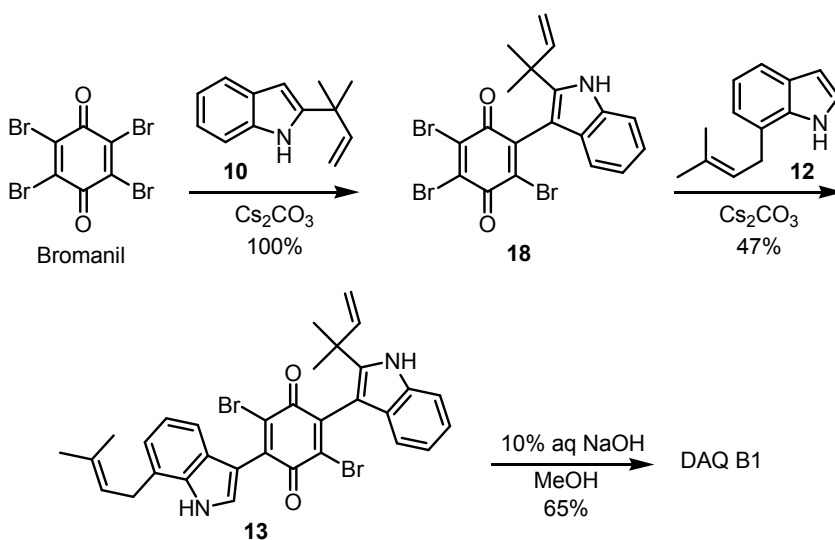


Figure 1.12 Aryl substitutions made to the quinone ring of DAQ B1 leading to the identification of “compound 2.”

1.7 Total Syntheses and SAR Studies of DAQ B1 by the Pirrung Group

The Pirrung group also worked toward a total synthesis of DAQ B1, with the goal of developing a divergent synthesis that could be applied to the production of analogs of this active natural product (Scheme 1.3).³⁸ In their first synthesis, bromanil and 2-isoprenylindole **10** were coupled in a base-catalyzed nucleophilic addition reaction. This reaction was highly selective, giving only the monoindolylquinone **18** in quantitative yield. Comparable conditions were applied to the coupling of **18** and **12**, with similar results for the yield, but issues arose concerning the reaction’s regioselectivity. The product was determined to be a 1:1 mixture of the meta-substituted quinone and the desired para-substituted quinone, but these two compounds were easily separable by chromatography. With the desired bis-indolyldibromoasterriquinone **13** in hand, conditions were developed for its hydrolysis. After much optimization, treatment of **13** in dilute MeOH with 10% aq NaOH provided a quick, scalable route to DAQ B1 (65%), a slight improvement over Tatsuta’s protocol which required two steps from **13** to obtain

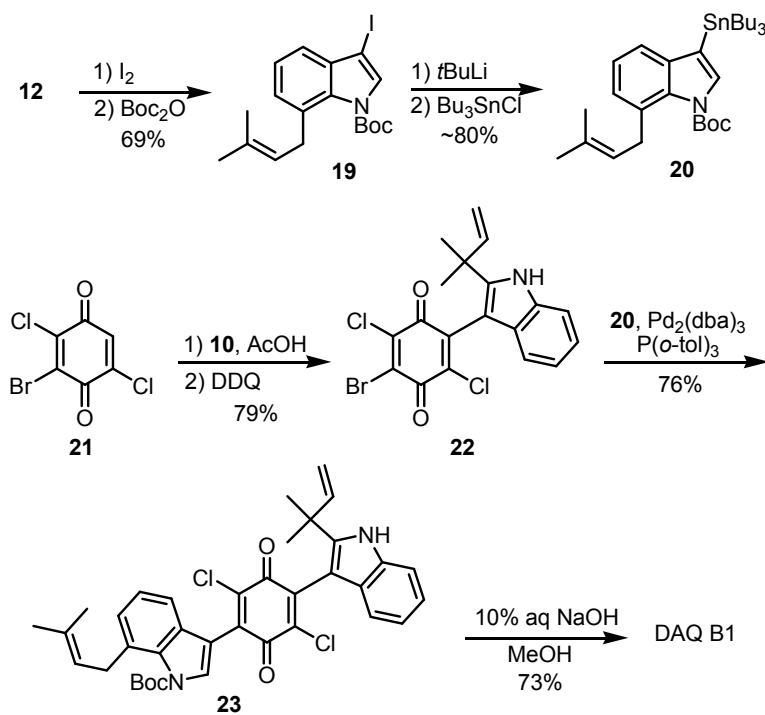
DAQ B1 in 58% yield. In all, this first attempt produced DAQ B1 in five steps and 12% yield.



Scheme 1.3 First total synthesis of DAQ B1 completed by the Pirrung group.

Not satisfied with the lack of regioselectivity of their first protocol, the Pirrung group developed a second synthesis that relied on a Stille coupling to achieve regioselectivity (Scheme 1.4). The requisite stannylated indole **20** was prepared by iodination and Boc (*N*-*tert*-butoxycarbonyl) protection of **12** to obtain 3-iodinated indole **19**, which was treated with *tert*-butyl lithium followed by tri-*n*-butyltin chloride. The brominated Stille coupling partner **22** was obtained through an acetic acid-promoted addition of **10** to bromo-2,5-dichlorobenzoquinone **21**, in the presence of 2,3-dichloro-5,6-dicyano-1,4-benzoquinone (DDQ) as reoxidant. The previous work in the area of this acid-catalyzed reaction involved the use of HCl, H_2SO_4 , or acetic acid for the synthesis of various monoindolylbenzoquinones,³⁹ but of the three acid sources, acetic acid proved

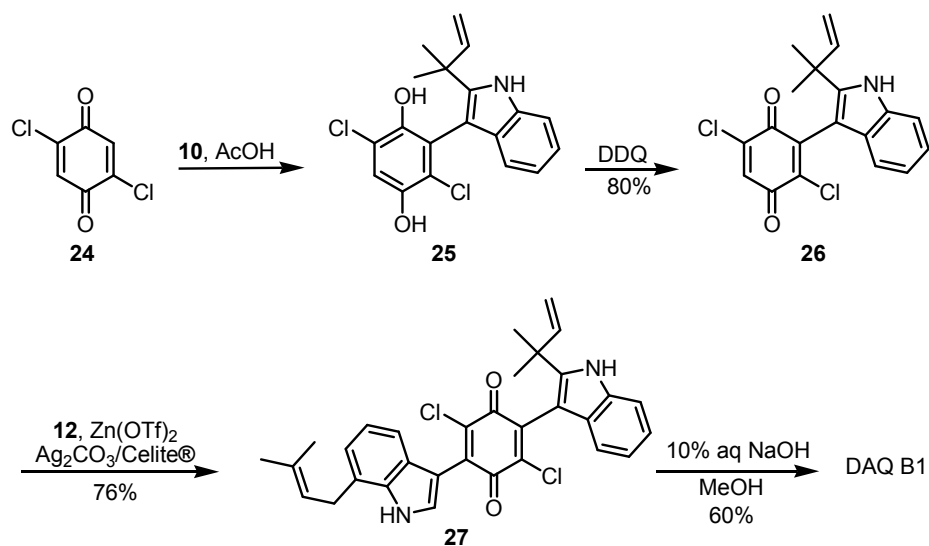
optimal for the synthesis of DAQ B1.³⁸ Due to the superior reactivity of vinyl bromides compared to vinyl chlorides, the Stille coupling of **22** with **20** proceeded as desired, producing only the para-substituted product **23**. Under the same conditions used in the prior synthesis, the Boc group was removed and the chlorides were hydrolyzed to yield DAQ B1 in seven steps and 13% overall yield.



Scheme 1.4 Second total synthesis of DAQ B1 reported by the Pirrung group.

Later, the Pirrung group further optimized their total synthesis of DAQ B1 and in the process attained their goal of developing a modular approach that could be applied to the synthesis of DAQ B1 derivatives (Scheme 1.5).⁴⁰ The potential selectivity issues that could arise with the use of 2,5-dichlorobenzoquinone **24** as the quinone source were

circumvented by applying methodology from their second synthesis (Scheme 1.4). The conjugate addition of **24** and **10** leads to the formation of hydroquinone intermediate **25**, which could be reoxidized in order to further react with indole to form a symmetrical astringinone. By adding in DDQ as oxidant in a separate step following consumption of indole, they were able to stop the reaction after a single addition and obtain only **26** in high yield. The second addition step was conducted in the presence of Lewis acid activator, $\text{Zn}(\text{OTf})_2$, and oxidant, silver carbonate on Celite®, with similar results. The second indole addition was mediated by $\text{Zn}(\text{OTf})_2$, due to lower reaction yields when the reaction was conducted in the presence of acetic acid and other Brønsted-Lowry acids. Final application of their optimized hydrolysis conditions led to the isolation of DAQ B1 in only 3 steps and 36% overall yield, a 3-fold improvement over the previous procedures.



Scheme 1.5 Concise synthesis of DAQ B1 by the Pirrung group.

In addition to the fact that this new synthesis was short, it also had the attractive quality of requiring no pre-activation of the indole or quinone subunits for the sake of regiocontrol, making it ideal for application to the synthesis of a library of analogs of DAQ B1 for SAR studies. A new method was developed for the SAR study of this compound, termed “methyl scanning.”⁴⁰ This method involves the systematic replacement of each hydrogen of the biologically active lead compound with a methyl group, in an attempt to create a steric hindrance at that position that blocks interaction with the receptor. A single methyl substitution that leads to a decrease in activity indicates the discovery of a “hot spot,”⁴⁰ meaning molecular locations potentially involved in receptor binding. Merging this data, a picture of the drug’s pharmacophore, or the features necessary for activity, can be formed.

Ten methylated derivatives of 2-isoprenylindole (**28**) and 7-prenylindole (**29**) were prepared. Indoles **28a-e** were condensed with **24** in the presence of acetic acid, then 7-prenylindole was coupled to this monoindolylquinone under the Zn(OTf)₂-mediated conditions. Hydrolysis in the presence of NaOH/MeOH led to the isolation of asterriquinone **30a-e**. Indoles **29f-j** were coupled to **26** using Zn(OTf)₂ then the vinyl halides were hydrolyzed to generate asterriquinones **30f-j**. Additionally, monomethoxy quinones **30k** and **30l** were synthesized for the methyl scan. Literature conditions developed for the synthesis of a DAQ A1 derivative⁴¹ were successfully applied to the synthesis of **30k**. A protocol for controlled hydrolysis of **27** was developed for the synthesis of **30l**.

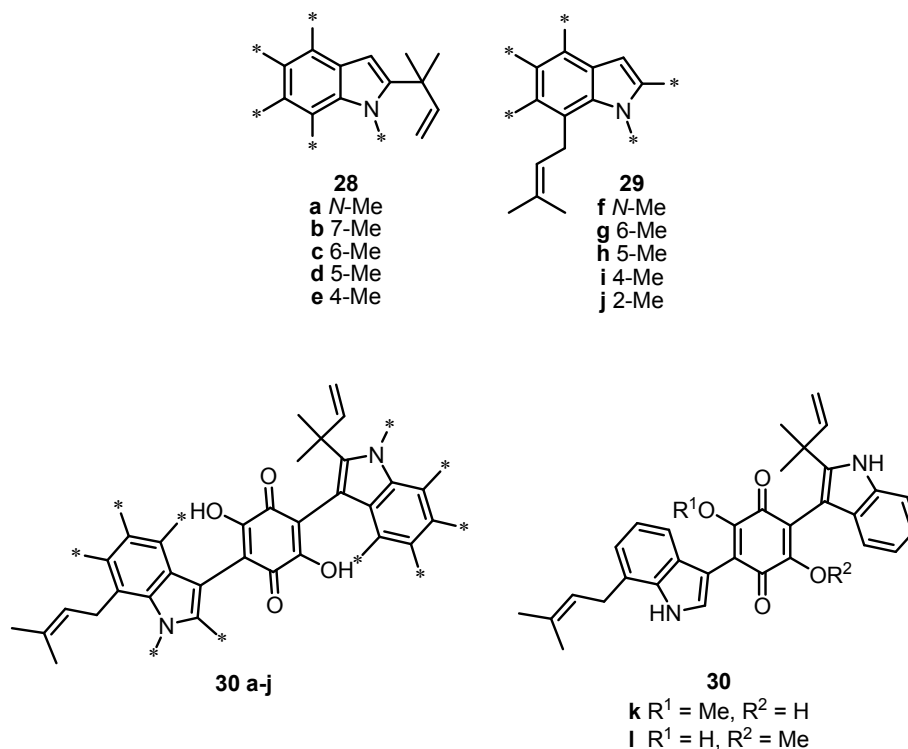


Figure 1.13 Methylated indoles and asterriquinones for the methyl scan study.

The 12 methylated derivatives were screened for their ability to activate the human insulin receptor (hIR) in rat fibroblasts at 30 μ M. Methylation was not tolerated at the 4-, 5-, and 6-positions of the 7-prenylindole moiety (**30g-i**) or at either hydroxyl group (**30k-l**), indicating that the “hot spot” of DAQ B1-IR binding is the region encompassing the 7-prenylindole and OH of the quinone (Figure 1.14). Interestingly, methylation at the 2-position of 7-prenylindole (**30j**) led to a slight improvement (1.5-fold) in tyrosine kinase activation relative to that of DAQ B1.

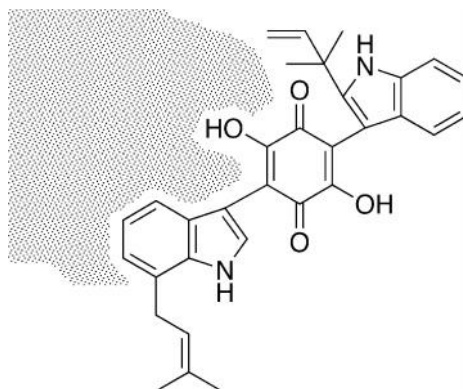


Figure 1.14 Regions of interaction between DAQ B1 and IR, as determined by methyl scanning experiment.

Image copied from Pirrung, M. C. et al. *J. Am. Chem. Soc.* **2005**, *127*, 4609-4624.

Compounds **31** and **32** (or ZL196),³⁹ composed of only the quinone ring and either 2-isoprenylindole or 7-prenylindole, respectively, were also tested in a tyrosine kinase autophosphorylation assay in the presence of DAQ B1 (Figure 1.15).⁴⁰ This experiment tested the hypothesis that the activity of DAQ B1 arises from the molecule spanning the two monomers of the receptor to cause dimerization and activation. If dimerization is indeed the mechanism of action for DAQ B1, the inclusion of **31** or **32** in the cellular media would block the binding of DAQ B1 and inhibit any dimerization. Compound **31** had no effect on the activity of DAQ B1, which is expected in light of the lack of “hot spots” on the side of DAQ B1 that is composed of 2-isoprenylindole. The data for ZL196 did not indicate any inhibition of activity, but instead revealed that this small molecule actually augments tyrosine kinase activity stimulated by DAQ B1. Alone, ZL196 was active in a cell-based assay for tyrosine kinase autophosphorylation, but its EC₅₀ was only about 100 μM. This data indicated that ZL196 represents the pharmacophore of DAQ B1.

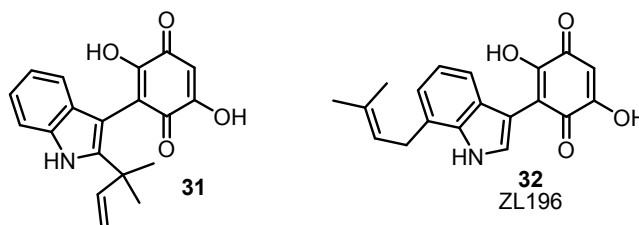


Figure 1.15 DAQ B1 derivatives for the study of IR dimerization induced by DAQ B1.

1.8 Derivatives of DAQ B1: Synthesis and Biological Activity

Application of the modular and concise synthetic route used to obtain DAQ B1 in only 3 steps (Scheme 1.5) led to the synthesis of a library of indolylquinones by the Pirrung group.⁴² One of the advantages of these conditions is that the reactions can be conducted in parallel using an automated synthesizer to quickly obtain pure products in typically moderate to high yields. To maximize yields, it was determined that less reactive indoles with electron-withdrawing groups or substitution at the 4-position should be added in the first step [mediated by either acetic acid or H₂SO₄], while the more reactive indoles with electron-donating groups should be added in the second step [Zn(OTf)₂-mediated step].

Indole building blocks for the library were chosen based on commercial availability, thus avoiding bias toward groups known to activate IR. From the parallel condensation reactions of 21 different indolylquinones **33** and 35 indoles **34** (Tables 1.1 and 1.2), a combinatorial library of 269 compounds (of 535 possible compounds) was constructed. When the library was screened for receptor autophosphorylation at concentrations ranging from 10-30 μM, four compounds (**35-38**, Figure 1.16) emerged as leads. A common structural feature among these four compounds is the presence of a

bulky group at the 2-position of one of the indole groups. This result was surprising due to previous work that had indicated that bulky substituents (isoprenyl) at the 2-position of the indole were not beneficial to activity, while hydrophobic groups, such as benzyloxy or prenyl, at the 7-position were integral to obtaining optimal activity.

Table 1.1 Indoles used in the combinatorial synthesis of an asterriquinone library.

33	Indole	33	Indole
A	5-benzyloxyindole	s	5-fluoroindole
B	5-methylindole	t	7-chloroindole
C	<i>N</i> -methylindole	u	5,6-methylenedioxyindole
D	6-chloroindole	v	6-fluoroindole
E	4-methoxyindole	w	2- <i>tert</i> -butylindole
F	4-benzyloxyindole	x	2-(3',5'-dimethoxyphenyl)indole
G	2-isopropylindole	y	7-methylindole
H	5-methoxyindole	z	7- <i>tert</i> -butylindole
I	2-methyl-5-chloroindole	aa	2,5-dimethylindole
J	2-methyl-5-methoxyindole	bb	5-bromoindole
K	5-chloroindole	cc	2-pentylindole
L	2-cyclopropylindole	dd	7-ethylindole
M	5-iodoindole	ee	7-methoxyindole
N	2-ethylindole	ff	2-isobutylindole
O	2-propylindole	gg	2-methyl-7-bromoindole
P	2-phenylindole	hh	2-phenyl-1-ethylindole
Q	2-methylindole	ii	2-(<i>p</i> -chlorophenyl)indole
R	indole		

Table 1.2 Indolylquinones in the combinatorial synthesis of an asterriquinone library.

34	Indolylquinone	34	Indolylquinone
a	2-methylindole	l	6-chloroindole
b	2-phenylindole	m	4-methoxyindole
c	2-isopropylindole	n	4-benzyloxyindole
d	2- <i>tert</i> -butylindole	o	7-ethylindole
e	5-bromoindole	p	5-methylindole
f	1-methylindole	q	5-methoxyindole
g	2- <i>n</i> -propylindole	r	6-fluoroindole
h	5-iodoindole	s	7-methoxyindole
i	7-methylindole	t	4-methyl-5-methoxyindole
j	5-chloroindole	u	5-fluoroindole
k	7-chloroindole		

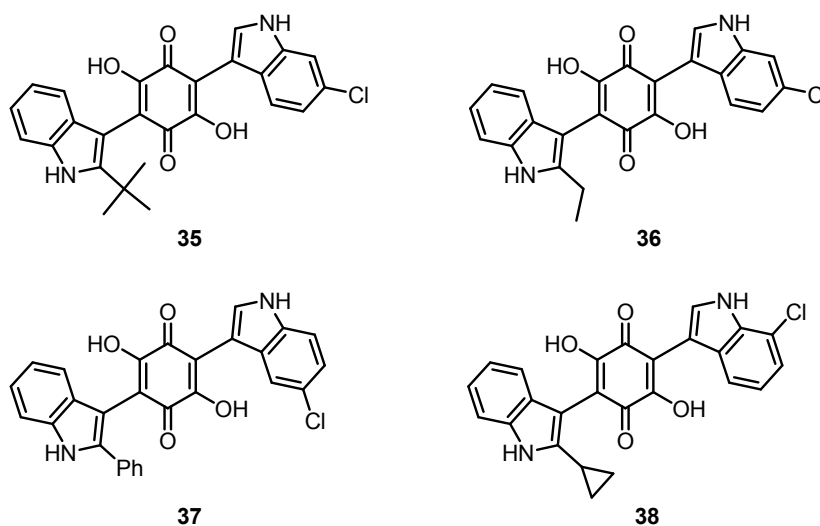


Figure 1.16 Potent IR-activators from library screen.

A library of benzoquinone and naphthoquinone derivatives were synthesized and tested for their ability to activate IR phosphorylation (Figure 1.17).⁴³ In this screen, only benzoquinone-containing compounds were active. It was also determined that

substitution at the 6- and 7-positions of indole led to a higher percentage of IR activation. Only ZL196 and LD-17 (with a 7-benzyloxyindole) were carried on for further study (Figure 1.18). A cell-based assay revealed LD-17 activated not only IR phosphorylation, but also that of Akt, in a dose-dependent manner. Just as with DAQ-B1, ZL196 showed some activity at IGFR and EGFR, though for IGFR, ZL196 was more active at low concentration than DAQ B1. On the other hand, LD-17 was much more selective for only IR. Glucose uptake was stimulated by the presence of LD-17 and ZL196. In vivo, when administered orally to hyperglycemic *db/db* mice, these compounds had the effect of gradually decreasing blood glucose levels. The in vitro and in vivo insulin mimetic activity of these two benzoquinones corroborates the methyl scan experiment that identified ZL196 as the pharmacophore of DAQ B1. It is quite advantageous to have relatively simple benzoquinones as opposed to asterriquinones as drug leads, as benzoquinones offer the benefit of fewer synthetic steps to make the active drug. A common issue hindering the use of DAQ B1 and other asterriquinones in vitro and in vivo is the poor cell clearance of these structures. The partition coefficient or log P of a compound is correlated to its ability to cross the cell membrane. Log P values of <5 suggest good cell permeability. The log P values for asterriquinone DAQ B1 and benzoquinones ZL196 and LD-17 were calculated to be 6.96, 2.65, and 1.97, respectively.⁴³ This indicates that benzoquinones with bulky substituents at the 7-position of the indole should be moderately active insulin mimics with good cell permeability.

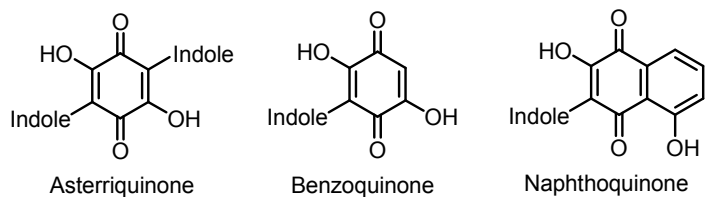


Figure 1.17 Different types of quinones.

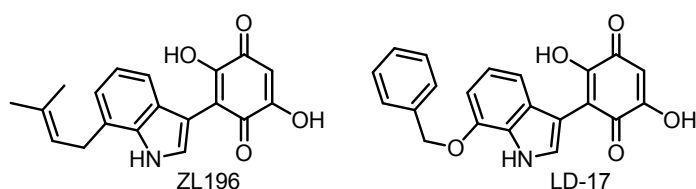


Figure 1.18 7-substituted mono-indolylbenzoquinones active as insulin mimics.

Despite the enticing results indicating the potential therapeutic utility of these small molecules, further development of this class of compounds has halted due to concerns over the safety of the quinone ring. Though there are a few drugs on the market that contain this substructure, quinone-containing compounds are generally viewed as toxic when used in the long-term. Interestingly, the beneficial activity and toxicity of some quinone-containing compounds has been attributed to the dual reactivity of these ring structures.⁴⁴ Quinones readily participate in redox chemistry. The generation of semiquinone can lead to the formation of reactive oxygen species (ROS), such as superoxide, H_2O_2 , or hydroxyl radical. Quinones also can act as electrophiles in 1,4-addition reactions with nucleophilic groups such as amines, thiols, and nucleic acids of DNA. This addition reaction to proteins or other endogenous molecules can lead to loss of normal cellular function. The potential oxidative stress or impaired cell function

caused by the administration of quinone could be quite harmful to a patient with chronic use.

A treatment for diabetes would require chronic dosing over the lifetime of the patient, but, of the drugs that are currently in use therapeutically, all of the drugs that contain the quinone ring are prescribed for acute use. For example, naphthoquinone-containing atovaquone is used as an antiparasitic and antimalarial agent and mitomycin C is an anti-cancer treatment (Figure 1.19). In both of these cases, the drug is only prescribed for a relatively short amount of time. For anti-cancer drugs, a certain level of toxicity is acceptable, as long as the drug has a higher toxicity profile in cancer cells than healthy cells and is only required for short periods of time.

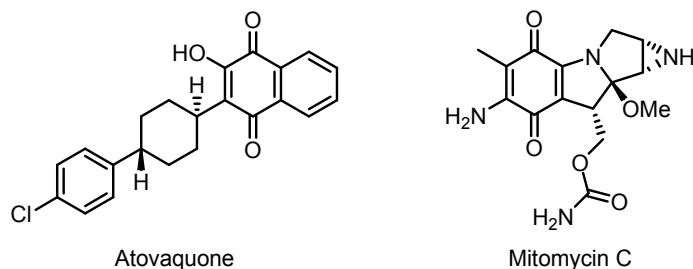


Figure 1.19 Quinone-containing drugs on the market.

1.9 Quinone Replacements

Despite the promising biological activity displayed by asterriquinone DAQ B1 and derivatives such as “compound 2,” ZL196, and LD-17, the presence of the quinone ring structure common to all of these small molecules has inhibited further development of this drug class. The Pirrung group has examined several other ring structures for their

ability to maintain the biological activity of the small molecule IR activators containing the offensive quinone.

As previously discussed, one of the factors contributing to the toxicity of a medicinal quinone is its ability to participate in redox chemistry. The methyl scan of DAQ B1 indicated the necessity of the enol subunit,⁴⁰ so ring structures that lacked the potential for redox reactions while preserving the α -hydroxy enone functionality of ZL196 were sought. Preliminary work involving the replacement of asterriquinone and benzoquinone with squaric acid to yield **39** (Figure 1.20) revealed that this substitution was detrimental to IR activation.⁴³ Tropolone was also auditioned by the Pirrung group as a possible alternative to quinone.⁴⁵ Treatment of CHO.IR cells with tropolone derivative **40** led to minimal IR autophosphorylation, though signs of cytotoxicity were noted. Compounds incorporating natural product maltol **41** and cyclohexadienone **42** have also been investigated in the Pirrung lab, though no biological data exists for these compounds to date.⁴⁶

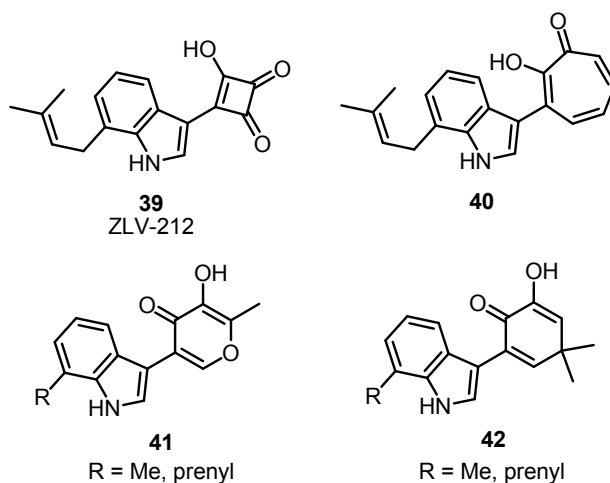


Figure 1.20 Early candidates for quinone replacements.

Another quinone substitute examined by the Pirrung group was kojic acid (Figure 1.21). Kojic acid is a fungal natural product derived from *Penicillium*, *Acetobacter*, and *Aspergillus*.⁴⁷ Kojic acid was discovered in 1916 by Yabuta as he investigated the *Aspergillus oryzae* mold, commonly called “koji” in Japanese, growing on steamed rice.⁴⁸ Kojic acid is present in many foods, a fact that indicates the safety of this pyrone. *Aspergillus* mold is used to manufacture Japanese foods including miso, sake, and soy sauce; fermentation of these foods leads to the production of kojic acid. Kojic acid has also found use as a food additive. Kojic acid inhibits the process by which cut fruit browns and also helps maintain the pink/red color of seafood. Kojic acid has additionally been used in the cosmetics industry as a skin-lightening agent. Current widespread public exposure to kojic acid implies the natural product would be safe to employ as a drug scaffold.

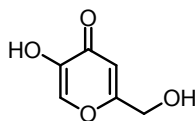
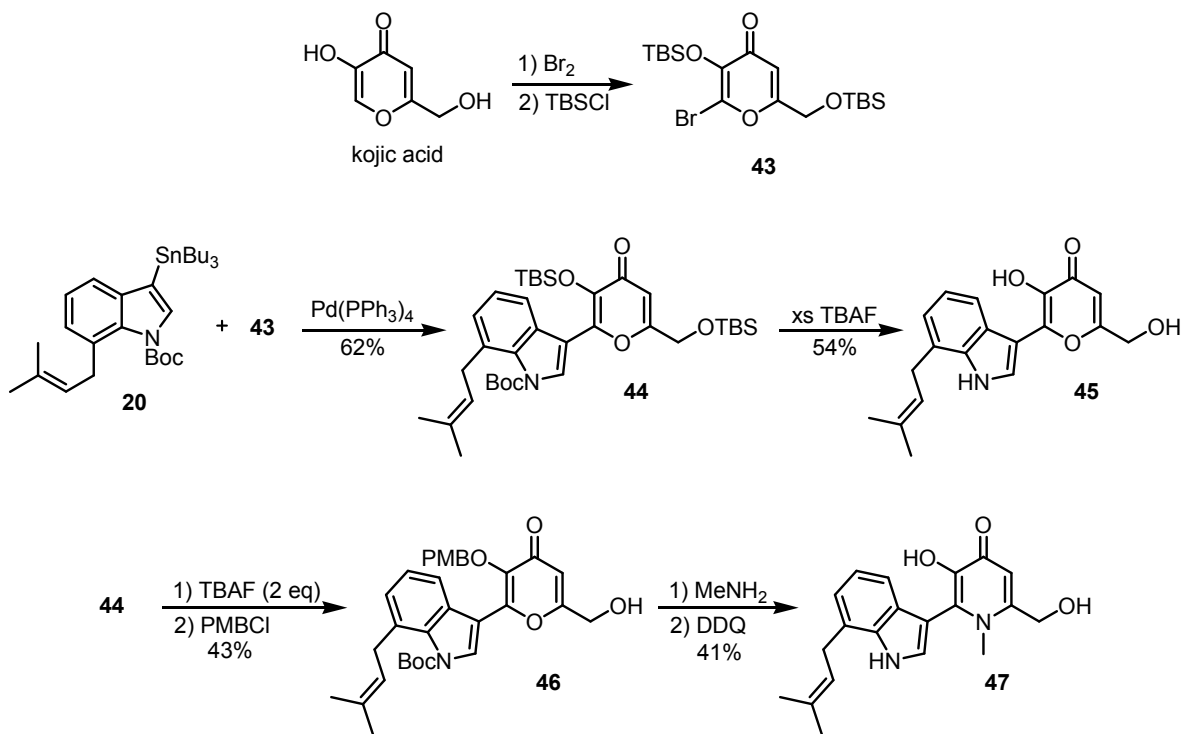


Figure 1.21 Kojic acid.

1.10 Kojate-Based Compounds Synthesized by Stille Coupling

Stille coupling was exploited to quickly access pyrone and pyridone kojate derivatives with a high degree of structural similarity to ZL196, the pharmacophore of DAQ B1 (Scheme 1.6).⁴⁵ Bromination of kojic acid according to a literature procedure,⁴⁹ followed by double TBS (*tert*-butyldimethylsilyl) protection afforded **43**. Compound **44**

was generated by coupling stannane **20** and bromide **43** under Stille conditions similar to those previously utilized in the synthesis of DAQ B1.³⁸ Fluoride ion was used in the subsequent deprotection steps. Using only 2 equiv of tetrabutylammonium fluoride (TBAF) removed both TBS groups of **44**, while an excess of TBAF under refluxing conditions cleaved the Boc group in addition to the TBS groups to afford **45**. Controlled removal of only the TBS groups from **44**, followed by selective protection of the α -hydroxy group using *para*-methoxybenzyl chloride (PMBCl) led to **46**, which was subjected to a pyrone to pyridone exchange reaction that also removed the indole nitrogen protection. Finally, DDQ was used to deprotect the enol and generate pyridone **47**.



Scheme 1.6 Preparation of kojate derivatives by Stille coupling.

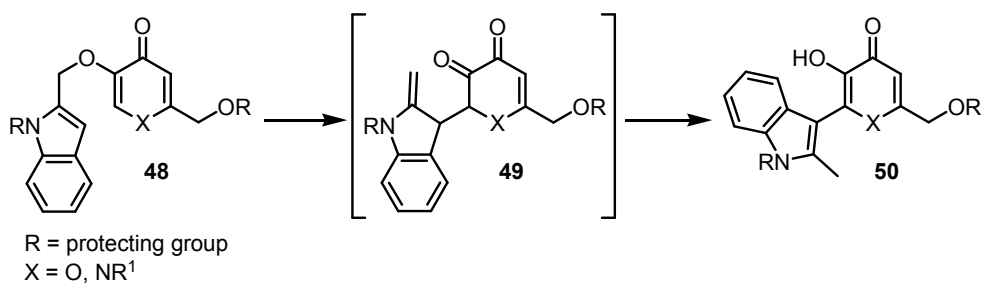
The IR activity of kojate derivatives **45** and **47** was probed through a receptor phosphorylation assay using CHO.IR cells. Both **45** and **47** were active initiators of IR phosphorylation, with EC₅₀ values similar to that of ZL196 (1, 1, and 30 μM, respectively). Additionally, pyrone **45** showed minimal inhibition of off-target processes (<20%) in over 40 different assays involving the activity of various human proteins, including phosphodiesterases, cyclooxygenases, and all four proteases classes, suggesting its safety.

The promising preliminary biological data pertaining to **45** and **47** confirms that the kojic acid ring is an acceptable replacement for the quinone present in DAQ B1 and other quinone-containing leads. In order to perform a full SAR study involving this new insulin mimic substructure, a diverse library of compounds would be required. Diversity could be accomplished through varying substitution patterns of the indole or by changing the groups attached to the pyridone nitrogen. One drawback to the use of the aforementioned Stille coupling route is that it is difficult to alter the substitution of the stannylated indole unit. To circumvent this issue, a new route involving the Claisen rearrangement was developed.⁵⁰

1.11 Kojate Library Synthesis by the Claisen Rearrangement

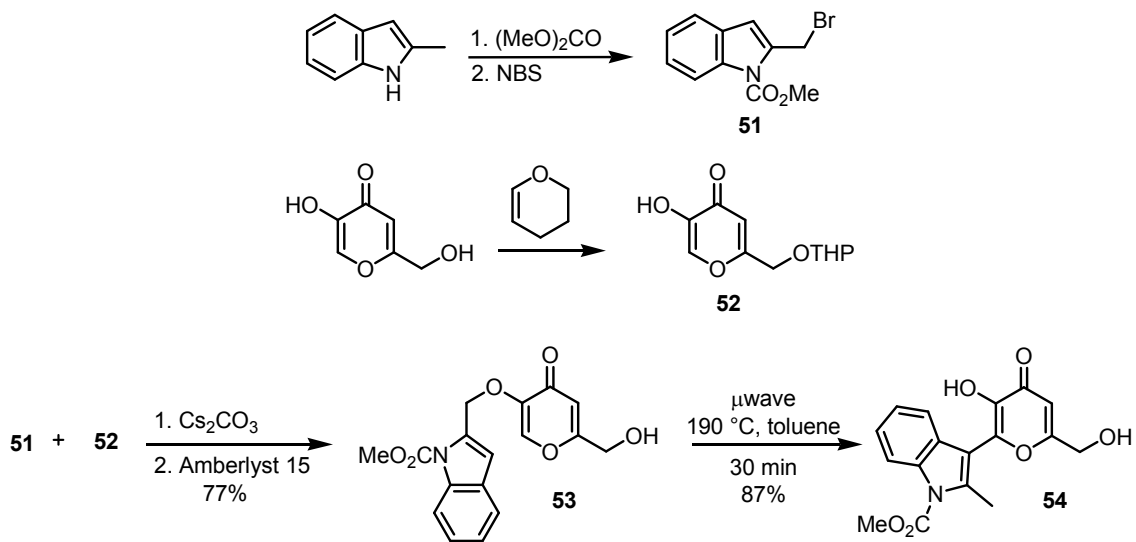
Mechanistically, this novel Claisen rearrangement of an (indole)methyl kojate is assumed to proceed by initial induction of the rearrangement of Claisen substrate **48** by heating to afford intermediate **49**. Restoration of conjugation in the indole and kojic acid rings creates target compound **50** (Scheme 1.7). Attempts to initiate the rearrangement

without protection on the indole nitrogen were unsuccessful. It was hypothesized that the indole kojate ether is solvolized in the absence of indole protection with an electron-withdrawing group, necessitating an additional protection step prior to the Claisen step. It should be noted that the Claisen rearrangement of (indole)methyl kojates installs a methyl group at the 2-position of the indole of **50**, but the methyl scan of DAQ B1 revealed that this methyl substitution enhanced the activity of the small molecule at the IR.⁴⁰



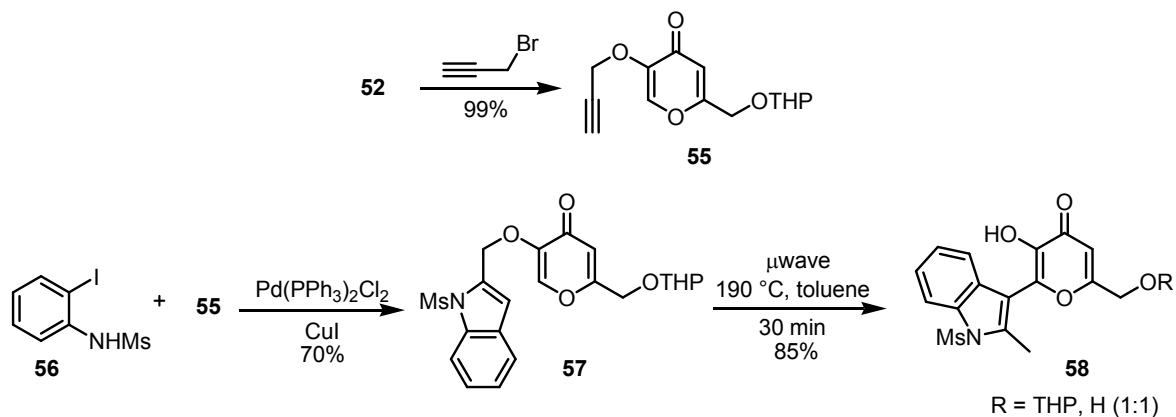
Scheme 1.7 Generic Claisen rearrangement of (indole)methyl kojates.

Synthesis of a precursor suitable for the Claisen rearrangement could be accomplished by coupling 2-bromomethylindole **51**⁵¹ and THP-protected (THP = tetrahydropyran) kojic acid **52**⁵² and removing the THP group by treatment with Amberlyst in high yield over two steps (Scheme 1.8).⁵⁰ Microwave irradiation was utilized to quickly conduct a test reaction of **53** and access target compound **54**. Use of halides like **51** limits the versatility of this approach, so further adjustments were made.



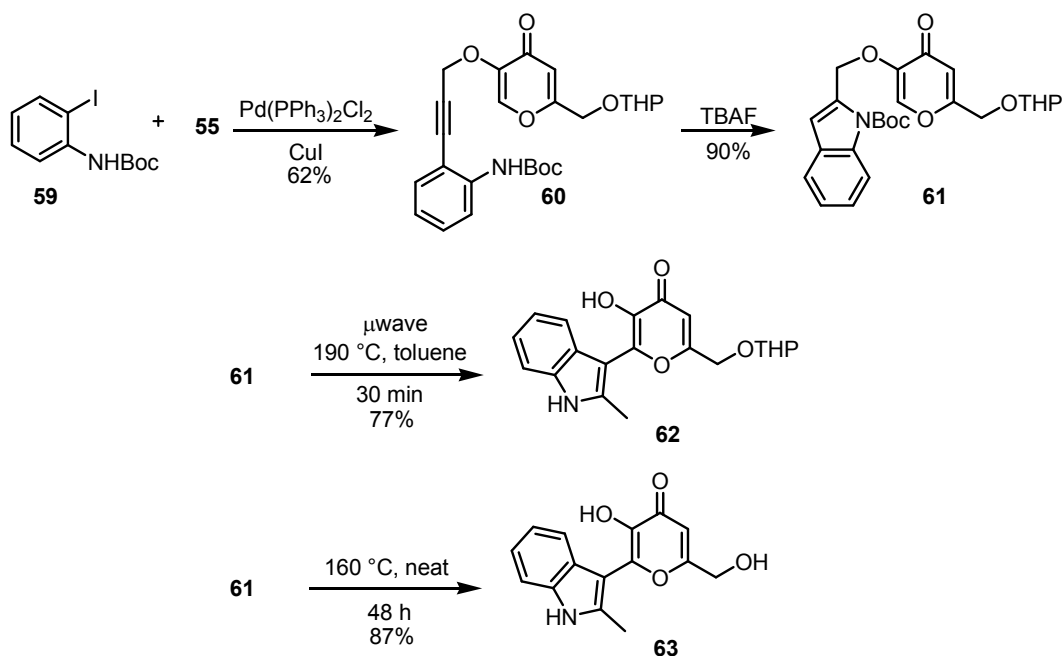
Scheme 1.8 Test reaction for the Claisen protocol.

The use of 2-ethynylanilines to form indoles is a well-known reaction, especially in the realm of natural product synthesis. The requisite 2-ethynylanilines can be accessed through a Sonogashira coupling reaction of a terminal alkyne and *o*-halogenated aniline. Iodoanilines were used to test the methodology due to their high reactivity under Sonogashira conditions. Enol **52** was efficiently converted into propargylated kojate **55** (Scheme 1.9). Sonogashira coupling of **55** and *N*-methylsulfonyl-protected (Ms) **56** and subsequent spontaneous cyclization yielded (indole)methyl indole **57**. The microwave-assisted Claisen rearrangement of THP-protected **57** gave a 1:1 mixture of products **58**, indicating that extended periods of heating could be used to effect the rearrangement and remove the primary alcohol protecting group in one pot. Despite the incomplete removal of the THP group, this test reaction proved the Sonogashira-cyclization-Claisen procedure could be used to conveniently generate potential insulin mimics.



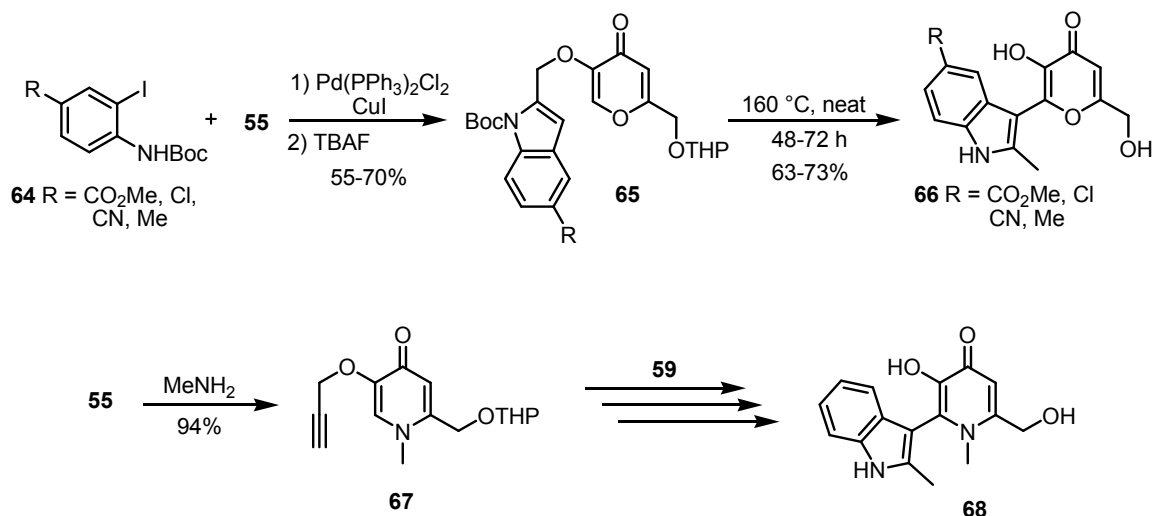
Scheme 1.9 Sonogashira-cyclization-Claisen sequence.

The *N*-methylsulfonyl group was swapped in favor of the easily cleavable Boc protecting group to aid in the production of deprotected target compounds prime for eventual biological testing (Scheme 1.10). Spontaneous cyclization did not occur in the product from coupling **55** and **59**, but treatment of **60** with stoichiometric TBAF⁵³ produced **61** in high yield. Application of microwave irradiation afforded target molecule **62**, with a loss of the Boc group yet retention of the THP moiety. Full deprotection was realized by modifying the mode of irradiation. As previously discussed, subjecting **57** to microwave heating induced a cascade presumed to involve Claisen rearrangement, followed by partial loss of the THP protection (Scheme 1.9). It was surmised that extended heating would allow for the reaction to progress to the point of rearrangement and double deprotection. Indeed, heating **61** neat, in an effort to avoid the use of solvents with high boiling points, at 160 °C for 2 days generated **63** in excellent yield.



Scheme 1.10 Claisen rearrangement protocol using a Boc-protected indole.

Using the conditions developed for the synthesis of **63**, a small library of diverse indolylkojates was created (Scheme 1.11). The Boc derivatives of four different iodoanilines **64** were coupled to propargyl kojate **55** and then treated with fluoride ion to form the indole of **65** in one-pot. Claisen precursor **65** was then heated neat for 2-3 days in order to obtain **66** in decent yields. The pyrone core is an additional site of potential diversification. Methylamine was used to convert pyrone **55** into *N*-methylpyridone **67** in exceptional yield. Using Boc-protected iodoaniline **59** under the developed conditions, indolylpyridone **68** is produced. These results, along with those with **63**, demonstrate the utility of this route: 5 different anilines were used with 2 different kojate derivatives to quickly and efficiently generate 6 different target compounds, though more are possible with this combination of reagents.



Scheme 1.11 Synthesis of an indolykajoate library.

1.12 Other Known Small Molecule Insulin Mimics

Since the discovery of DAQ B1, several other compounds have been reported that have been proven to increase glucose uptake by myocytes and adipocytes *in vitro* and *in vivo* (Figure 1.22). Small molecules including sennidin A⁵⁴ and DDN (5,8-diacetoxy-2,3-dichloro-1,4-naphthoquinone)⁵⁵ have been disclosed that exhibit glucose-lowering effects, but these compounds both contain the offensive quinone substructure. The quinone ring of DAQ B1 can be converted to furoic acid by biotransformation. This fact was exploited by Tsai and Chou in order to develop bisindolyhydroxyfuroic acid D-410639, a potent insulin mimic *in vitro* that is 128-fold less cytotoxic compared to DAQ B1.⁵⁶ Small molecule D-410639 was not specific for IR though, as it was determined to act as an inhibitor of both EGFR and fibroblast growth factor receptor (FGFR). Symmetrical urea TLK19781, discovered from SAR studies of insulin sensitizer TLK16998, was found to induce autophosphorylation of IRTK *in vitro* in the absence and

presence of insulin.⁵⁷ The fact that the insulin mimetic effects of TLK19781 in the absence of insulin were only observed at high concentrations ($\geq 18 \mu\text{M}$) suggests it is more useful as an insulin sensitizer.

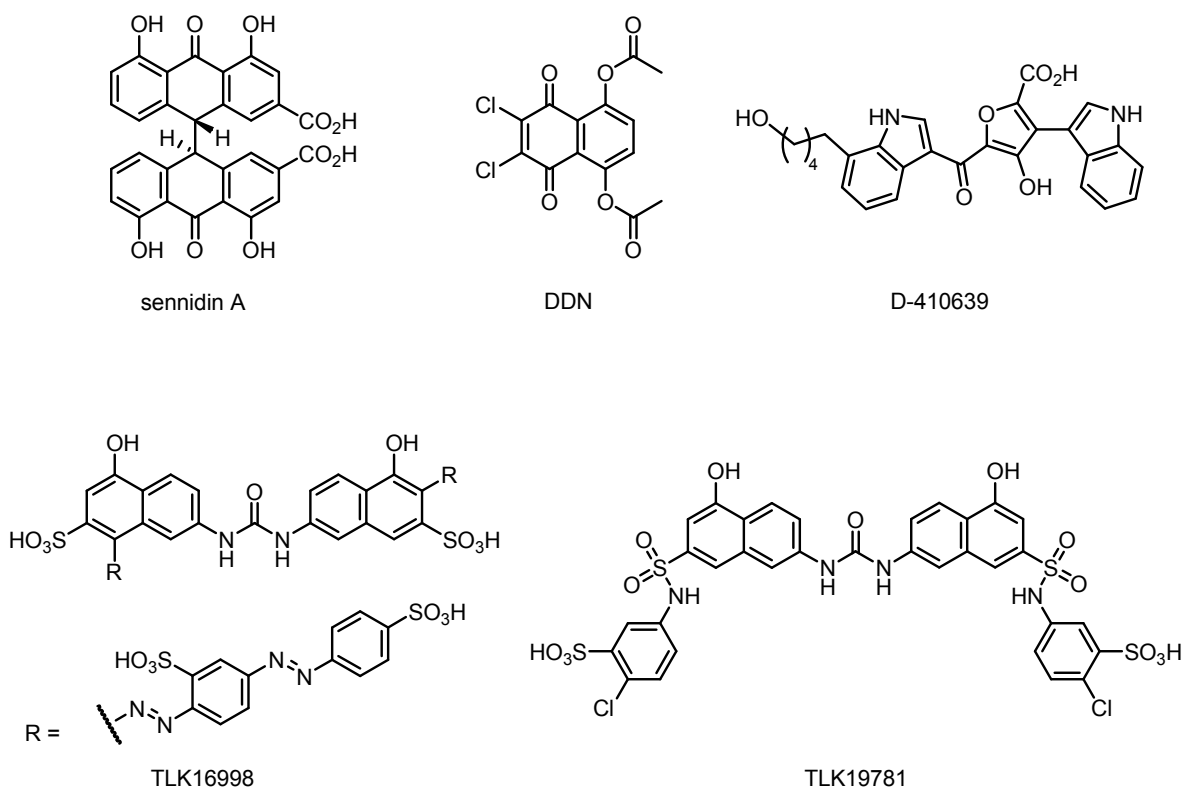


Figure 1.22 Examples of small molecule insulin mimics.

A few natural products have also been reported to exhibit activity at the insulin receptor (Figure 1.23). The insulin mimetic effects of cinnamon extract have been studied recently.⁵⁸ Oral administration of an aqueous solution of cinnamon extract to diabetic rats lowered their blood glucose levels and induced GLUT4 translocation in adipose and muscle tissue. Despite these promising results, insulin is 50-fold more active than

cinnamon extract, with respect to GLUT4 translocation. Triterpenoid ursolic acid is an active insulin sensitizer above 1 $\mu\text{g}/\text{mL}$ in the presence of 1 nM insulin and an insulin mimic at doses above 50 $\mu\text{g}/\text{mL}$, but this promising data is reported only for cell-based assays.⁵⁹ Penta-*O*-galloyl- α -D-glucopyranose (α -PGG), derived from natural product tannic acid, has been identified as a potent IR activator in vitro and in vivo.⁶⁰ Despite an SAR study that revealed additional glycosidic compounds with activity akin to insulin, data indicated that these compounds compete with insulin for binding at the α subunit of the receptor. Recently, a number of disaccharides, including neohesperidose,⁶¹ trehalose, isomaltose, and gentiobiose,⁶² have been reported by Kato to stimulate glucose uptake by muscle cells at as low as subnanomolar concentrations, in the case of neohesperidose.⁶¹ The mode of action of these disaccharides remains a mystery, as this area of research is still in its infancy. Inositols D-pinitol and *myo*-inositol are orally active stimulators of GLUT4 translocation, though biological data for these compounds revealed that they also have the effect of reducing plasma insulin levels.⁶³ Though most of the aforementioned compounds avoid the offensive quinone substructure found in DAQ B1, these synthetic and natural alternatives to our indolykajates lack sufficient evidence to date, such as positive in vivo results from oral administration or minimal off-target activity, that would currently make them superior to our indolykajates as drug leads.

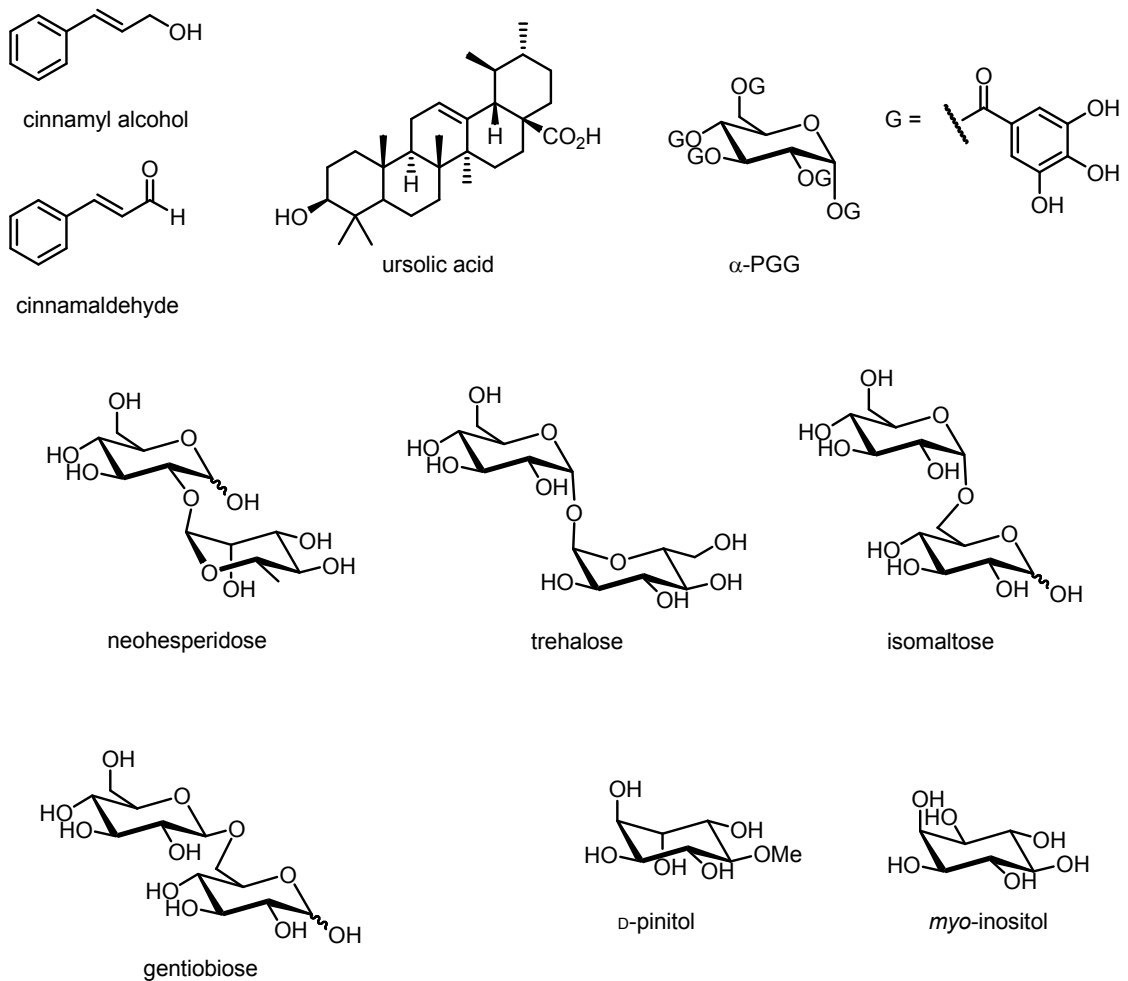


Figure 1.23 Naturally-occurring insulin mimics.

1.13 Conclusion

With the alarming increase in the number of diabetes patients yearly, it is apparent that the development of novel prevention and treatment measures is necessary. Many of these individuals suffer through painful and inconvenient daily insulin injections. Despite the existence of numerous diabetes medications, none of these drugs act on the IR, effectively mimicking the activity of insulin. Natural product DAQ B1 is the first known

orally-active insulin mimic, offering the hope of the development of a pill that could replace insulin injections. Various total syntheses and subsequent SAR studies of DAQ B1 have led to the identification of a few compounds that have comparable or better activity. Though these small molecules, including DAQ B1, “compound 2,” ZL196, and LD-17, have shown promising biological activity, none of these potent insulin mimics have reached clinical trials and testing in humans.

Fears over the safety of quinones have led to the abandonment of research concerning the use of asterriquinones or benzoquinones as insulin mimics. In an effort to maintain the biological activity of DAQ B1 and its analogs, while avoiding the toxicity issues surrounding the use of the quinone structure, the Pirrung group has explored replacements for the offending ring structure.

Kojic acid was determined to be a productive replacement based on the promising biological activity displayed by **45** and **47**. A novel approach to the synthesis of potential pyrone- and pyridone-based insulin mimics was developed in our lab. This approach relies on the Claisen rearrangement as its key step. The demonstrated utility of this approach makes it a promising starting point for the synthesis of a diverse library of potential insulin mimics.

Chapter 2. Synthesis of a Library of Candidate Insulin Mimics

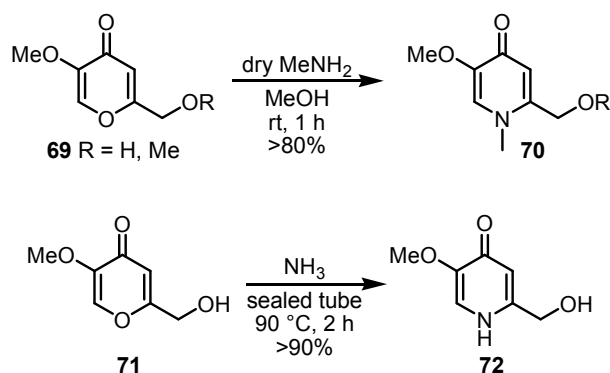
2.1 Introduction

The present work is focused on the extension of our group's early modular synthesis of potential insulin mimics via the Claisen rearrangement.⁵⁰ The overarching goal has been the synthesis of a more varied library of targets, enabling a full SAR study of this novel class of insulin mimics. By combining the data from an SAR study of kojate-based compounds with that from previous SAR studies of DAQ B1 derivatives,^{40,42,43} it will be possible to assemble potent small molecule activators of the insulin receptor. Though high yields were achieved in our previous work using iodoanilines for the synthesis of indolylkojates by the Claisen rearrangement,⁵⁰ their further use in a synthetic scheme seeking diversity would be limited by their commercial availability. In an effort to evade this potential difficulty, various functionalized arenes, including aryl fluorides, bromides, and triflates, have been explored for their ability to couple with a terminal alkyne, with the hope of eventually generating a library with a variety of substituted indoles and pyrone/pyridone cores.

2.2 Pyridone Synthesis

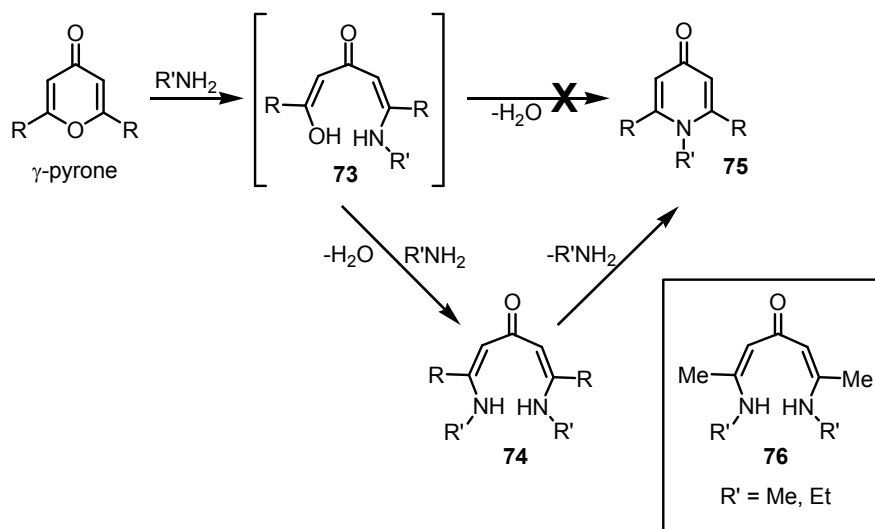
Initial work toward assembling a kojate-based library of potential insulin mimics centered on the utilization of the pyrone to pyridone exchange reaction in an effort to diversify the kojic acid scaffold. In 1931, Armit and Nolan were the first to report the derivatization of kojic acid by treatment with primary amines (e.g., ammonia and methylamine) (Scheme 2.1).⁶⁴ The reactions with methylamine and mono- and dimethyl kojate derivatives **69** were conducted at ambient temperature, but the reaction of

monomethyl kojate **71** and ammonia required more stringent conditions (90 °C in a sealed tube).

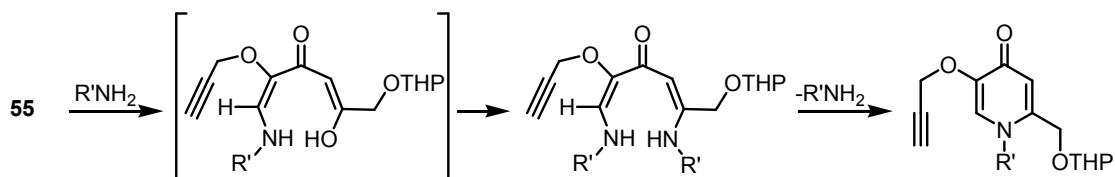


Scheme 2.1 Early report of an exchange reaction using kojic acid.

The generally accepted mechanism for this exchange reaction involves aza-1,4-conjugate addition to a γ -pyrone (Scheme 2.2). Attack of the primary amine results in ring-opening of the pyrone. Jones and coworkers have postulated that intermediate **73** recyclizes with a loss of water to arrive at **75**.⁶⁵ Garratt sought to prove that another intermediate, **74**, lies between **73** and **75**.⁶⁶ Compound **74** would arise from attack of **73** with another molecule of amine. Diamines **76** have been isolated by Garratt in the synthesis of lutidone, lending credibility to her proposed mechanism. From **74**, a final ring-closure can occur with loss of amine to obtain pyridone **75**. The mechanism for the conversion of propargylated kojate **55** to various pyridones would most likely involve initial nucleophilic attack at the less hindered side of the pyrone, closest to the propargyl ether (Scheme 2.3).



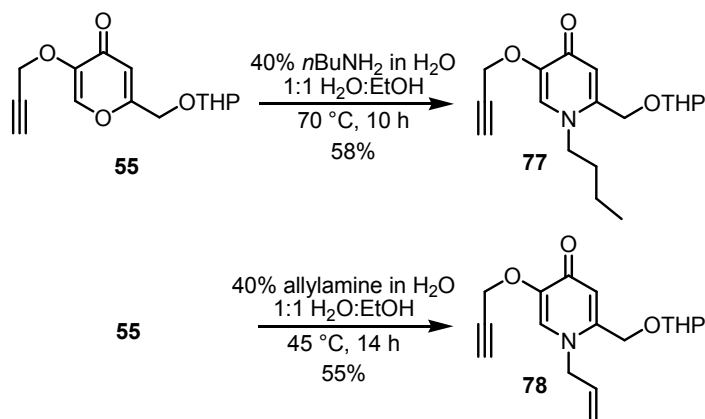
Scheme 2.2 Proposed reaction mechanism for the pyrone to pyridone exchange reaction.



Scheme 2.3 Proposed mechanism for the exchange reaction of pyrone **55**.

In light of our group's early success with the conversion of **55** to *N*-methylpyridone **67**, identical conditions (40% w/w solution of amine in H₂O, 1:1 H₂O:EtOH, 65-70 °C) were applied to the synthesis of novel propargylated pyridones. Heating *n*-butylamine and **55** for 6 h led to only 44% yield of desired pyridone **77** (Scheme 2.4). Extending the heating period (16 h) was actually detrimental to the reaction, as evidenced by the isolated yield of only 30%. We postulated that long reaction times at elevated temperatures would result in evaporation of the amine (bp 77-79 °C)

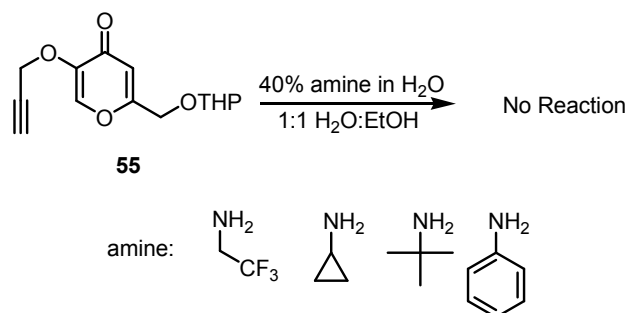
though it is present in excess. Furthermore, decomposition of pyrones with long periods of heating has been reported.^{65b} Though the destruction of starting material could be viewed as advantageous when viewed from the perspective of product isolation and purification, in our case this decomposition combined with loss of amine decreased the yield of **77**. To improve this reaction, the reaction mixture was heated for a short amount of time (4-6 h) then concentrated. The residue was then resubmitted to the reaction conditions again only briefly. Employing this resubmission technique, the yield improved to 58%. The resubmission method was also used for the synthesis of *N*-allylpyridone **78**, though the reaction temperature was lowered to accommodate the boiling point of allylamine (bp 55-58 °C).



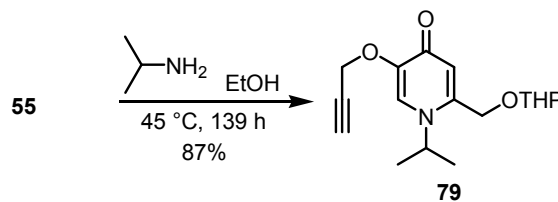
Scheme 2.4 Exchange reaction for the synthesis of *N*-butyl- and *N*-allylpyridones.

Using the solvent combination of H₂O and EtOH, exchange reactions with 2,2,2-trifluoroethylamine, cyclopropylamine, *t*-butylamine, and aniline all failed (Scheme 2.5). Conducting the aniline exchange reaction in pure EtOH also led to no starting material

conversion, while doing the same for a reaction with isopropylamine furnished the desired *N*-isopropylpyridone **79** (Scheme 2.6). Initially the reaction of **55** and isopropylamine (bp 31-35 °C) was conducted at room temperature for almost 2 days, but no reaction occurred. Heating the reaction at 45 °C encouraged product formation, but made the periodic addition of isopropylamine necessary. Instead of concentrating the reaction mixture and resubmitting the residue to the reaction conditions, additional portions of amine were added to the reaction mixture every 4-6 h. This method did allow for the product to be isolated in high yield (87%), but it required 60 equiv of amine (compared to 20 equiv for the resubmission of **77** and **78**) and almost 6 days of reaction time.



Scheme 2.5 Failed exchange reactions.

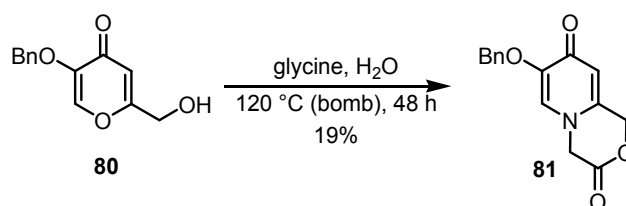


Scheme 2.6 *N*-isopropylpyridone synthesis in EtOH.

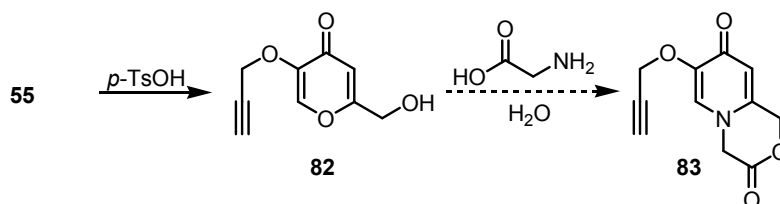
The lack of success encountered in the reaction involving aniline and trifluoroethylamine can be explained by the fact that the electron-withdrawing groups on the nitrogen make these amines poor nucleophiles. Sterics could be used to explain the failure of the reactions involving *t*-butylamine and cyclopropylamine, though steric effects seem to be an implausible explanation in light of the successful synthesis of **79**. A cyclopropyl group would be more compact spatially than isopropyl, making it more likely that both isopropylamine and cyclopropylamine would not yield products if sterics were truly to blame for an absence of reactivity. Presumably, this difference in reactivity can be attributed to solvent effects, as the isopropylamine reaction was conducted in EtOH, whereas the cyclopropylamine reaction was in a mixture of water and EtOH. The exchange reaction of cyclopropylamine and various substituted γ -pyrones has been recently reported in THF,⁶⁷ MeOH,⁶⁸ and water,⁶⁹ so it is possible that a solvent screen would have been beneficial to the reaction of **55** and cyclopropylamine.

A bicyclic pyridone was also the target of synthetic efforts. Teitei reported the treatment of benzyl-protected kojate **80** with glycine to yield fused heterocycle **81** (Scheme 2.7).⁷⁰ This exchange reaction-condensation cascade was facilitated by heating the aqueous reaction mixture at 120 °C in a bomb for 2 days but only afforded the desired product in low yield (19%). In order to apply these conditions to the direct synthesis of **83**, pyrone **55** was treated with *para*-toluenesulfonic acid (*p*-TsOH) to remove the THP group, yielding **82** (Scheme 2.8). In the absence of a bomb reactor, the reaction was simply heated under N₂. Unfortunately, decomposition was observed by heating at 120 °C for 48 h and at only 80 °C for 24 h. Using **80**, the literature procedure was replicated

(Scheme 2.7), employing a resealable pressure tube instead of Teitei's reported bomb. With 3 days of heating at 125 °C, there was no conversion to **81**. Increasing the reaction time to 4 days, a white solid was isolated whose physical data did not match that of the literature (mp 117-120 °C vs. lit. mp 171-173 °C).



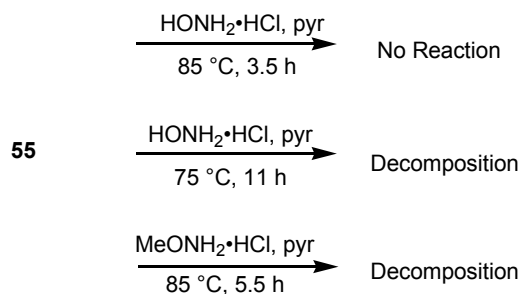
Scheme 2.7 Teitei's reported pyrone to pyridone exchange reaction and condensation cascade.



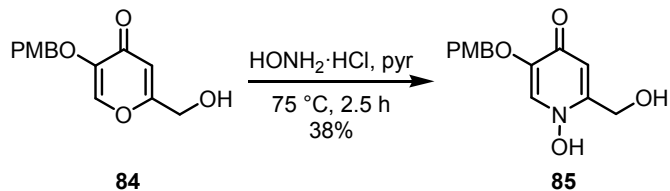
Scheme 2.8 Exchange reaction/condensation attempt with **55**.

Finally, hydroxylamine and methoxylamine were examined in the synthesis of pyridones from **55** (Scheme 2.9). Due to the amines being supplied as hydrochlorides, the reactions were run in pyridine. No conversion of **55** was observed following the reaction in the presence of hydroxylamine hydrochloride at 85 °C for 3.5 h. Extending the reaction time, while slightly lowering the temperature, led to signs of decomposition. The same was true for the reaction of methoxylamine hydrochloride and **55** at 85 °C for 5.5 h. Tsuruoka and coworkers reported an analogous exchange reaction of hydroxylamine with

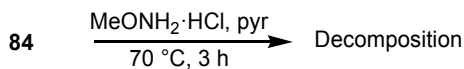
PMB-protected kojate **84**,⁷¹ and this literature protocol was replicated to obtain **85** (Scheme 2.10). With the successful replication of the literature, a similar reaction was attempted with methoxylamine but to no avail (Scheme 2.11).



Scheme 2.9 Failed exchange reactions with hydroxyl- and methoxylamine.



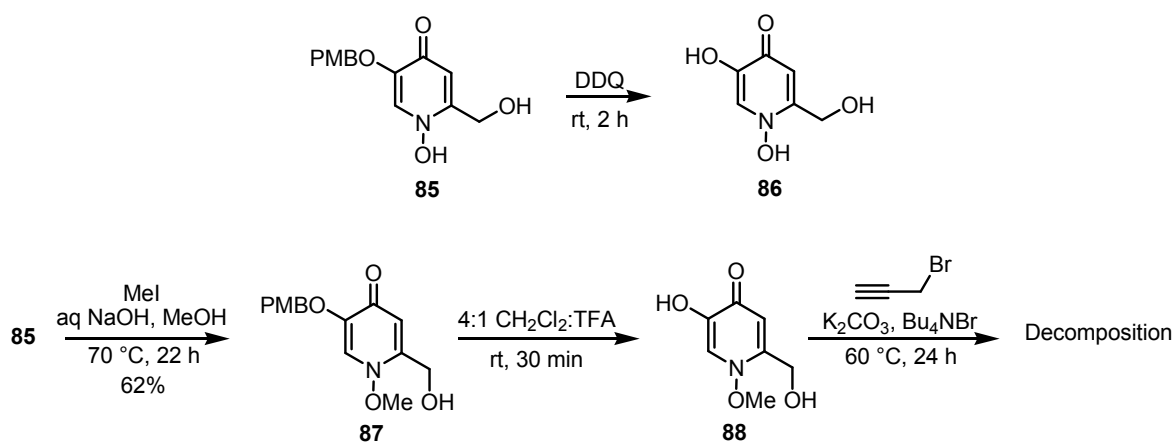
Scheme 2.10 Tsuruoka's reported *N*-hydroxypyridone synthesis.



Scheme 2.11 Failed application of the Tsuruoka synthesis.

With **85** in hand, it was possible to attempt conversion of this PMB-protected pyridone into the needed propargylated derivative. To do this, removal of the PMB group was necessary, but deprotection trials afforded a highly polar product **86** that was difficult

to manipulate (Scheme 2.12). Due to this difficulty, further work with *N*-hydroxypyridones was abandoned so that efforts could be focused on the synthesis of an *N*-methoxypyridone that would be more easily handled. To do so, the *N*-hydroxy group of **85** was selectively methylated, then the PMB group was removed from **87** upon treatment with trifluoroacetic acid (TFA) to obtain **88**. This crude product was too polar for column purification, so the crude material was directly subjected to the propargylation conditions previously developed in the Pirrung group.⁵⁰ Unfortunately, the product from this reaction lacked a methoxy peak in the ¹H NMR spectrum, indicating decomposition.



Scheme 2.12 Manipulations of *N*-hydroxypyridone **85**.

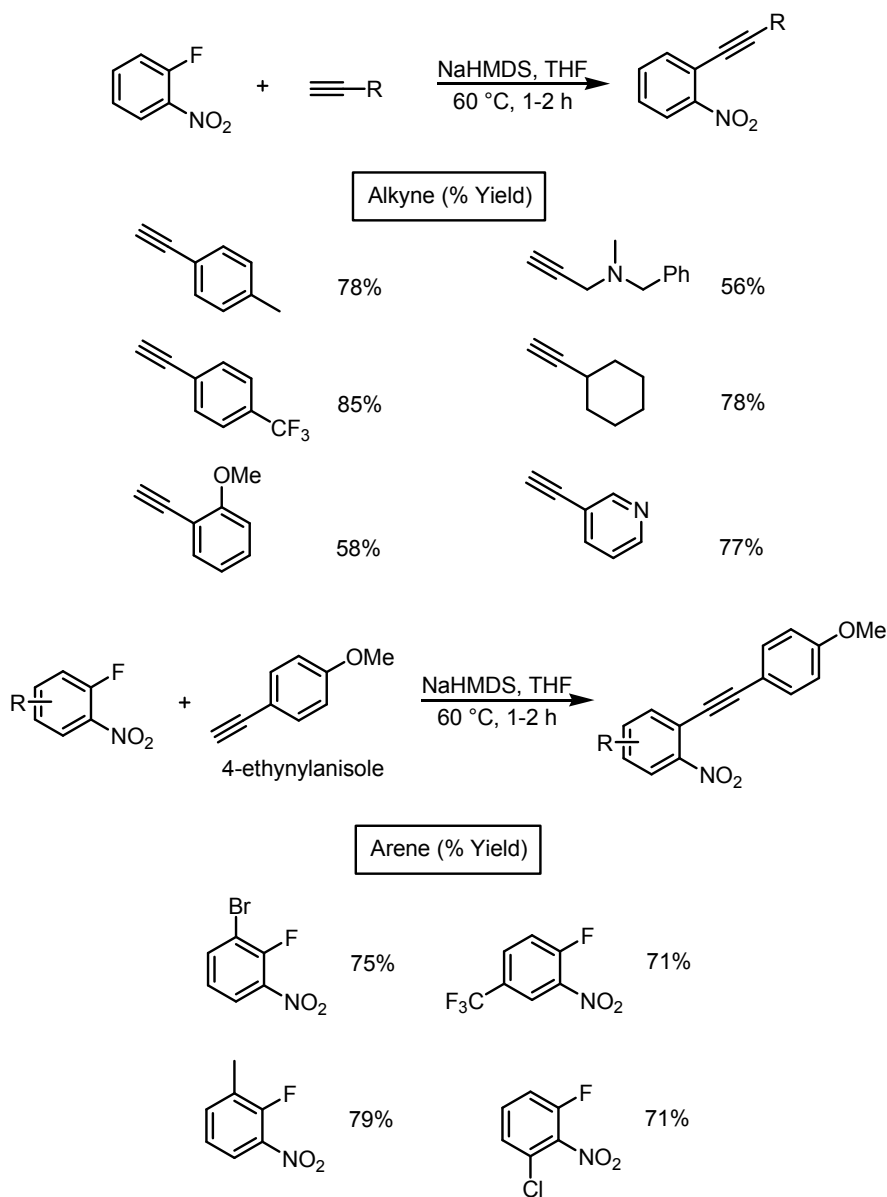
The successful preparation of novel pyridones **77**, **78**, and **79**, along with known compounds **55** and **67** enabled the assembly of a satisfactory collection of kojate-based building blocks. At this point, attention was shifted to the development of an efficient procedure for coupling the terminal alkyne moiety of these kojic acid derivatives to a functionalized arene.

2.3 Coupling of *o*-Halonitrobenzene and Alkyne

The low commercial availability of aryl iodides required the development of aryl fluoride and bromide building blocks as productive coupling partners with propargylated kojates (**55**, **67**, **77**, **78**, and **79**). To do so, *o*-fluoro- and *o*-bromonitrobenzenes were investigated. It was envisioned that using an electron-withdrawing nitro group as an amine precursor would allow for an efficient coupling reaction, enabling the use of these less reactive aryl halides. Making use of nitroarenes in our synthetic scheme requires an additional reduction step, but a number of mild reductants (e.g. SnCl₂,⁷² In-HI,⁷³ Fe/NH₄Cl,⁷⁴ Fe/HCl, and FeSO₄/Zn⁷⁵) are known that have been reported to accomplish the transformation of a nitro moiety to amino in the presence of other reducible functional groups.

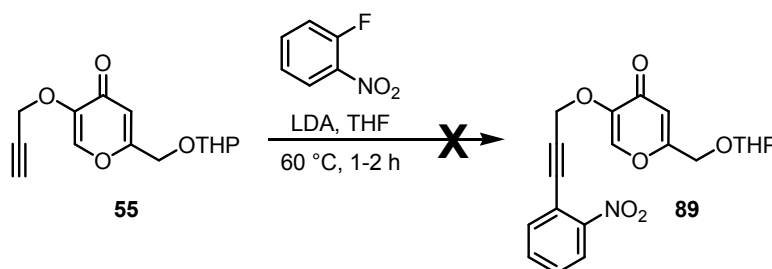
Yoakim reported the facile nucleophilic aromatic substitution (S_NAr) reaction between a terminal alkyne and *o*-fluoronitrobenzene.⁷⁶ Unlike the classical transition metal-mediated Sonogashira cross-coupling, this novel reaction only required sodium hexamethyldisilazide (NaHMDS) as base, making it an attractive option for application to our kojate building blocks. Yoakim reported moderate to excellent yields by adding base to a THF solution of alkyne and aryl fluoride and stirring the solution at 60 °C for only 1-2 h typically. Select examples of the wide scope of this reaction are depicted in Scheme 2.13. Various alkyl and aromatic (electron-poor and electron-rich) substituted alkynes worked well with *o*-fluoronitrobenzene. Additionally, reactions of 4-ethynylanisole and aryl fluorides with electron-withdrawing and electron-donating substituents present were

successful, even when sterically hindered aryl fluorides (with moieties ortho to the fluorine) were used.



Scheme 2.13 Select examples of Yoakim's S_NAr protocol.

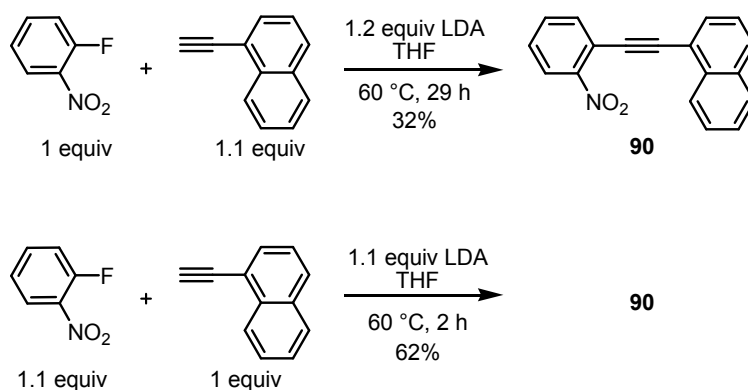
Instead of NaHMDS, lithium diisopropylamide (LDA) was employed in our work. LDA is a stronger base than NaHMDS, as evidenced by their pK_a values (36 vs. 26, respectively). Early efforts toward exploiting this base-mediated strategy in order to synthesize **89** were unfruitful, resulting in the recovery of **55** (Scheme 2.14). It is reasonable to assume that changing the base would require optimization of the reaction conditions. To avoid the loss of large amounts of precious material through numerous trial reactions, 1-ethynynaphthalene and *o*-fluoronitrobenzene were used as a model system to improve the reaction conditions in the presence of LDA (Scheme 2.15).



Scheme 2.14 Failed S_NAr between **55** and *o*-fluoronitrobenzene.

Following Yoakim's procedure (1 equiv aryl fluoride, 1.1 equiv alkyne, 1.5 equiv base, 60 °C, 1-2 h), none of **90** was detected in the reaction mixture. The reaction time was increased and the reaction progress was monitored by gas chromatography (GC). After 29 h at 60 °C, the desired product was isolated, but in only 32% yield (Scheme 2.15). In a separate trial reaction, additional aryl fluoride was accidentally added to the reaction mixture, making the alkyne the limiting reagent, but this mishap proved advantageous, as the alkyne was fully consumed in only 2 h. The modified S_NAr

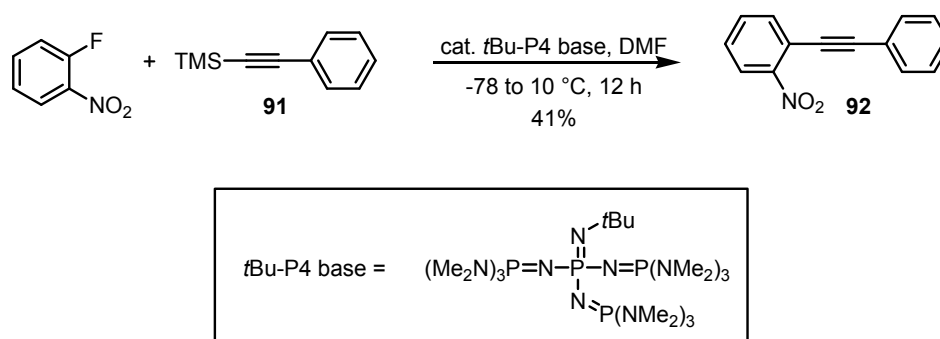
conditions (1.1 equiv aryl fluoride, 1 equiv alkyne, 1.1 equiv base, 60 °C, 1-2 h) afforded **90** in a moderate yield (62%) that was comparable to Yoakim's yields with ortho-substituted alkynes. Unfortunately, when these optimized conditions were applied to the reaction of **55** and *o*-fluoronitrobenzene, no reaction occurred.



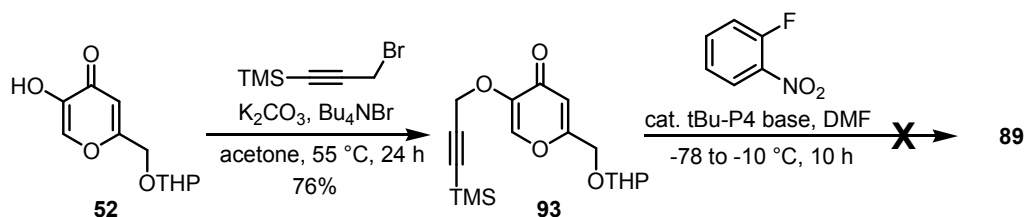
Scheme 2.15 Optimization of model system for S_NAr reaction.

Another example of a transition metal-free S_NAr ⁷⁷ was examined for the synthesis of **89**. The report detailed the use of catalytic phosphazene base, *t*Bu-P4, as a desilylating agent. This strong organic base (pK_{BH^+} of 42.1 in CH_3CN) activates silylated nucleophiles to reveal an anion that can participate in a nucleophilic substitution reaction in the presence of an electrophile, such as an aryl fluoride. To test this methodology in the presence of a *C*-silylated nucleophile, the acetylide of phenylacetylene was protected with a trimethylsilyl (TMS) moiety to obtain **91** (Scheme 2.16). When a mixture of **91** and *o*-fluoronitrobenzene in DMF was treated with *t*Bu-P4, S_NAr product **92** was generated in 41% yield, along with unreacted starting material. Though this literature

procedure bears further investigation to improve the yield, these preliminary results prove the synthetic utility of phosphazene base catalysts in cross-coupling reactions. Synthesis of the requisite TMS-protected propargyl kojate **93** was accomplished by the reaction of TMS-protected propargyl bromide and **52** (Scheme 2.17). Treatment of **93** and *o*-fluoronitrobenzene with *t*Bu-P4 indeed resulted in desilylation but no subsequent coupling occurred.



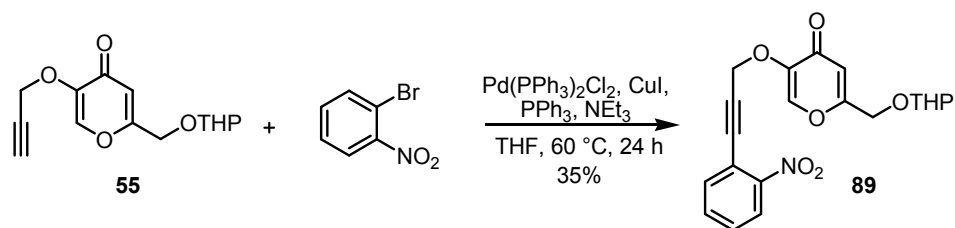
Scheme 2.16 $\text{S}_{\text{N}}\text{Ar}$ reaction catalyzed by phosphazene base.



Scheme 2.17 Failed phosphazene base-catalyzed cross coupling.

With the lack of success encountered in the production of **89** using aryl fluorides in transition metal-free reactions, Sonogashira couplings with aryl bromides became the subject of investigation. The low reactivity of aryl bromides compared to aryl iodides in

the Sonogashira reaction necessitates harsh reaction conditions (i.e. high temperatures) for the former.⁷⁸ To avoid Glaser homocoupling, oxygen-free conditions were achieved by evacuating and backfilling the reaction vessel with N₂ three times prior to the addition of alkyne and base to the reaction mixture.⁷⁹ Homocoupling is a consequence of the use of copper catalysts, as oxidation of the copper acetylide intermediate generates the alkyne dimer. Triphenylphosphine (PPh₃, 0.2 eq) was also included in the reaction mixture in order to improve the stability of the palladium (II) catalyst used [Pd(PPh₃)₂Cl₂] and ensure high yields in spite of the use of aryl bromides. Although extensive care was taken with the reaction, the isolated yield of product **89** was only 35% (Scheme 2.18). Sonogashira has reported that an extra two equivalents of PPh₃ are necessary for the reaction of aryl bromides at elevated temperatures.⁸⁰ The additional ligand serves the purpose of preventing decomposition of the active metal species, Pd(0), thereby improving the reaction efficiency. Unfortunately, when 2.2 equiv of PPh₃ were present in the reaction of **55** and *o*-bromonitrobenzene, only unreacted starting materials were isolated. Total exclusion of supplemental ligand led to decomposition of **55**.



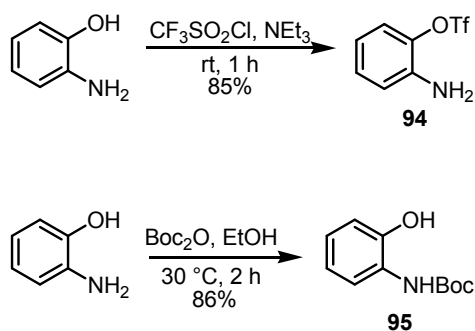
Scheme 2.18 Attempted Sonogashira cross-coupling reactions of *o*-bromonitrobenzene and **55**.

Despite numerous adjustments to the reaction (e.g. extended reaction time, increase/decrease of the equiv of alkyne and catalyst present, solvent change to toluene), the yield of this novel product never exceeded 35%. Questions were raised as to whether the isolated product was indeed the desired Sonogashira product. Spectroscopically, the ^1H NMR spectrum contained all of the expected peaks, but the ^{13}C NMR lacked one carbon signal, though this observation could be attributed to symmetry. Using infrared (IR) spectroscopy, nitroarenes can be characterized by two strong absorptions at around 1550 and 1365 cm^{-1} (N-O stretching vibrations), yet the IR spectrum for the isolated product lacked bands with strong absorptions in this region. In light of the low yields of debatable product formed in this reaction, research interests were diverted to the exploration of 2-aminoaryl triflates as coupling partners for the terminal alkyne of **55**.

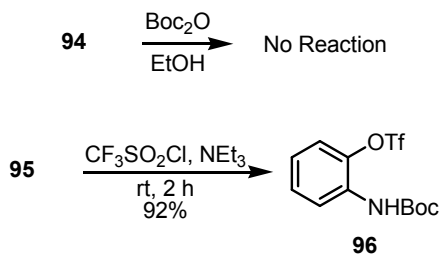
2.4 Coupling of 2-Aminoaryl Triflate and Alkyne

Though less reactive than aryl iodides, aryl triflates are more reactive than aryl bromides,⁸¹ allowing the use of 2-aminoaryl triflates, instead of the corresponding 2-nitroaryl triflates, under Sonogashira coupling conditions. Aryl triflates are easily prepared from phenols, which have wide commercial availability and are inexpensive. Synthesis of the required 2-aminoaryl triflate **96** began by following a known procedure to obtain **94** from 2-aminophenol and trifluoromethanesulfonyl chloride (Scheme 2.19).⁸² Subsequent treatment of **94** with di-*tert*-butyl dicarbonate (Boc anhydride or Boc_2O) in order to protect the free nitrogen with an electron-withdrawing group was futile (Scheme 2.20). The synthesis of Boc-protected 2-aminophenol **95** is also known, by treatment of 2-aminophenol with Boc_2O in EtOH (Scheme 2.19).⁸³ Employing

trifluoromethanesulfonyl chloride, **95** was efficiently converted to **96** in high yield with no need for purification (Scheme 2.20). The use of triflic anhydride as triflating agent did not generate any of the desired product from **96**, a result that is in accord with the reported low yields when 2-aminophenol was treated with triflic anhydride.⁸²



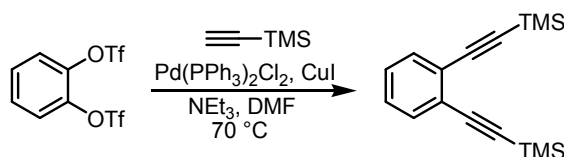
Scheme 2.19 Literature transformations of 2-aminophenol.



Scheme 2.20 Synthesis of aryl triflate **96**.

Rychnovsky demonstrated that the presence of tetrabutylammonium iodide (*n*Bu₄NI or TBAI) in excess accelerated the Sonogashira coupling reactions of terminal alkynes and aryl triflates (Scheme 2.21).⁸⁴ The degree of rate acceleration was directly related to the number of iodide equivalents used; with 300 mol% *n*Bu₄NI, the yield was

91% after only 3 h, while with 30 mol% the yield was only 59% after 19 h. Decent yields were obtained in the absence of additive, but the reaction required almost two days of heating to do so. Quaternary ammonium salts are commonly used as phase-transfer catalysts, but it is more likely that the added iodide ion activates the Pd(0) catalyst, since the reaction rate depends on the amount of *n*Bu₄NI present. Rychnovsky postulated that the addition of iodide does not lead to an aryl iodide intermediate, but instead stabilizes the active catalyst, enabling a facile oxidative addition to the triflate-arene bond.

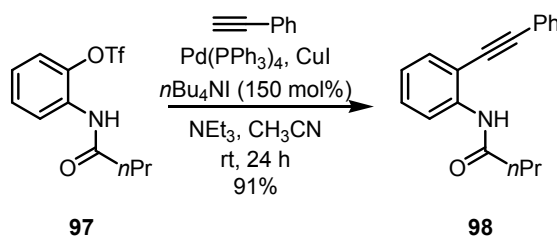


mol% <i>n</i> Bu ₄ NI	Time	% Yield
0 mol%	44 h	71%
30 mol%	19 h	59%
100 mol%	5 h	83%
300 mol%	3 h	91%

Scheme 2.21 Rate acceleration of the alkylation of catechol ditriflate by the addition of *n*Bu₄NI.

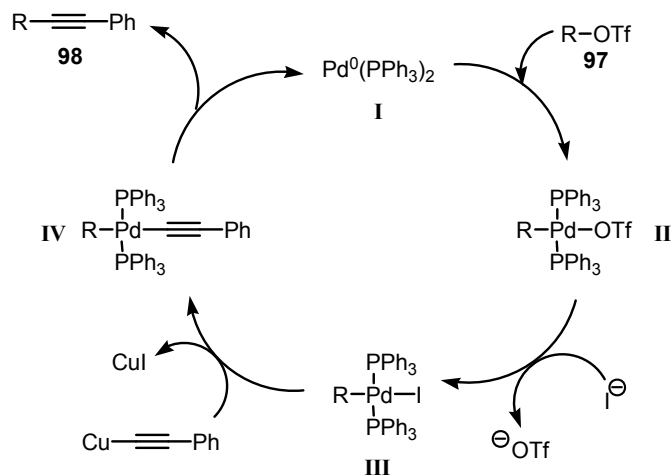
The literature on Pd-catalyzed alkylation of 2-aminoaryl triflates is sparse, with all of the work emerging from the Dai lab in their quest for biologically active indole-based small molecules.⁸⁵ Dai's results for the cross-coupling of phenylacetylene and aryl triflate **97**, which has an amide ortho to the triflate moiety (Scheme 2.22),^{85a} were similar to those previously reported by Rychnovsky.⁸⁴ Reactions with *n*Bu₄NBr as additive or with no additive were both inferior to the addition of excess *n*Bu₄NI. Various sources of palladium were tested, including Pd(PPh₃)₄, Pd(PPh₃)₂Cl₂, Pd(PhCN)₂Cl₂, and Pd(OAc)₂, and it was determined that the PPh₃ ligands are necessary for reaction success,

with Pd(PPh₃)₄ giving the highest yields in the shortest amount of time. The optimized conditions were also applied to various aryl triflates with comparable success, though electron rich arenes required refluxing conditions.⁸⁵



Scheme 2.22 Sonogashira coupling of 2-amidoaryl triflate **97** and phenylacetylene.

Dai rejected Rychnovsky's assumption that the iodide ion was needed for activation of Pd(0) prior to the oxidative addition step. Instead, Dai emphasized the fact that the coupling reaction does occur initially in the absence of *n*Bu₄NI, indicating that the iodide may aid in the subsequent transmetalation or reductive elimination. Dai hypothesized that, in the absence of additive, the palladium catalyst is poisoned by triflate ion as the reaction proceeds. This poisoning is alleviated by the addition of iodide ion, which acts by displacing the triflate ligand on the Pd(II) intermediate **II** (Scheme 2.23). Transmetalation of intermediate **III**, followed by reductive elimination of **IV** generates the cross-coupled product **98**.

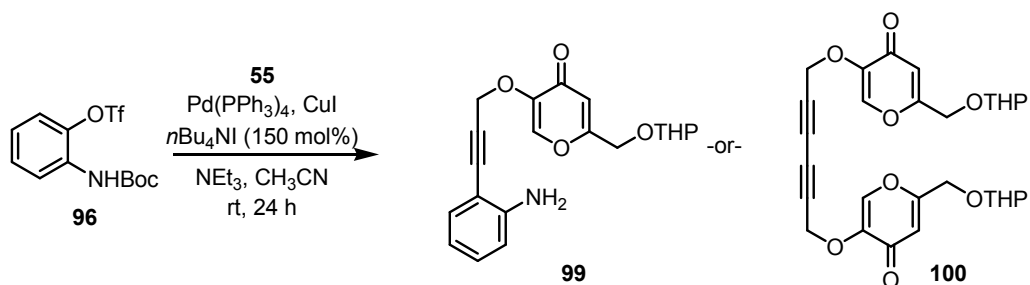


Scheme 2.23 Dai's proposed palladium cycle.

With Dai's promising report of successful alkynylations with the structurally similar 2-amidoaryl triflate **97** in mind, the alkynylation of **96** was attempted. After a day at room temperature, the crude reaction mixture was mostly unreacted starting materials along with another compound present in small quantity. Surprisingly, isolation of this product revealed it to be identical to the questionable product previously isolated from the Sonogashira reaction of **55** and *o*-bromonitrobenzene (Scheme 2.18).

One possible explanation for the fact that two different reactions gave the same product would be that both reactions lead to aniline **99** (Scheme 2.24). For the nitroarene, this could arise from cross-coupling, followed by in situ reduction of the nitro moiety, whereas for the aryl triflates, this transformation would involve coupling and Boc removal. The absence of N-H stretches in the IR spectrum for this compound disproved this theory, though. The only other explanation for these convergent coupling reactions is Glaser homocoupling of **55** generating **100**, despite attempts to maintain oxygen-free

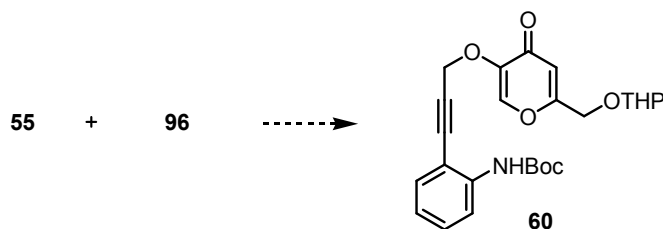
conditions. Homocoupling was disregarded initially, due to the presence of aromatic protons in the ^1H NMR of this product. These misleading peaks are most likely due to some impurity that co-spots with **100** by TLC (thin-layer chromatography), since the IR data lacks any indication of an aromatic amine or nitro group being present.



Scheme 2.24 Sonogashira coupling of **55** and **96** in the presence of $n\text{Bu}_4\text{NI}$.

Though the iodide-mediated Sonogashira reaction of **55** and **96** yielded a small amount of homocoupled product **100**, the majority of the product mixture was unreacted starting material, suggesting no reaction overall under these conditions. Classical Sonogashira conditions were applied to the alkylation of **96**, but none of these attempts were fruitful (Table 2.1). To begin, $\text{Pd}(0)$ was employed due to Dai's reported success with this catalyst, but under these conditions (entry 1) decomposition of **55** resulted. Changing the base to diisopropylethylamine (DIPEA) and heating the reaction for a short amount of time (entry 2), yielded mainly the undesired product of homocoupling (**100**) and unreacted starting materials. The same was true of the reaction in the presence of $\text{Pd}(\text{II})$ at ambient temperature (entry 3).

Table 2.1 Unsuccessful Sonogashira coupling of **55** and **96**.



Entry	Reactants	Solvent	Temp (°C)	Time (h)	Result
1	Pd(0), CuI, Et ₃ N	DMF	25	23	Decomposition
2	Pd(0), CuI, DIPEA	DMF	55	2	100
3	Pd(II), CuI, DIPEA	THF	25	24	100

2.5 Synthesis of *tert*-Butyl 2-(Benzyloxy)-6-iodophenylcarbamate

Given that aryl triflates were found to be unreactive in cross-coupling reactions with pyrone **55**, iodoanilines became the coupling partner of choice, due to prior success with these substrates in our lab.⁵⁰ As previously discussed in chapter 1 (section 1.8), LD-17 (Figure 1.18) has been identified as a potent activator of human IR.⁴³ It stands to reason that, just as **45** and **47** (Scheme 1.6) had similar activity compared to the quinone-containing analog ZL196 (Figure 1.18),⁴⁵ pyrone and pyridone analogs of 7-benzyloxyindolyl-benzoquinone LD-17 will likewise be active small molecule insulin mimics.

To test this theory, iodobenzene **101** was targeted (Figure 2.1). Treatment of 2-amino-3-iodophenol with Boc₂O in EtOH⁸³ or CH₂Cl₂⁸⁶ surprisingly yielded the *O*-Boc protected product **102**, instead of the expected *N*-Boc product (Scheme 2.25). The structural assignment of the unanticipated product was confirmed by treating **102** with

benzyl bromide (BnBr), potassium hydride (KH) and *n*Bu₄NI. Interestingly, under these conditions, the *O*-Boc group was exchanged for the *O*-benzyl group and **103** was isolated in 60% yield. All subsequent attempts to introduce an *N*-Boc group into **103** were unsuccessful.

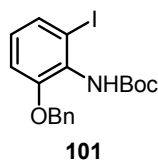
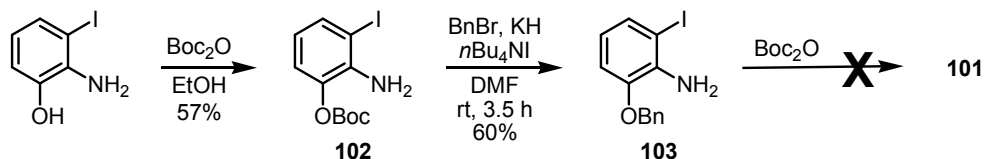


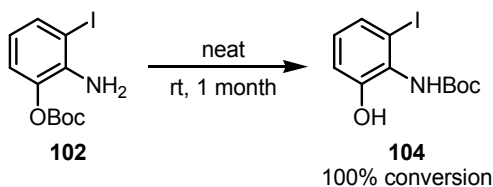
Figure 2.1 *tert*-Butyl 2-(Benzyloxy)-6-iodophenylcarbamate **101**.



Scheme 2.25 Unexpected *O*-Boc product formation.

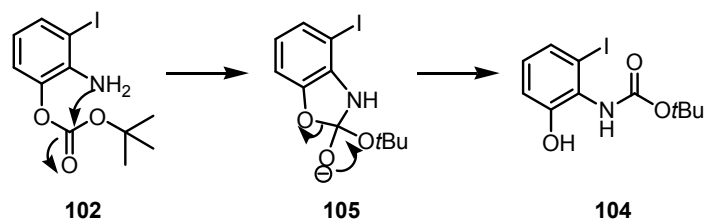
Though numerous groups have found success selectively Boc-protecting the amine of 2-aminophenol under mild conditions,^{83,86,87} the presence of ortho-substituents flanking the amine on both sides proved to be problematic for our specific substrate, 2-amino-3-iodophenol. Steric hindrance inhibits reaction of Boc₂O with the amine, so the reaction takes place at the less nucleophilic site, the alcohol. This steric hindrance is only exacerbated in **103** with the addition of the benzyl moiety, which accounts for the absence of reactivity of this intermediate in the presence of Boc₂O (Scheme 2.25).

Treatment of 2-amino-3-iodophenol with Boc₂O in EtOH at room temperature for only 5.5 h generated **102** in 57% yield (Scheme 2.25). This *O*-substituted arene was initially a red-orange oil, but, after being stored on the bench for 1 week at ambient temperature, it began to appear biphasic, indicating decomposition or transformation of some sort on the molecular level. After one month at room temperature, ¹H NMR revealed the presence of only the *N*-Boc protected product **104**, confirming that **102** rearranges over time, shuttling the protecting group from the oxygen to the more nucleophilic, yet hindered nitrogen of the amine (Scheme 2.26).

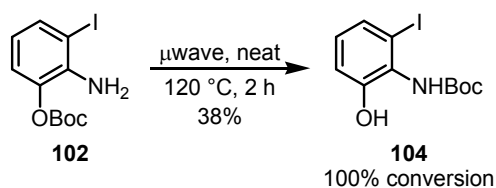


Scheme 2.26 Room temperature rearrangement of **102**.

This unprecedented aromatic *O*→*N* *tert*-butoxycarbonyl transfer is analogous to a transacylation recently reported by our lab.⁸⁸ The mechanism for the conversion of **102** to **104** presumably involves formation of benzoxazole intermediate **105**, which then ring-opens to yield the desired product with the Boc group on the amine (Scheme 2.27). Reactions that require a reaction time of one month are hardly practical, so microwave irradiation was employed to quickly convert **102** to **104**. Neat irradiation of **102** (sealed reaction vessel, 120 °C, 2 h) caused total conversion of starting material and an isolated yield of 38% for **104** (Scheme 2.28).



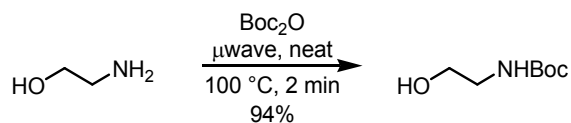
Scheme 2.27 Proposed mechanism for $O \rightarrow N$ Boc transfer.



Scheme 2.28 Microwave-assisted rearrangement of **102**.

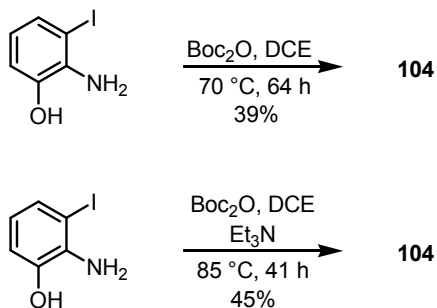
Facile methods for the direct formation of **104** from 2-amino-3-iodophenol were sought. Encouraged by the success of the Boc-transfer reaction under microwave heating conditions (Scheme 2.28), a similar reaction was examined, gaining guidance from a recent paper detailing selective *N*-Boc protection mediated by microwave irradiation.⁸⁹ Though the report only gave one example of a substrate with both an amine and an alcohol present, we felt it was a good model since that substrate was ethanolamine, a compound we have used in the past to demonstrate the aforementioned transesterification-transacylation cascade.⁸⁸ Microwave heating of a neat mixture of ethanolamine and Boc_2O generated the *N*-Boc protected product in 94% yield after only 2 min (Scheme 2.29).⁸⁹ Subjecting 2-amino-3-iodophenol to microwave irradiation at 100 °C for 7 min, afforded a mixture of starting material, **102**, and **104**. The authors also

reported the use of methanol giving identical yields compared to the neat reactions, with the same reaction times.⁸⁹ A solution of 2-amino-3-iodophenol and Boc₂O in MeOH at 100 °C required 75 min of microwave heating to achieve full conversion from starting material. The resulting product mixture exhibited a low crude mass and was comprised of **104** and a product from decomposition of the starting material.



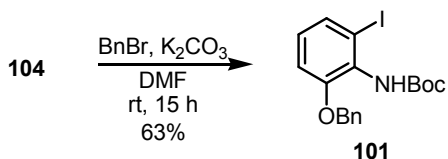
Scheme 2.29 Literature example of the selective, solvent-free *N*-Boc protection of ethanolamine.

Conventional heating was also utilized in the pursuit of a facile method for selectively synthesizing **104**. Heating a solution of 2-amino-3-iodophenol and Boc₂O at 70 °C for 16 h, there was only a 40% conversion to desired product observed by ¹H NMR. Increasing the reaction time to 48-64 h, the conversion improved, typically with little to no *O*-Boc product **102** present (Scheme 2.30). Despite the high conversion and selectivity, the yields were consistently low (~40%), prompting an examination of base additives. Including DIPEA in the reaction mixture (85 °C, 48 h), the resulting product was solely **102**, with none of the desired product present. The results were better in the presence of triethylamine. After about 40 h at 85 °C, **104** was isolated in 45% yield.



Scheme 2.30 Syntheses of **104** using conventional heating.

Though the routes to **104** were only moderately yielding, this product was carried forward in the synthetic scheme. Treatment of phenol **104** with benzyl bromide cleanly produced aryl iodide **101** (63% yield; Scheme 2.31). With **101** in hand, attention could be focused on the cross-coupling of iodide **101** and the alkyne of **55**, **67**, **77**, **78**, and **79**.

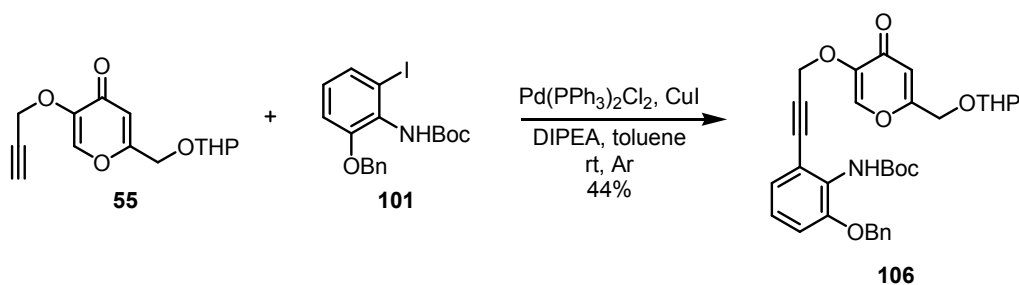


Scheme 2.31 Synthesis of Sonogashira substrate **101**.

2.6 Synthesis of Claisen Rearrangement Precursors

Exploiting the Sonogashira conditions previously reported by our lab, **55** and **101** were successfully coupled to generate **106** (Scheme 2.32). Homocoupled product **100** was not observed, possibly due to the switch from a nitrogen atmosphere to an argon atmosphere, leading to an improved oxygen-free environment. A preliminary trial Sonogashira coupling reaction only produced a small amount of the desired product **106**

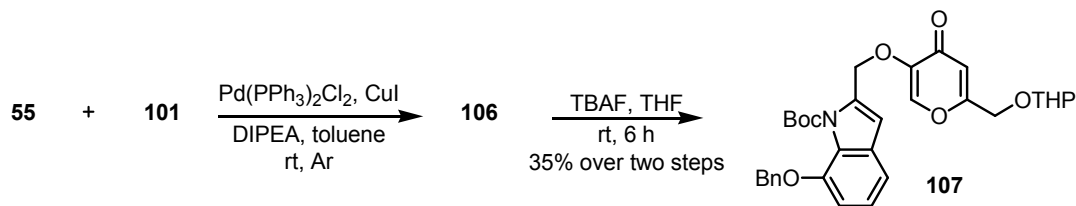
(15%), but the yield was improved to 44% by periodically adding 2 equiv portions of **55** to the reaction mixture until aryl iodide **101** was consumed.



Scheme 2.32 Production of **106** by Sonogashira coupling.

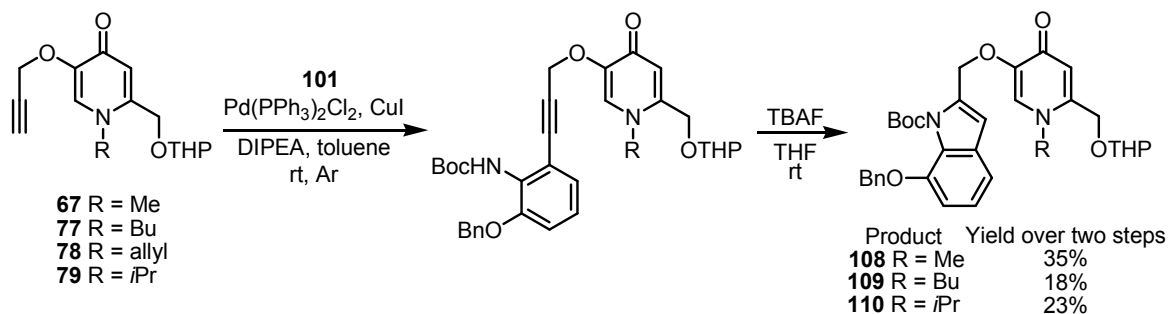
The transformation of alkyne **55** and aryl iodides **64** to indolylojates **65** was previously accomplished in one-pot by the addition of TBAF following completion of the Sonogashira reaction (Scheme 1.11).⁵⁰ All present attempts at accomplishing this two-step reaction in one-pot to form **107** were unproductive, thus making necessary a separate TBAF-mediated cyclization step with the crude residue containing **106** (Scheme 2.33). The low yield of this two-step reaction compared to the yields obtained previously using this methodology for the assembly of (5-substituted-indole)methyl kojates **65** indicates that the substitution of the starting aryl iodide dictates the reaction's success. Electronics are not responsible for the reaction outcome, due to the fact that electron-donating and electron-withdrawing groups in the 5-position of the indole similarly generated **65** in good yields (Scheme 1.11).⁵⁰ These results indicate that the installation of a bulky benzyloxy group in the 7-position of the indole of **107** is detrimental to the reaction yield

over the two steps, most likely due to steric effects retarding the initial Sonogashira reaction.



Scheme 2.33 Two-step protocol to yield (indole)methyl kojate **107**.

This two-step procedure was also applied to the reaction of pyridones **67**, **77**, **78**, and **79** (Scheme 2.34). By coupling **67** and **101** and cyclizing the intermediate, (indole)methyl *N*-methyl pyridone **108** was obtained in a yield identical to that with pyrone **55**. The *N*-butyl pyridone **77** was much less reactive than **55** or **67**, evidenced by the low isolated yield of **109**. *N*-Allyl pyridone **78** was completely unreactive in the Sonogashira step. This is most likely due to the allyl moiety forming a complex with the palladium complex, thus impeding the requisite Sonogashira catalytic cycle. Finally, *N*-isopropyl pyridone **79** produced **110**, though the yield was low for this conversion also. In all, the yields for the Sonogashira coupling reaction of the terminal alkynes of various pyrone and pyridones with aryl iodide **101** were low ($\leq 35\%$). Among the pyridone substrates, a trend emerged where the efficiency of the Sonogashira step decreased as the size of the *N*-alkyl group increased.

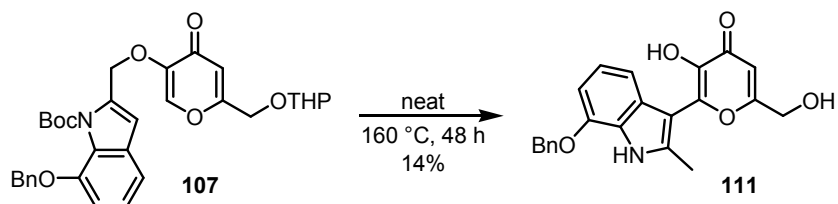


Scheme 2.34 Sonogashira-indole cyclization procedure for the synthesis of pyridone-based derivatives.

2.7 Claisen Rearrangement of 7-Benzyloxyindole Kojic Acid Derivatives

With the successful synthesis of four different Claisen substrates, **107-110**, it became possible to attempt the final step in the sequence in order to potentially obtain a small library of candidate insulin mimics. As previously discussed, extended heating of **61** and **65** was sufficient to activate the Claisen rearrangement and subsequently remove both the Boc and the THP protecting groups (Schemes 1.10 and 1.11).⁵⁰

Minor success was encountered heating pyrone **107** neat at 160 °C for 2 days. Indolylkojate **111** was isolated in only 14% yield (Scheme 2.35). Subjecting *N*-methyl pyridone **108** to high temperatures for 48 h did not cause any reaction to occur with this substrate. The product mixture resulting from heating *N*-butyl pyridone **109** indicated negligible loss of the THP group, but lacked evidence of Claisen rearrangement. Similarly, heating **110** resulted in the removal of the THP group with no Claisen rearrangement occurring. Decomposition was observed when the THP-deprotected residue from this reaction was subjected to additional heating (200 °C, 2 h).



Scheme 2.35 One-pot Claisen rearrangement and deprotection to obtain indolylkojate **111**.

The resistance of these (indole)methyl kojate derivatives to Claisen rearrangement is puzzling, especially in light of our group's past achievements in this area. It is conceivable that the presence of the electron-donating benzyloxy moiety makes the indole sufficiently electron-rich that destroying the aromaticity of the ring system to commence the rearrangement is disfavored. Though the utility of this reaction pathway was previously demonstrated with 5 different indole subunits, the majority of these examples were electron-deficient. While it is true that (5-methylindole)methyl kojate **65** underwent Claisen rearrangement and deprotection in 70% yield,⁵⁰ the benzyl ether of **107** is much more electron-donating than a simple alkyl group. Despite the low yield of the final step, target compound 7-benzyloxyindolylpyrone **111** will be submitted for biological testing in the near future.

2.8 Conclusion

In the present work, various arene alkynylation reactions were explored in order to obtain a diverse set of substrates perfect for the Claisen rearrangement, with the goal of constructing a library of indolylkojates. The low commercial availability of aryl iodides used in our lab's original study of this synthetic route prompted the examination of aryl fluorides, bromides, and triflates. Unfortunately, none of these substrates were successful

coupling partners with our kojate derivatives, so the target compound **111** was finally synthesized through the use of aryl iodide **101**, albeit in low overall yield.

Chapter 3. Examination of the Biaryl Bond of Prospective Kojate-Based Insulin

Mimics by Chiral HPLC

3.1 Atropisomerism

It is well known that chirality is an important consideration in the pharmaceutical industry. This is due to the fact that often only one stereoisomer of a chiral drug is biologically active.⁹⁰ The biologically active stereoisomer is designated the eutomer. In most cases, the other stereoisomer (or distomer) is merely an impurity, as it has no biological activity. In rare cases, the distomer has adverse biological activity. Due to the potential efficacy and safety issues surrounding the use of racemic mixtures of a drug, the U.S Food and Drug Administration (FDA) has adopted strict policies regarding the use of therapeutic stereoisomers.⁹¹ Prior to FDA approval of a drug candidate, it is necessary to perform a pharmacological study of the behavior of each individual stereoisomer. Such a study will establish the activity of each isomer in vitro and in vivo and will answer the key question of whether the isomers interconvert readily.

An oft-overlooked class of chirality is that of axial chirality.⁹² A molecule exhibits axial chirality when the groups surrounding an axis of rotation are held in a spatial arrangement that prevents the molecule from superimposing on its mirror image. The most common example of axial chirality is found in biaryl systems. If rotation about the biaryl bond is restricted due to the presence of bulky groups, two nonplanar stereoisomers, called atropisomers, are possible. Interconversion between the two isomers must be slow, with a half-life of greater than 1000 s, for the system to qualify as atropisomeric.⁹³ If interconversion is slow enough, it is possible to separate and isolate

the atropisomers. Endothelin receptor antagonist BMS-207940 is an example of a biaryl compound that exhibits atropisomerism due to steric hindrance created by the presence of only two bulky substituents ortho to the biaryl bond (Figure 3.1).⁹⁴ At ambient temperature, BMS-207940 has a half-life of interconversion of about 15 h, despite the fact that it lacks the conventional three non-hydrogen substituents surrounding the biaryl bond expected to be required for atropisomerism.

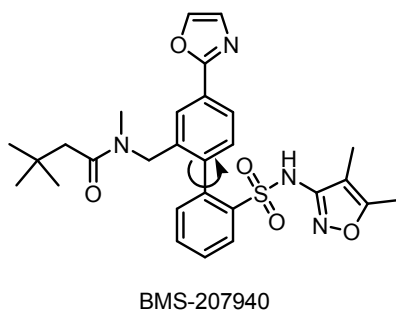


Figure 3.1 Example of atropisomerism in a biologically active biaryl compound.

The indole-kojate single bond of our target compounds (such as **45**, **47**, **63**, **66**, **68**, and **111**) is akin to a biaryl bond, making it essential to examine the potential chiral attributes of these small molecule drug candidates. If a kojate such as **112** displays restricted rotation about the biaryl bond, the resulting atropisomers would be enantiomers of one another (Figure 3.2). Steric congestion about the biaryl bond could arise from the use of non-hydrogen substituents at the 2- and 4-positions of the indole, furnishing a product with sufficient barrier to rotation that study by chiral HPLC (high-performance liquid chromatography) is possible. Any process with an energy barrier of less than 14.3

kcal/mol is facile at room temperature, but the barrier for interconversion about the biaryl bond of **112** is almost 30 kcal/mol (according to theoretical calculations performed by Prof. Pirrung). This suggests that the enantiomers should be stable and separable on the laboratory time scale.

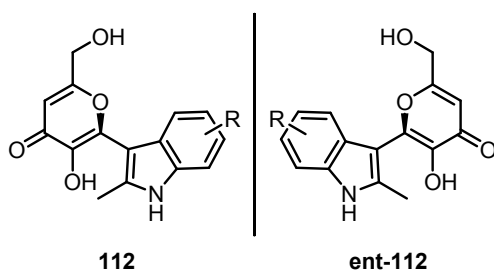


Figure 3.2 Potentially atropisomeric indolylkojate derivative.

The biaryl bonds of monoindolyldichlorobenzoquinones **113** and **114**, with non-hydrogen substituents at indole positions 2 and 4, were interrogated by a past graduate student from the Pirrung lab, Dr. Liu Deng (Figure 3.3).⁹⁵ Each of these pure compounds was analyzed by chiral HPLC (Chiralpak AD column, 30% isopropanol in hexanes, 1 mL/min). The results for each compound were similar, in that they both displayed two peaks in their chromatograms that had widely different retention times. The atropisomers of **113** had elution times that differed by over 11 min (4.538 min vs. 15.880 min), while for **114**, the retention times of the atropisomers differed by over 17 min (12.765 min vs. 30.160 min). This HPLC study proved that these monoindolylbenzoquinones indeed exist as chiral compounds on the laboratory time scale. Subsequent endeavors toward the development of a catalytic asymmetric route to these chiral molecules were unsuccessful.

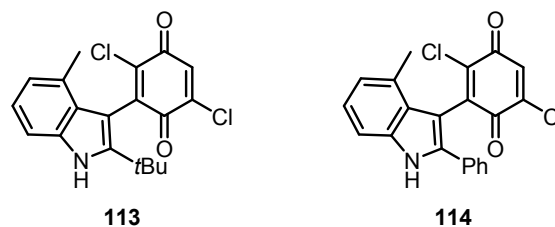


Figure 3.3 Atropisomeric monoindolyldichlorobenzoquinones.

3.2 Synthesis of a 4-Bromoindolylkojate Derivative

The current work began with the application of Deng's methods to the analysis of **63**, previously synthesized by postdoctoral researcher Dr. Xin Xiong in our lab (Scheme 1.10). Subjecting this kojate to chiral HPLC (Chiralpak AD, 30% isopropanol in hexanes, 1.2 mL/min) yielded only one peak with a retention time of almost 5 min, even when HPLC analysis was continued for an hour (Figure 3.4). This result led us to conclude that a methyl group in the 2-position of the indole subunit did not provide the steric bulk necessary for restricted rotation about the biaryl bond of **63**. This result is expected, as **63** lacks large substituents that could cause steric hindrance and restrict bond rotation. In order to obtain a kojate derivative that exists as two discreet atropisomers, structural modification became necessary. The Claisen rearrangement route to indolylkojates installs a 2-methyl group in the indole moiety, so alterations at the 4-position of the indole could provide a product that exhibits restricted rotation at room temperature.

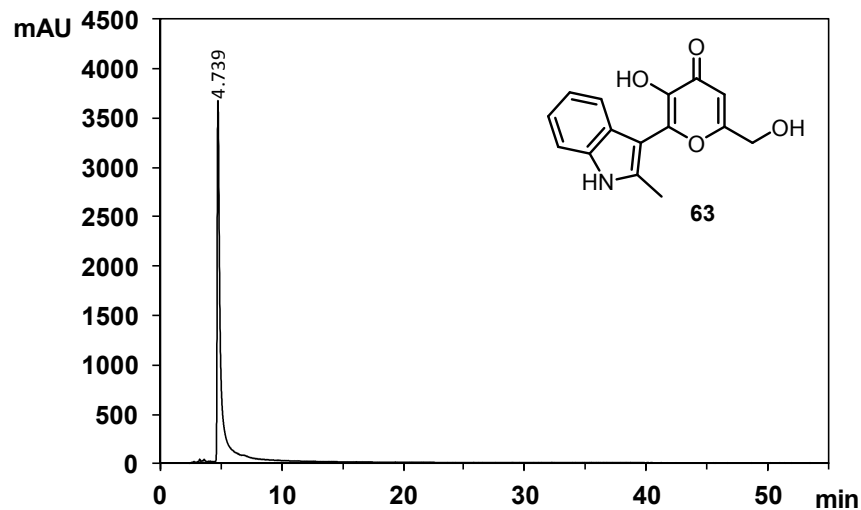


Figure 3.4 HPLC chromatogram of **63**.
(Chiralpak AD, 30% isopropanol in hexanes, 1.2 mL/min, 254 nm).

We hypothesized that a large group at the indole 4-position, such as a bromo substituent, could create ample steric hindrance, such that two atropisomers would be revealed through chiral HPLC analysis. In order to verify this theory, a synthetic route to 4-bromoindolylkojate **115** (Figure 3.5) was developed. Moody and coworkers reported the synthesis of a 4-bromoindole that we felt could be a useful intermediate in our synthesis.⁹⁶

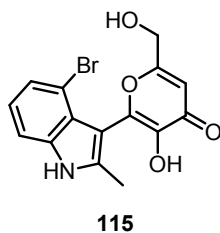
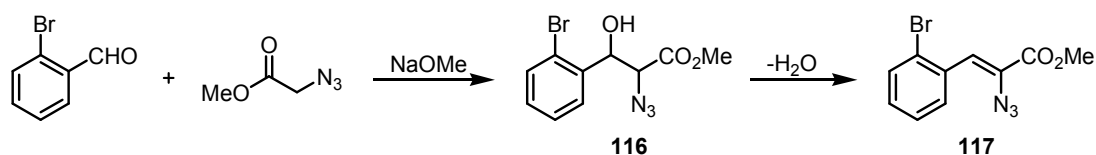


Figure 3.5 Model kojate system for chirality study.

The initial aldol/dehydration reaction of 2-bromobenzaldehyde and methyl azidoacetate was attempted according to Moody's procedure, but the product ^1H NMR spectrum was messy and indicated the presence of mainly the β -hydroxy ester intermediate **116** (Scheme 3.1). It was determined that dropwise addition of the methyl azidoacetate/2-bromobenzaldehyde mixture to the NaOMe solution over a time period of 40 minutes led to a cleaner conversion to the desired product **117**, but the isolated yield of pure product was negligible. Repeating the reaction and decreasing the temperature during the dropwise addition step gave consistently low yields.



Scheme 3.1 Aldol/dehydration reaction.

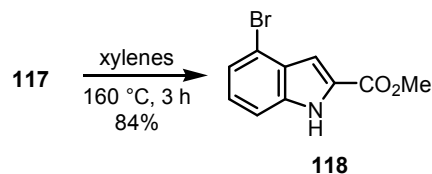
Finally, it was determined that the ratio of the sodium metal and methyl azidoacetate was important to the reaction outcome (Table 3.1). Moody reported the use of 1 equiv of 2-bromobenzaldehyde, 3.8 equiv of methyl azidoacetate, and 3.8 equiv of sodium metal to achieve a moderate yield of **117** (entry 1).⁹⁶ Conversely, in the present work, similar reaction conditions (3.9 equiv methyl azidoacetate, 4 equiv sodium metal, entry 2) led to no desired product, but decomposition of the starting materials instead. Increasing the equivalents of the sodium metal used (entry 3) only gave a 19% yield. When the molar equivalents of both methyl azidoacetate and sodium metal were increased, using more methyl azidoacetate than sodium metal (entry 4), the desired

product was isolated in a much improved yield of 83%. It was determined that such an excess of these reagents is unnecessary, as the reaction with 5.1 equiv of methyl azidoacetate and 3.8 equiv of sodium metal led to an 85% yield of **117** with no need for purification (entry 5). By incorporating a slow dropwise addition and by using 1.3 additional equivalents of methyl azidoacetate compared to sodium metal, this reaction was improved drastically over the reported 51% yield.⁹⁶ With **117** in hand, the azide was cyclized to indole **118**, according to the literature procedure (Scheme 3.2).⁹⁶

Table 3.1 Optimization of the Aldol reaction.

Entry	Equivalents		% Yield
	Azide	Na	
1	3.8	3.8	51 ^a
2	3.9	4	0
3	3.8	4.4	19
4	11	9.1	83
5	5.1	3.8	85

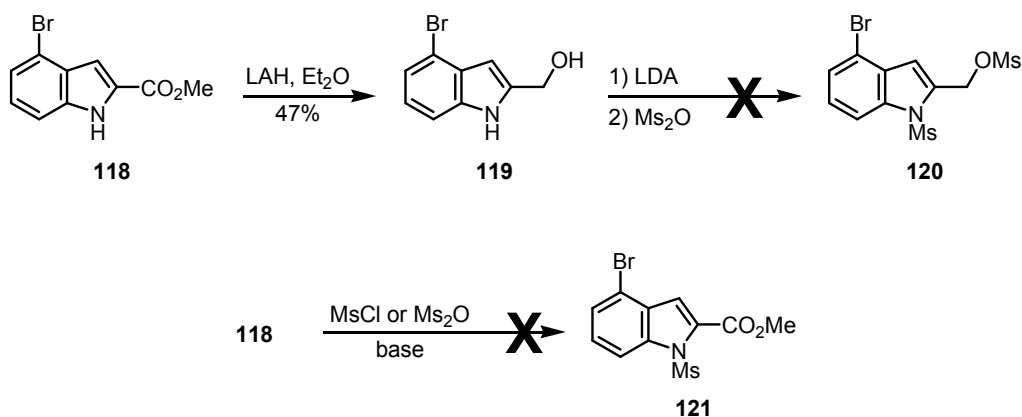
^a Literature results.⁹⁶



Scheme 3.2 Indole-cyclization of **117**.

A method was sought for the protection of the indole nitrogen of **118** with an electron-withdrawing protecting group, because this is critical for the success of the Claisen rearrangement used in the final step. It was envisioned that initial reduction of the

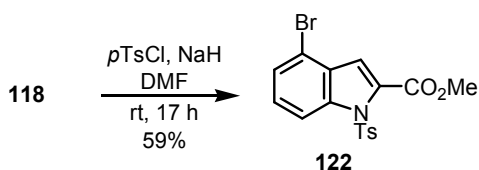
methyl ester, followed by treatment of the resulting alcohol with a source of protection could induce protection of both the indole nitrogen and the alcohol, leading to an intermediate that could then be coupled directly to kojate **52**. Reduction of **118** was accomplished using lithium aluminum hydride (LAH) to produce alcohol **119** in moderate yield (47%; Scheme 3.3). Treatment of **119** with LDA, followed by mesyl anhydride failed to give the desired double mesylated product **120**. Alternatively, the protection of the indole nitrogen of **118** in the presence of the methyl ester was attempted. Mesyl chloride or mesyl anhydride with various bases (Et₃N, LDA, NaH, K₂CO₃) failed to give good conversions of **118** to desired product **121**.



Scheme 3.3 Failed mesyl protection reactions.

Switching to *p*-toluenesulfonyl chloride (*p*TsCl) in the presence of NaH as base finally provided indole **122**, with an electron-withdrawing tosyl protecting group. The reaction conditions (DMF, rt, overnight) provided inconsistent yields, the highest being 59%. Though an excess of *p*TsCl was used (4-5 equiv), TLC analysis of the reaction

mixture indicated consumption of *p*TsCl, with unreacted indole **118** remaining following the reaction.

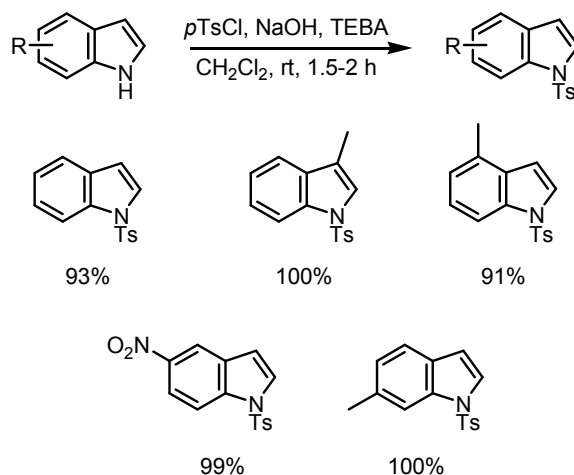


Scheme 3.4 Successful protection of indole with *p*TsCl.

In order to improve the conversion of indole **118**, it was thought that adding the *p*TsCl in portions could improve the reaction outcome, since the *p*TsCl was always consumed under the reaction conditions. Unfortunately, the periodic addition of *p*TsCl in portions led to very little desired product present. It was hypothesized that the basic medium was responsible for the degradation of *p*TsCl and, by extension, the low isolated yields of this protection method. This was verified when the reaction in the presence of 5.1 equiv of NaH (instead of 1.2 equiv) generated **122** in only 27% yield. To combat the damaging effects NaH had on the tosyl source, the time **118** and NaH were allowed to react prior to the addition of *p*TsCl was extended from only 30 min to 4 h. This modification did improve the conversion of **118**, but the isolated yield was still moderate (49%). DMF was found to be a better solvent for this reaction, as switching to THF was detrimental to the isolated yield of **122** (6% yield).

Concurrently with these optimization trials a paper was published by Hui and Yangyang⁹⁷ that detailed the efficient synthesis of tosyl-protected indoles in high yields

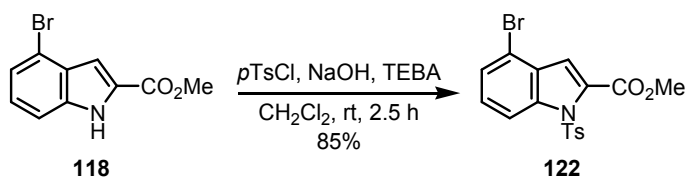
with short reaction times. Their novel reaction involved treatment of various indoles in CH_2Cl_2 with *p*TsCl in the presence of NaOH and triethylbenzylammonium chloride (TEBA) as a phase transfer catalyst. The reaction worked well with a variety of indoles with electron-donating or electron-withdrawing groups present, with reaction times of only 1.5-2 h and yields ranging from 91-100% (Scheme 3.5).



Scheme 3.5 Examples of the utility of Hui's novel tosyl protection protocol.

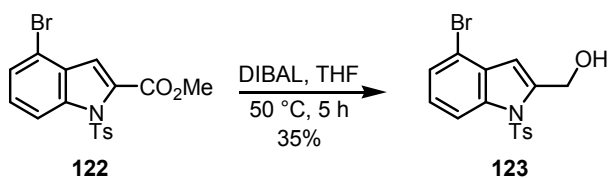
Successful application of Hui's conditions⁹⁷ to the conversion of **118** to **122** reduced the reaction time from 17 h with NaH/DMF to only 2 h, though the yield was only 47%. This transformation was optimized by decreasing the reaction concentration from 0.25 M as prescribed in Hui's paper⁹⁷ to 0.13 M. This change in concentration led to complete conversion of starting indole **118** to typically produce **122** in quantitative yield, without the need for any purification measure other than filtration following the reaction.

Alternatively, when subjected to column chromatography, **122** was isolated in as high as 85% yield (Scheme 3.6).



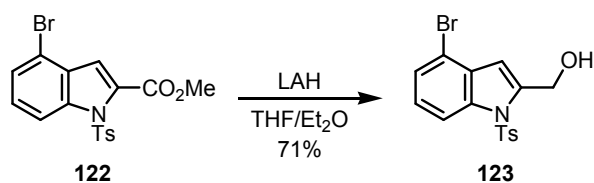
Scheme 3.6 Optimization of the indole protection step.

With satisfactory conditions for the protection of indole **118** in hand, attention was focused on the development of an efficient procedure for the reduction of the methyl ester of **122**. Using diisobutylaluminum hydride (DIBAL) in THF and stirring the reaction at room temperature for about a day did not lead to any change in the reaction mixture by TLC. Heating this reaction mixture to 50 °C for 5 h finally led to consumption of the starting material by TLC, with alcohol **123** being isolated in 35% yield (Scheme 3.7).



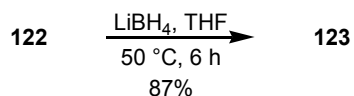
Scheme 3.7 DIBAL-mediated ester reduction.

Despite the moderate activity of LAH in Et₂O for the reduction of **118** to **119** (Scheme 3.3), use of this reducing agent in an Et₂O solution of **122** was fruitless, though this was most likely due to the insolubility of this tosyl-protected indole in Et₂O. Running the reaction in THF led to an isolated yield of only 5% of the desired product, a result that could be attributed to the low solubility of LAH in THF compared to Et₂O. In an effort to improve these conditions, a mixed solvent system was used, adding dropwise a THF solution of **122** to a solution of LAH in Et₂O. This adjustment proved advantageous, as **123** was generated in 71% isolated yield (Scheme 3.8).



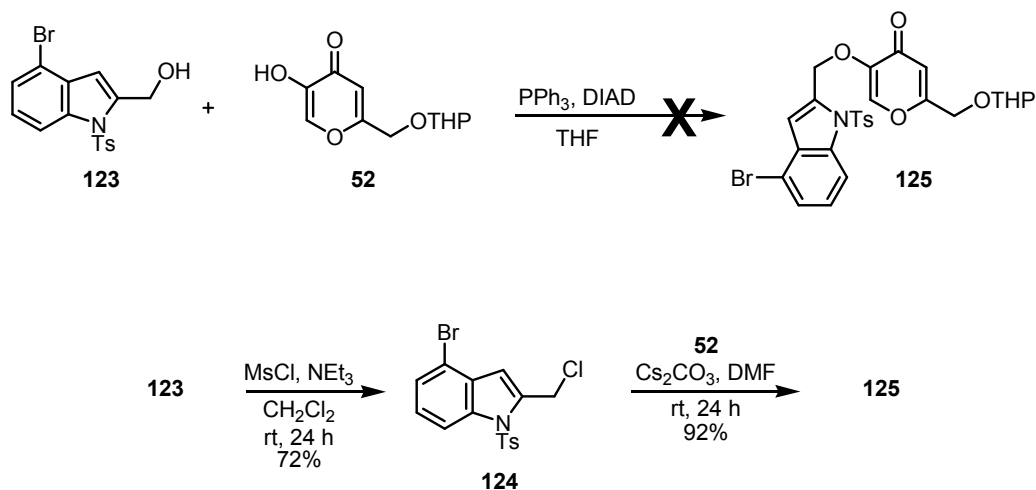
Scheme 3.8 Optimized ester reduction in the presence of LAH.

Besides DIBAL and LAH, lithium borohydride was also examined in the reduction of **122**. Moderate success was achieved by treating **122** with LiBH₄ and then heating the resulting solution at 50 °C for 6.5 h (65% yield). Dropwise addition of LiBH₄ to a THF solution of **122** preheated to 50 °C proved integral to reaction progress, as a clean product was isolated, typically in near quantitative yield with no need for purification. Purification by column chromatography afforded the product in as high as 87% yield (Scheme 3.9).



Scheme 3.9 Methyl ester reduction, mediated by LiBH₄.

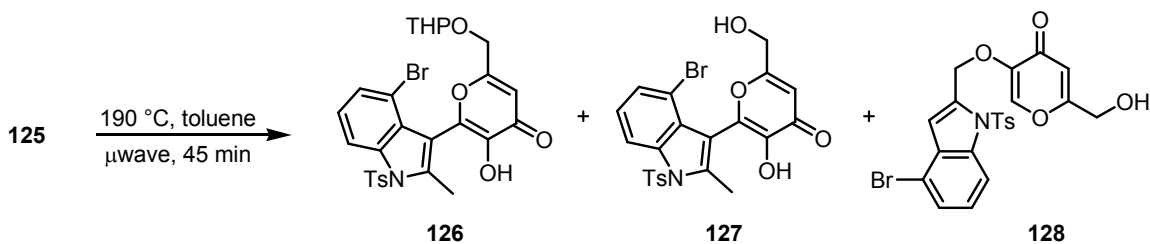
Direct Mitsunobu coupling of **123** with **52** was unproductive, suggesting that an additional step would be necessary to convert the alcohol of **123** into a better leaving group so an S_N2 reaction would be possible. This was accomplished easily by treatment of **123** with mesyl chloride and Et₃N in CH₂Cl₂ to furnish chloride **124** in good yield (Scheme 3.10). Coupling of **124** and **52** produced the requisite Claisen precursor **125** in excellent yield.



Scheme 3.10 Synthesis of kojate derivative **125**.

An early microwave-assisted Claisen rearrangement of **125** (190 °C, 45 min, toluene, sealed vessel) afforded a complex mixture of products, determined to be the

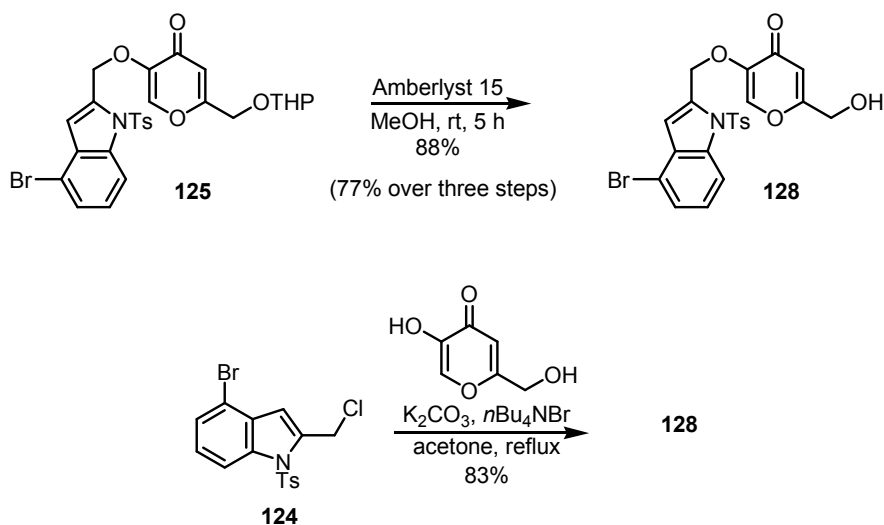
THP-protected and -deprotected products of the Claisen rearrangement (**126** and **127**, respectively), along with the product from only THP removal, **128**, and unreacted starting material **125** (Scheme 3.11). Separation of desired product **127** from **128** was difficult, as the two products are virtually indistinguishable by chromatography. Partial removal of the THP group using microwave irradiation is known (Scheme 1.9),⁵⁰ though incomplete Claisen rearrangement under these conditions is unprecedented.



Scheme 3.11 Incomplete Claisen rearrangement and deprotection.

The bulky 4-bromo substituent of the indole moiety can be credited with the difficulty encountered when attempting the Claisen rearrangement of **125**. It is apparent that the same group installed to restrict rotation about the biaryl bond of **127** also provides some steric congestion such that the rearrangement of **125** is inefficient. The isolation of **128** under the reaction conditions implied that the THP moiety was a microwave energy sink. In order to devote all of the microwave energy exclusively to the rearrangement, the THP protecting group was removed from **125** to generate **128** in excellent yield (88%). This (indole)methyl kojate can also be accessed quickly and in high yield by coupling **124** with kojic acid (83%). Though the overall yields were similar

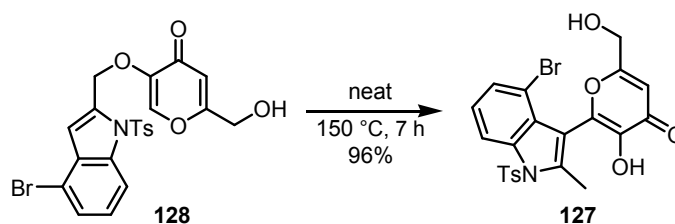
(83% vs. 77% over three steps), the direct reaction is clearly superior to the protection-coupling-deprotection strategy, due to the need for fewer steps.



Scheme 3.12 Methods for the synthesis of **128**.

The microwave-promoted Claisen rearrangement was attempted with **128**, extending the time to over an hour, but the conversion was still incomplete, as evidenced by the 1:1 ratio of **127**:**128** (Scheme 3.13). As previously discussed, purification of a mixture of these two compounds was problematic, as **127** and **128** are practically inseparable. Conventional heating measures were determined to be more effective than microwave irradiation. Heating **128** neat at 150 °C for only 7 h, target compound **127** was isolated in exceptional yield. By TLC analysis of pure samples of **127** and **128**, it became apparent why purification of a mixture of **127** and **128** was exceedingly difficult (Figure 3.6). Though visualization of the TLC plate by vanillin revealed that **127** stains a yellow-orange color and **128** stains a black color, the R_f values for starting material and product

are nearly identical. The successful development of a method that allows for full conversion and excellent yields allayed any potential purification issues.



Scheme 3.13 Claisen rearrangement of **128**.

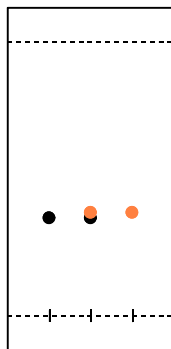


Figure 3.6 Example of TLC analysis of **127** and **128**, eluting with 25% hexanes in EtOAc and stained with vanillin. From left to right, **128**, mixed spot, **127**.

3.3 Analysis by Chiral HPLC

Analysis of **127** on a Chiralpak AD HPLC column, eluting with 30% isopropanol in hexanes, displayed only one peak during the hour-long run (Figure 3.7). This result could indicate the need for a different chiral column, but this same column was previously used by Dr. Deng with great success to analyze chiral mixtures of monoindolyquinones **113** and **114**,⁹⁵ which have a great degree of structural similarity to

indolylkojate **127**. It is more likely that this result disproves our theory that a bromo substituent at the 4-position of the indole would provide sufficient steric congestion, such that rotation about the biaryl bond is restricted. Though the existence of atropisomers would be possible if a larger group, such as phenyl or *tert*-butyl ester, was used in place of the bromo moiety, we sought to modify the kojic acid core instead, by converting the pyrone of **127** into a pyridone analog. The rationale behind this proposed modification was that the combination of an alkyl group on the pyridone nitrogen along with the steric bulk of a bromine at the 4-position of the indole should hinder rotation about the single bond enough that the compound would exist as enantiomers on the laboratory time scale.

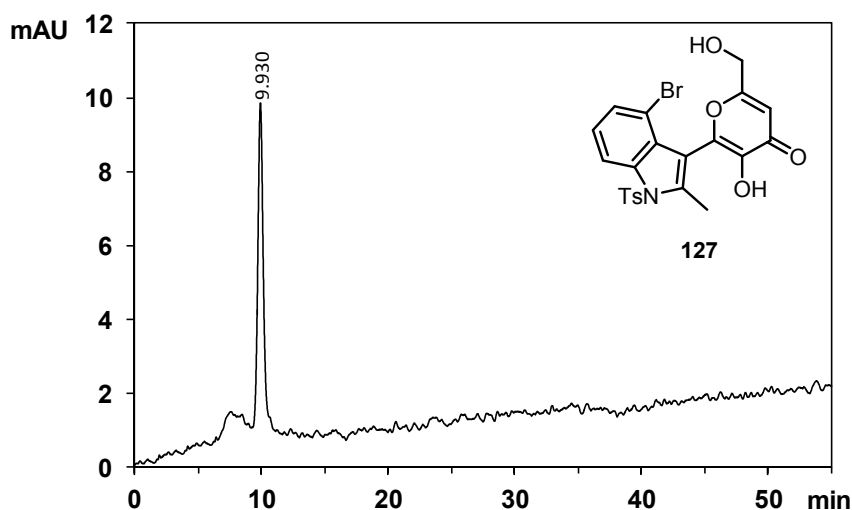
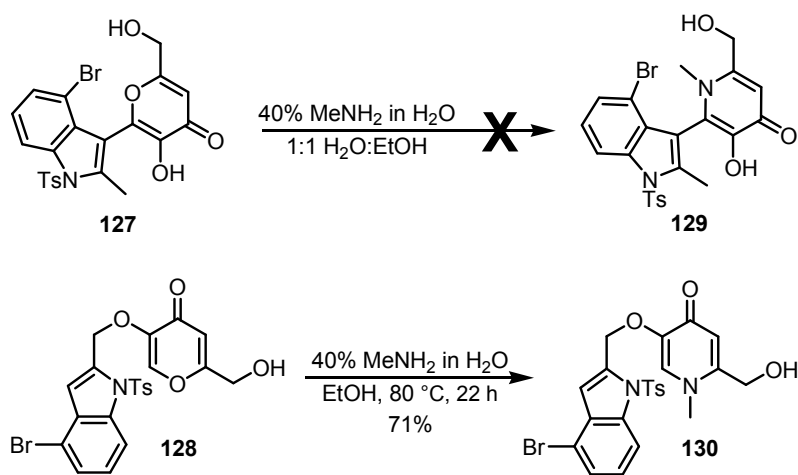


Figure 3.7 HPLC chromatogram of **127**.
(Chiralpak AD, 30% isopropanol in hexanes, 1.2 mL/min, 254 nm).

3.4 Synthesis of a 4-Bromoindolyl Pyridone Derivative

Though our group^{45,50,95} and others^{64,70,71} have enjoyed great success performing the pyrone to pyridone exchange reaction on substrates where the enol oxygen is protected (Schemes 1.6, 1.11, 2.1, 2.4, 2.6, 2.10, 2.13), a direct exchange reaction was attempted to convert **127** into **129**. A successful exchange reaction in the presence of a free enol oxygen is not unprecedented,⁶⁵ but it failed with **127** as the substrate. Alternatively, (indole)methyl kojate **128** was treated with methylamine to obtain **130** in good yield (71%; Scheme 3.14).



Scheme 3.14 Pyrone-to-pyridone exchange reactions.

Heating pyridone **130** neat at temperatures ranging from 150-170 °C caused decomposition of the starting material, even for reaction times as short as only 4 h. The product derived from the use of microwave irradiation (190 °C, 45 min) for the rearrangement of **130** also showed signs of decomposition with only traces of

rearrangement product **129** present. Utilizing Lewis acid $\text{Zn}(\text{OTf})_2$ to catalyze the rearrangement (see Chapter 4), **130** was heated to 120 °C for up to 200 min under microwave heating conditions in toluene, but no conversion of the starting material was observed.

3.5 Conclusion

When targeting a biaryl system during the course of drug development, it is crucial to gain a full understanding of the chirality of the candidate molecule. The same is true of the indolylkojates that have been the subject of much research in the Pirrung lab. Though benzoquinones **113** and **114** have been identified as being atropisomeric, kojate **63** displayed no evidence of chirality.

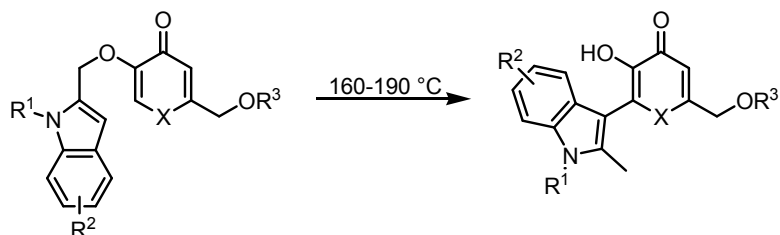
Substitutions at the 2- and 4-positions of the indole subunit are responsible for creating the steric hindrance necessary to observe restricted rotation about the biaryl bond. We envisioned that the presence of a large group, such a bromo, at the 4-position of the indole would allow for the existence of two discrete enantiomers at ambient temperature. The synthesis and subsequent analysis of **127** by chiral HPLC refuted that theory, suggesting that further structural modification would be necessary to obtain a molecule that is sufficiently hindered to permit the existence of atropisomers. To serve this purpose, pyridone **130** was synthesized, but all efforts to effect the Claisen rearrangement of this substrate were unsuccessful, typically resulting in decomposition. Conditions for the successful Claisen rearrangement of **130** or perhaps its THP-protected derivative should be developed by future members of the Pirrung group.

Chapter 4. Catalytic Claisen Rearrangements of *O*-Allyl Kojates

4.1 Introduction

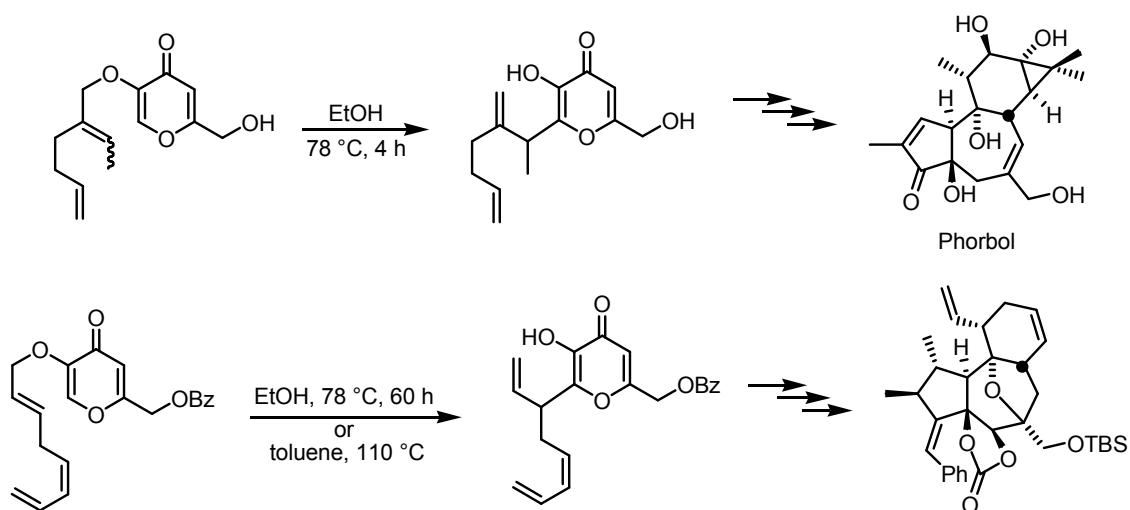
Since its discovery 100 years ago,⁹⁸ the Claisen rearrangement has been a widely used tool for the formation of C-C bonds. Typically, the reaction requires harsh conditions, such as high temperatures and long reaction times, which can limit the substrates that can be used with this method. To combat this issue, many groups over the last century have sought catalysts that would allow for the rearrangement to be performed under milder conditions.

As previously discussed (Section 1.11), the thermal Claisen rearrangement is a key step in the synthesis of potential insulin mimics (Scheme 4.1). We have determined that it is essential to protect the nitrogen of the indole subunit with an electron-withdrawing group.⁵⁰ This is due to the fact that, at the high temperatures required for this transformation (as high as 190 °C), solvolysis of the indolyl ether bond is faster than the desired rearrangement without this protection in place. In an effort to avoid the use of high temperatures as well as time-consuming protection and deprotection steps, we have been stimulated to think about ways to catalyze this rearrangement. There are very few examples of the thermal Claisen rearrangement of kojic acid derivatives^{50,99,100} and even fewer examples of catalysis of these reactions.^{100c,101}

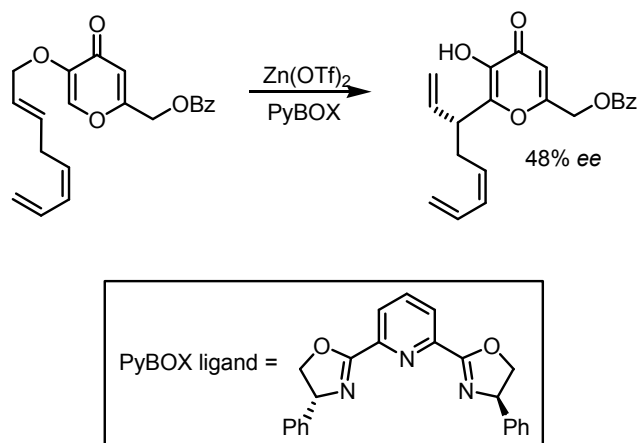


Scheme 4.1 Crucial Claisen rearrangement in the synthesis of prospective kojate-based insulin mimics.

Wender has been at the forefront of research concerning the Claisen rearrangement of *O*-allyl kojate ethers, with his work toward the synthesis of various natural products and their analogs.¹⁰⁰ He has reported thermal rearrangements of these substrates successfully being conducted at as high as 110 °C^{100c} and as low as 78 °C (Scheme 4.2).^{100a,b} Wender also hinted at some promising preliminary work toward asymmetric catalysis of this rearrangement, with the combination of Zn(OTf)₂ and PyBOX giving enantiomeric excesses of up to 48%, though the report was devoid of any experimental details (Scheme 4.3).^{100c}



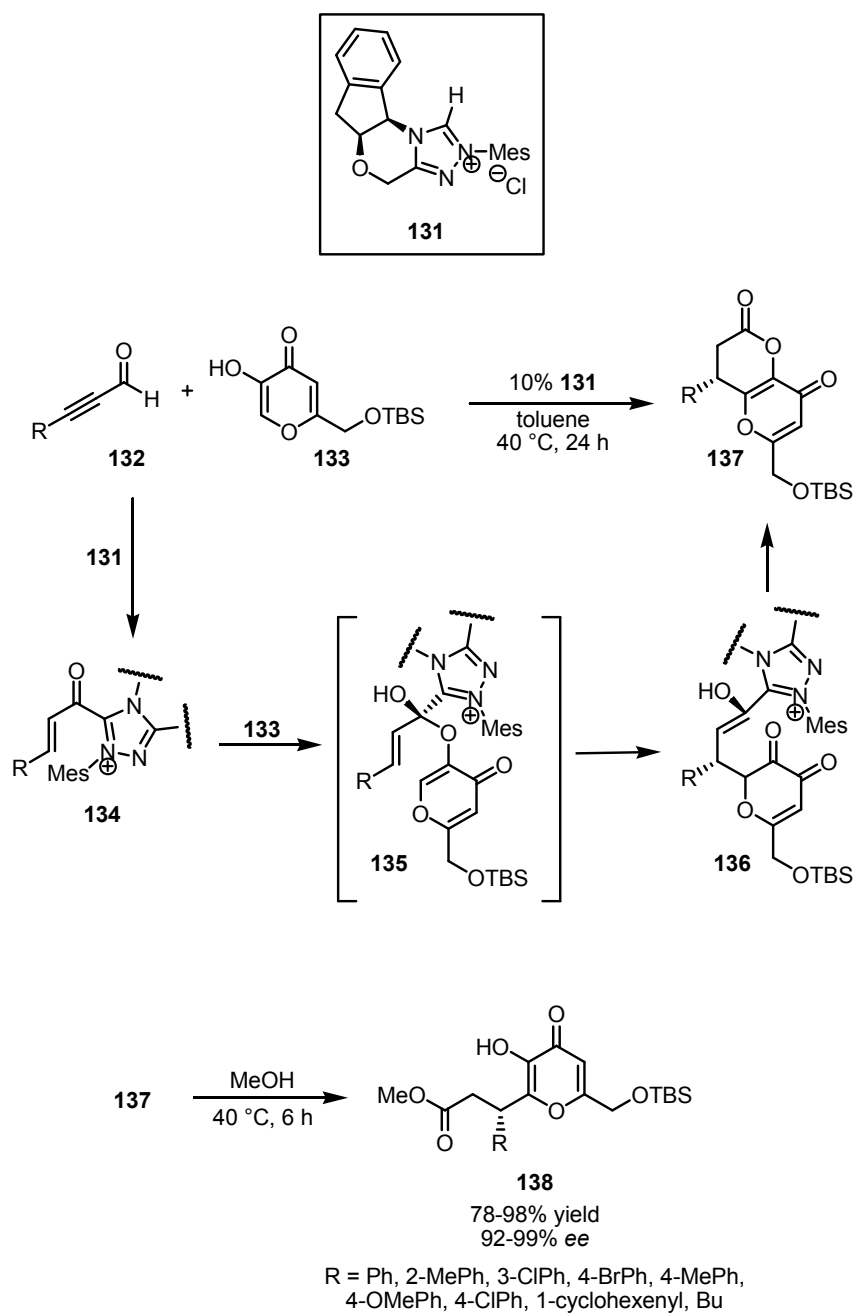
Scheme 4.2 Wender's thermal Claisen rearrangement.



Scheme 4.3 Claisen rearrangement of an *O*-allyl kojate, catalyzed by Zn(OTf)_2 -PyBOX.

Bode disclosed some interesting work on catalytic Claisen rearrangements using chiral carbenes.¹⁰¹ The proposed mechanism for this transformation is depicted in Scheme 4.4. When treated with *N*-heterocyclic carbene (NHC) catalyst **131**, various ynals **132** likely form α,β -unsaturated acyl azolium species **134**. Surprisingly, Bode and coworkers found that the reaction did not require the addition of base to generate the carbene, as the chloride counterion of **131** was a competent surrogate. In the presence of the enol of kojic acid derivative **133**, hemiacetal **135** is presumably formed. A subsequent Coates-Claisen rearrangement would produce intermediate **136**, which then can undergo lactonization and tautomerization to generate dihydropyranone **137**. The possibility of the reaction proceeding by a 1,4-addition was excluded, based on failed attempts to effect such a reaction using various nucleophiles, such as azide, thiols, and electron-rich aromatic compounds. Dihydropyranones **137** are moderately unstable, so the products were stirred in MeOH for 6 h to obtain ring-opened products **138** that were suitable for isolation. Employing a wide range of ynals, where R corresponds to various electron-poor

and electron-rich aryl groups and alkyl chains, the reaction cascade furnished **138** in good to excellent yields and excellent enantioselectivities.



Scheme 4.4 Bode's enantioselective NHC-catalyzed Claisen rearrangement.

The relative scarcity of literature surrounding the catalyzed rearrangement of kojic acid derivatives prompted us to turn our attention to catalysts known to be effective for the Claisen rearrangements of allyl aryl ethers and (allyloxy)acrylates. Electronically, *O*-allyl kojates, with their conjugated 6π -electron ring systems, would be expected to react similarly to allyl aryl ethers under catalytic Claisen conditions. Though *O*-indolylkojates are formally vinyl benzyl ethers, substrates that have been established as unreactive to the Claisen rearrangement,¹⁰² past work from our lab with *O*-indolylkojates has proven these substrates exhibit reactivity akin to allyl aryl ethers.⁵⁰ Structurally, *O*-allyl kojates and (allyloxy)acrylates are very similar (Figure 4.1). This structural similarity has led us to reason that catalysts that have been proven effective for facilitating the rearrangement of (allyloxy)acrylates would be able to bind in a similar manner to *O*-allyl kojates and catalyze this reaction as well. Catalysts for the rearrangement of (allyloxy)acrylates are believed to bind in a bidentate fashion to the ether oxygen and the ester carbonyl oxygen of the substrate.¹⁰³ The ring of the kojate should provide much conformational rigidity to the *O*-allyl kojates, which should allow for our substrates to be pre-organized for metal binding. We hypothesized that this rigid conformation could even make our *O*-allyl kojates better substrates than the more conformationally flexible (allyloxy)acrylates, which have been found to be some of the best substrates for catalytic Claisen rearrangements (*vide infra*).¹⁰⁴⁻¹⁰⁷

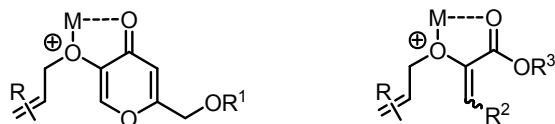
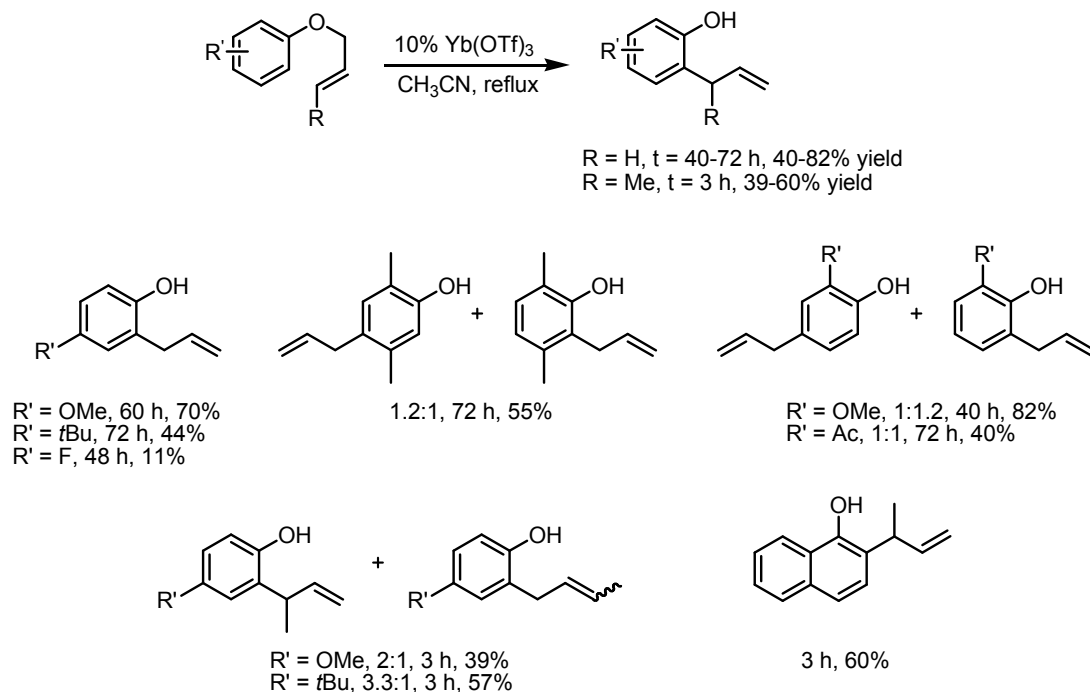


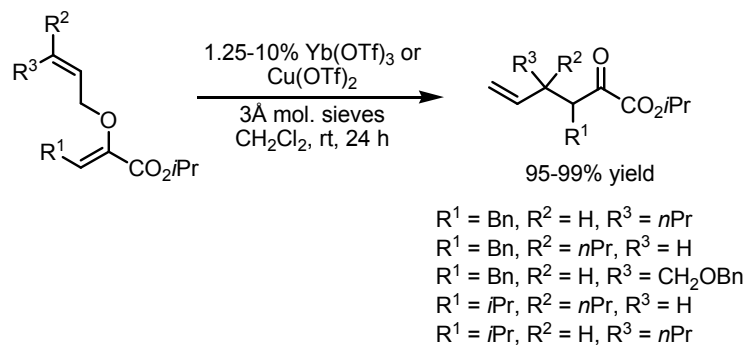
Figure 4.1 *O*-allyl kojates vs. (allyloxy)acrylates, both depicted as complexed to a metal catalyst.

4.2 Literature Examples of Catalytic Claisen Rearrangements of (Allyloxy)acrylates and Allyl Aryl Ethers

Lewis acid catalyst $\text{Yb}(\text{OTf})_3$ has been applied to the rearrangements of both allyl aryl ethers¹⁰³ and (allyloxy)acrylates.¹⁰⁴ The $\text{Yb}(\text{OTf})_3$ -catalyzed rearrangement of various allyl aryl ethers was conducted with 10 mol% of the catalyst in refluxing CH_3CN for 40-72 h, while the rearrangement of crotyl aryl ethers required only 3 h of reaction time to consistently achieve moderate yields (Scheme 4.5).¹⁰³ $\text{Cu}(\text{OTf})_2$ has been reported as a successful catalyst for the rearrangement of (allyloxy)acrylates¹⁰⁴ and this methodology has been extended to the asymmetric version with the incorporation of BOX ligands.¹⁰⁵ The Claisen rearrangements of (allyloxy)acrylates with $\text{Cu}(\text{OTf})_2$ and $\text{Yb}(\text{OTf})_3$ were conducted at room temperature in various halogenated solvents [CH_2Cl_2 , CHCl_3 , and $(\text{ClCH}_2)_2$] in the presence of pulverized molecular sieves (3Å; Scheme 4.6).¹⁰⁴ Generally, the reactions were complete within 24h, with high yields yet low diastereoselectivities.



Scheme 4.5 Yb(OTf)₃-catalyzed Claisen rearrangements of allyl and crotyl aryl ethers.



Scheme 4.6 Cu(OTf)₂- and Yb(OTf)₃-catalyzed Claisen rearrangements of (allyloxy)acrylates.

Jacobsen has disclosed the efficient rearrangement of (allyloxy)acrylates and allyl aryl ethers in the presence of achiral and chiral hydrogen-bond donor catalysts (Figure 4.2).¹⁰⁶ Inclusion of achiral guanidinium catalyst Ph₂GuanBArF was found to greatly

enhance the conversion of these substrates under rearrangement conditions. For example, a scant 12% conversion was observed in the reaction of (allyloxy)acrylate **140** in the absence of catalyst, while the addition of 20 mol% Ph₂GuanBArF dramatically improved the conversion of **140** to **141** (76%; Scheme 4.7). The use of chiral catalyst **139** in the rearrangement of various (allyloxy)acrylates permitted the isolation of α -ketoesters in good yields and excellent enantioselectivities (Scheme 4.8). The binding mode for these guanidinium catalysts with (allyloxy)acrylates is presumed to involve hydrogen bonding between the catalyst and the oxygens of the ether and ester carbonyl of the substrate (Figure 4.3).^{106b}

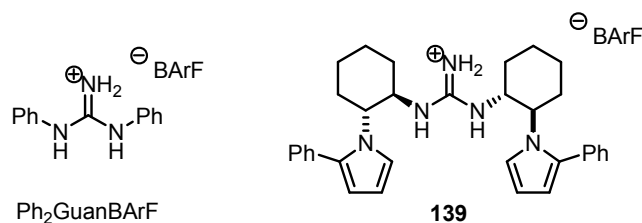
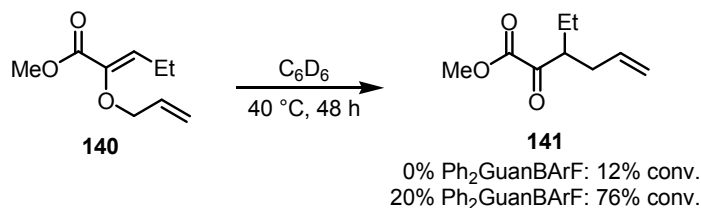
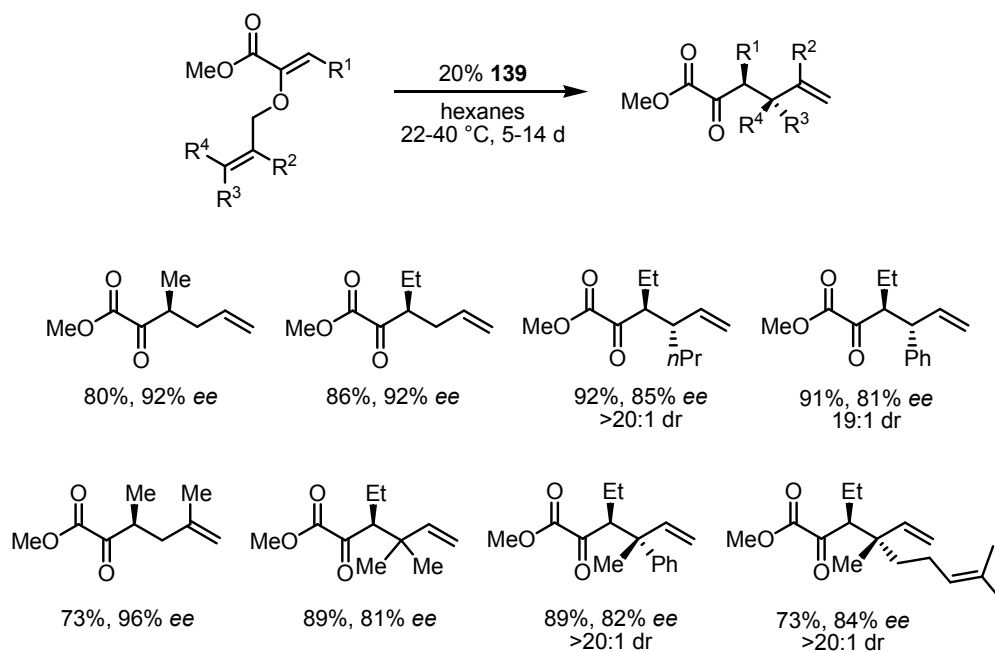


Figure 4.2 Guanidinium catalysts.



Scheme 4.7 Rate enhancement in the presence of Ph₂GuanBArF.



Scheme 4.8 Enantioselective Claisen rearrangements catalyzed by **139**.

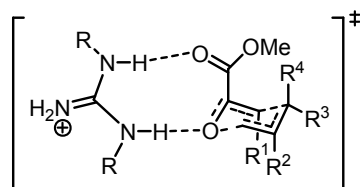
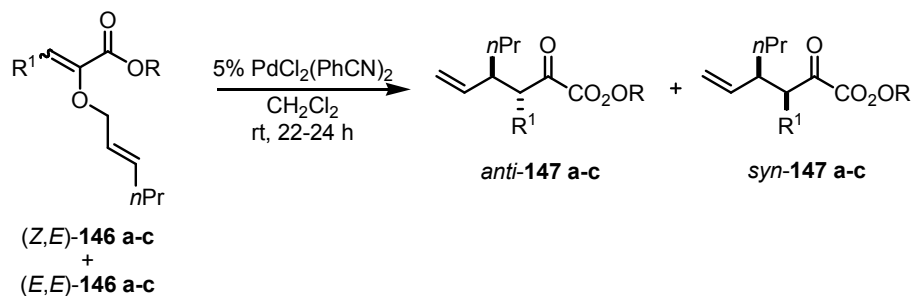


Figure 4.3 Proposed model of guanidinium catalyst binding.

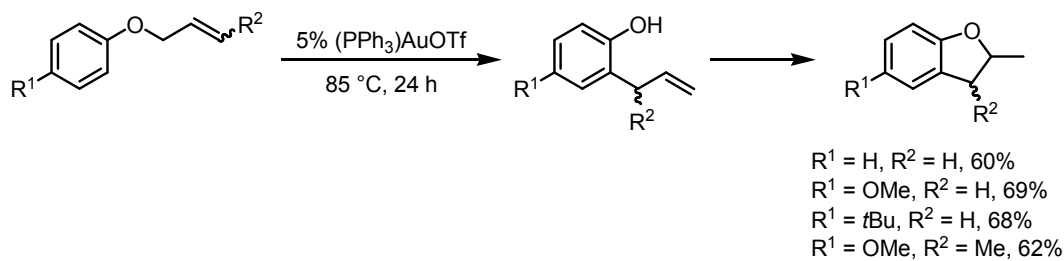
Hiersemann reported the use of Pd(II) catalysts for the rearrangement of (allyloxy)acrylates (Table 4.1).¹⁰⁷ A mixture of *Z,E* and *E,E* isomers of **146a-c** and 5 mol% PdCl₂(PhCN)₂ was stirred at room temperature for a day to determine the effect the configuration of the vinyl group had on reactivity. Hiersemann found that the *Z,E* isomers were practically unreactive, while *E,E* isomers rearranged under these conditions to yield the corresponding *anti* products (**147**) in near quantitative yield.

Table 4.1 Pd(II)-catalyzed Claisen rearrangements of (allyloxy)acrylates.

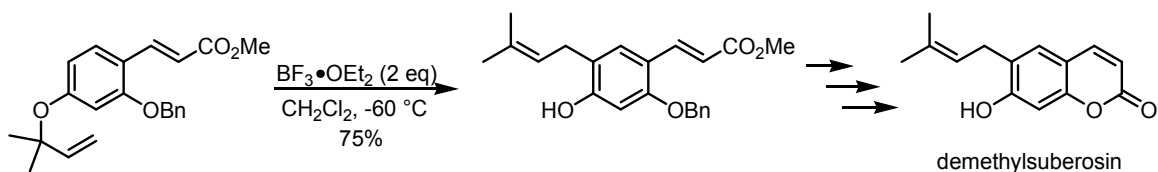


Substrate	Substrate Ratio	Product Mixture			
	<i>Z,E</i> : <i>E,E</i>	% (<i>Z,E</i>)- 146	% (<i>E,E</i>)- 146	% <i>anti</i> - 147	% <i>syn</i> - 147
146a	59:41	58	0	37	4
146b	64:36	54	0	39	6
146c	67:33	68	0	32	0

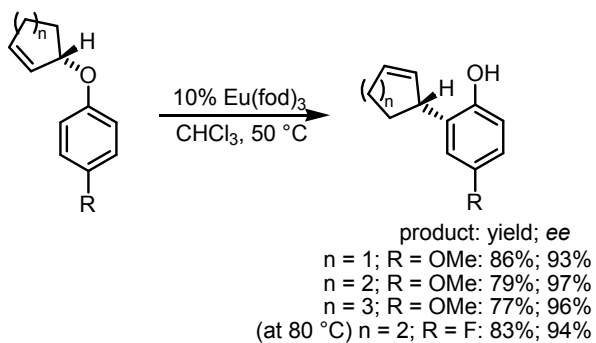
Gold (I) catalysis has been used for the Claisen rearrangement of allyl aryl ethers.¹⁰⁸ He and coworkers reported the use of 5 mol% (PPh₃)AuOTf, generated in situ from (PPh₃)AuCl and AgOTf, for the tandem Claisen rearrangement/cyclization of allyl aryl ethers to form dihydrobenzofurans in one pot (Scheme 4.9). The reaction required temperatures of up to 85 °C for 24 h to obtain the desired products in good yields. Lewis acid catalyst BF₃•OEt₂, known to catalyze the Claisen rearrangement of allyl aryl ethers, has been exploited in the regioselective synthesis of demethylsuberosin (Scheme 4.10).¹⁰⁹ NMR shift reagent Eu(fod)₃ was successfully employed in the asymmetric Claisen rearrangement of allyl aryl ethers by Trost (Scheme 4.11)¹¹⁰ and in the syntheses of various flavonoid derivatives with interesting biological activity.¹¹¹



Scheme 4.9 Gold (I) catalyst for the rearrangement of allyl aryl ethers.



Scheme 4.10 $BF_3 \cdot OEt_2$ -catalyzed Claisen rearrangement for the synthesis of demethylsuberosin.

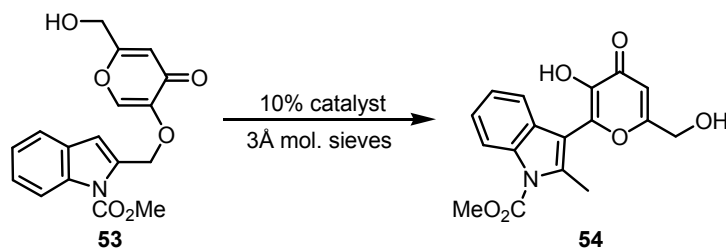


Scheme 4.11 Europium(III)-catalyzed Claisen rearrangement.

4.3 Attempted Catalytic Claisen Rearrangement of an Indolykjoate

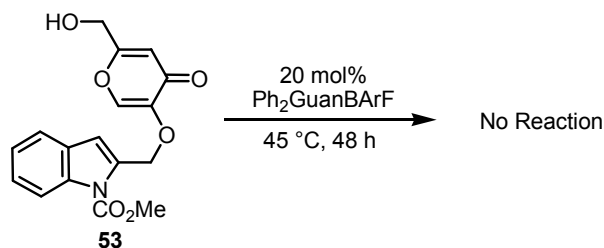
Known indolykjoate **53**⁵⁰ (Scheme 1.8) was exploited to examine the efficacy of various catalysts. Due to the demonstrated utility of Cu(OTf)₂ and Yb(OTf)₃ in the catalytic Claisen rearrangements of (allyloxy)acrylates and allyl aryl ethers,¹⁰³⁻¹⁰⁵ similar conditions were applied to the rearrangement of **53** (Table 4.2). Using Yb(OTf)₃ (10 mol%) at room temperature for 93 h did not afford any of the desired product **54**. Heating the reaction mixture to 55 °C for 1 h led to decomposition. In the presence of 10 mol% Cu(OTf)₂ at 60 °C, slight product formation was observed by ¹H NMR after only an hour, but extending the reaction time to 4 h only generated a product from decomposition. Similarly, the reaction conducted at 35 °C for a day also showed signs of decomposition. These reaction conditions were extended to the use of Zn(OTf)₂ as the catalyst (10 mol%), but no product was formed at all at room temperature, even with protracted reaction times. Minimal product formation was observed upon briefly heating the Zn(OTf)₂ reaction (60 °C, 1.5 h). Solvent had no effect on any of these reactions, as there was no difference in reactivity with the use of CH₂Cl₂ or (ClCH₂)₂, which was used for the reactions above 55 °C.

Table 4.2 Metal triflates as catalysts for the Claisen rearrangement of **53**.

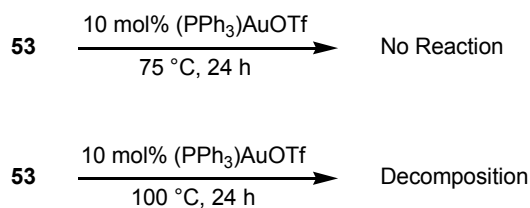


Catalyst	Solvent	Temp (°C)	Time (h)	Result
Yb(OTf) ₃	CH ₂ Cl ₂	25	24	NR
Yb(OTf) ₃	CH ₂ Cl ₂	25	93	NR
Yb(OTf) ₃	(ClCH ₂) ₂	55	1	Decomposition
Cu(OTf) ₂	(ClCH ₂) ₂	60	1	<1% yield
Cu(OTf) ₂	(ClCH ₂) ₂	60	4	Decomposition
Cu(OTf) ₂	(ClCH ₂) ₂	35	24	Decomposition
Zn(OTf) ₂	CH ₂ Cl ₂	25	24	NR
Zn(OTf) ₂	CH ₂ Cl ₂	25	64	NR
Zn(OTf) ₂	(ClCH ₂) ₂	60	1.5	<1% yield

Jacobsen's achiral guanidinium catalyst Ph₂GuanBARF was also examined in the catalytic rearrangement of kojate **53**. Unfortunately, application of the literature conditions for the rearrangement of (allyloxy)acrylates^{106a} (20 mol% Ph₂GuanBARF, 45 °C, 48 h) did not generate any of the desired rearrangement product, **54** (Scheme 4.12). Gold(I) complex (PPh₃)AuOTf [10 mol%, based on (PPh₃)AuCl] was employed for the rearrangement of **53**, due to the reported success of this catalyst in the Claisen rearrangement of allyl aryl ethers.¹⁰⁸ Disappointingly, heating **53** in the presence of (PPh₃)AuOTf at 75 °C for a day did not generate any of the desired rearrangement product (Scheme 4.13). By increasing the temperature in a separate trial reaction (100 °C, 24 h), the starting kojate **53** began to decompose to kojic acid.



Scheme 4.12 Attempted Ph₂GuanBARF-catalyzed Claisen rearrangement.

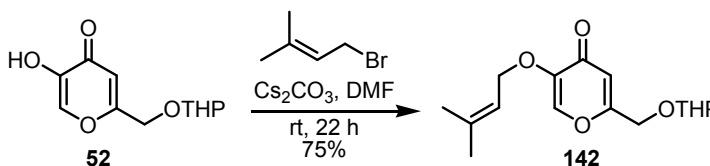


Scheme 4.13 Unsuccessful Claisen rearrangements in the presence of (PPh₃)AuOTf.

4.4 Preliminary Results from the Catalytic Claisen Rearrangements of *O*-Prenyl Kojates

Numerous fruitless attempts to catalyze the rearrangement of **53** caused us to focus our efforts on a simpler substrate, namely *O*-prenyl kojate **142**, easily accessed by treating **52** with prenyl bromide (Scheme 4.14). Wender's mention of the productivity of Zn(OTf)₂ in combination with PyBOX^{100c} inspired our investigation of the rearrangement of **142** under similar catalytic conditions. The use of various BOX ligands in conjunction with metal triflates has been a successful approach to asymmetric catalytic Claisen rearrangements.^{100c,105} Furthermore, rate acceleration has been reported for the Cu(OTf)₂-catalyzed rearrangement of (allyloxy)acrylates.^{105a} With Cu(OTf)₂ alone, the reaction requires 24 h to go to completion (Scheme 4.6),¹⁰⁴ whereas with both Cu(OTf)₂ and a

BOX ligand, the reaction is complete in only an hour.^{105a} For the present trial reaction of **142**, a BOX ligand previously synthesized by Dr. Yunfan Zou (Figure 4.4)¹¹² was chosen to pair with Zn(OTf)₂. Unfortunately, no rearrangement product was detected even with extended periods of heating (50 °C, 3 days).



Scheme 4.14 Facile synthesis of **142**.

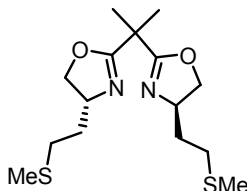
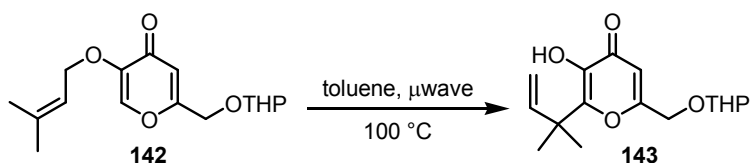


Figure 4.4 BOX ligand synthesized by Dr. Zou.

With the lack of success encountered using conventional heating methods, the mode of heating was changed to microwave irradiation. Substantial conversion of **142** to **143** was observed in the presence of Zn(OTf)₂ (10 mol%) and PyBOX (10 mol%) after only 50 min at 100 °C (Table 4.3, entry 2). To determine if the ligand was responsible for the rate acceleration, the amount of ligand was doubled to 20 mol%, which would lead to more of the Zn-ligand complex being present at equilibrium (entry 3). The result of this test reaction was that the conversion decreased to only 10%, suggesting that catalysis of

the rearrangement actually decreases in the presence of PyBOX for this substrate. To corroborate this observation, the reaction was run in the absence of PyBOX ligand giving rise to full conversion to **143** after only 1 h at 100 °C (entry 4). The apparent inhibitory effect of the PyBOX ligand on the rearrangement of **142** was quite surprising. Gratifyingly, these results established microwave irradiation as the optimal heating mode for relatively rapid Claisen rearrangements of *O*-allyl kojates.

Table 4.3 Microwave-assisted catalytic Claisen rearrangements.

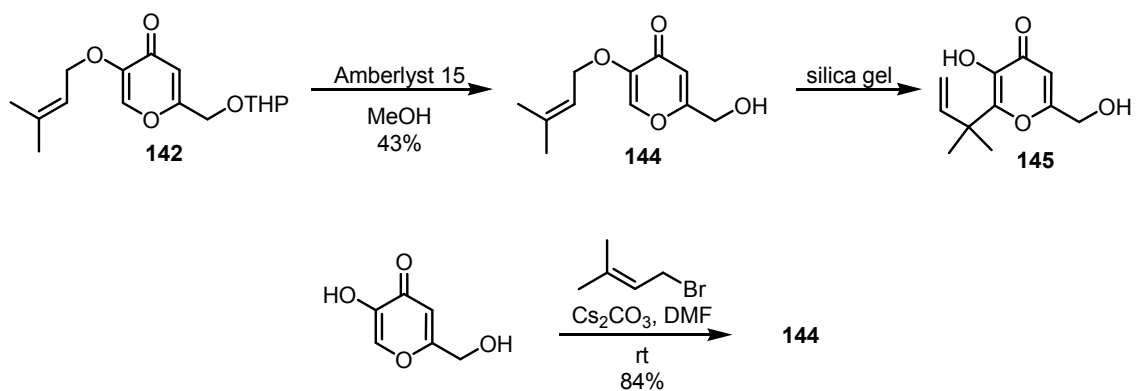


Entry	mol%		Time (min)	% conversion ^a
	Zn(OTf) ₂	PyBOX		
1	10	10	25	7
2	10	10	50	42
3	10	20	60	10
4	10	0	60	100

^aPercent conversion calculated from ¹H NMR integrations of crude product mixture.

In some of the catalytic trial reactions of **142** mentioned above, loss of the THP group was also observed in the ¹H NMR of the crude material. Previously in our lab, we have demonstrated that partial removal of the THP group is observed in the microwave-mediated Claisen rearrangement of (indolyl)kojic acids (Scheme 1.9).⁵⁰ With **142**, this partial loss of the THP protection often caused a messy crude spectrum, which hindered our ability to follow the reaction's progress by ¹H NMR.

To further simplify the substrate for ease of use in a catalyst screen, the THP group was removed from **142** upon treatment with Amberlyst® 15 to yield **144** (Scheme 4.15). Great care had to be taken with kojate **144** during the purification process, as the acidity of silica gel ($pK_a \approx 6.5$)¹¹³ is sufficient to cause some premature rearrangement, leading to contamination by **145**. To circumvent this issue, the silica gel was neutralized (1% Et₃N added into the solvent used to equilibrate the column) prior to the addition of product to the column. Despite the avoidance of material loss by inopportune rearrangement, the yield for this transformation was only as high as 43%. Consistent with the determination that THP protection and deprotection steps are unnecessary for the synthesis of indolykojate **128** (Scheme 3.12), **144** was synthesized directly from kojic acid and prenyl bromide without the need for THP protection of the primary alcohol of kojic acid prior to reaction with prenyl bromide. The yield is excellent at 84%, especially when compared to the 32% overall yield to obtain **144** by way of the THP protected intermediate **142**.



Scheme 4.15 Methods for the synthesis of *O*-prenyl kojate **144**.

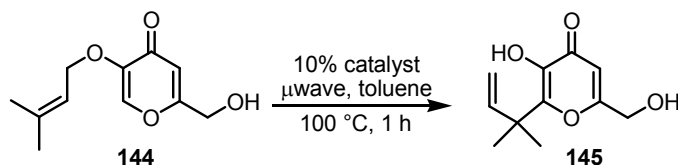
4.5 Catalyst Screen

With the promising preliminary results for the rearrangement of **142**, a screen was developed utilizing various catalysts known to effectively induce the Claisen rearrangement of *O*-allyl kojates and aryl allyl ethers.^{103,104,106-111} To compare the catalytic reactions to the thermal rearrangement, **144** was heated neat at 160 °C for 1 h to obtain **145** in 94% yield. Under the conditions reported by Wender for the thermal Claisen rearrangement (EtOH, 78 °C, 60 h; Scheme 4.2),^{100b} **145** was formed in 79% yield.

The catalyst screen for the rearrangement of **144** was conducted in anhydrous toluene (0.028 M) under microwave irradiation at 100 °C for 1 h, with 10 mol% catalyst present (Table 4.4). The crude product ¹H NMR spectra was typically clean, allowing for the reaction progress to easily be determined by integration of the vinylic protons. Additionally, the crude products were purified to determine isolated yields. All of the reactions were performed in duplicate.

Employing BF₃•OEt₂¹⁰⁹ for the rearrangement of **144**, only a trace amount of desired product was formed, though the background reaction in the absence of catalyst yielded 4% of the desired product, indicating BF₃•OEt₂ is an inhibitor of the rearrangement of this substrate. As previously discussed, Hiersemann's report on Pd(II)-catalyzed Claisen rearrangements of (allyloxy)acrylates established that substrates with *E* vinyl groups worked best.¹⁰⁷ Kojate **144** contains an *E* vinyl group, but unfortunately, using PdCl₂(CH₃CN)₂ for the rearrangement in the present study furnished only a trace amount of **145**.

Table 4.4 Catalyst Screen.



Catalyst	% Conversion	% Yield
None	7	4
BF ₃ ·OEt ₂	<1	<1
PdCl ₂ (CH ₃ CN) ₂	<1	<1
Eu(fod) ₃	^a	8
(PPh ₃)AuCl	1	<1
(PPh ₃)AuOTf	8	5
Ph ₂ GuanBArF	10	14
Yb(OTf) ₃	100	15
Cu(OTf) ₂	100	12
AgOTf	9	5
Zn(OTf) ₂	100	31
Zn(OTf) ₂ ^b	100	39
HOTf	1	<1

^aEuropium salts present in the crude reaction mixture caused a messy ¹H NMR spectrum, therefore % conversion could not be calculated. ^bAcid scavenger, *t*Bu₂Pyr, was added to the reaction mixture.

With Eu(fod)₃^{110,111} as the catalyst for the rearrangement of **144**, the yield was only 8%. Gold (I) catalysis¹⁰⁸ was also attempted, but neither Ph₃PAuCl nor PhP₃AuOTf were able to successfully catalyze the rearrangement of kojate **144**. Using Jacobsen's achiral hydrogen-bond catalyst Ph₂GuanBArF,¹⁰⁶ we saw a modest improvement in the yield to 14%.

The metal triflates Yb(OTf)₃, Cu(OTf)₂, AgOTf, and Zn(OTf)₂ were also examined in the rearrangement of **144**. With Yb(OTf)₃ and Cu(OTf)₂,¹⁰⁴ full conversion to product was achieved, though the yields were still low at only 15% and 12% respectively. Minimal catalysis was observed using AgOTf to effect the rearrangement of **144**.

Similar to Yb(OTf)₃ and Cu(OTf)₂, employing Zn(OTf)₂ as catalyst led to full conversion to product and an isolated yield of 31%, the highest yield of all the catalysts screened. To determine whether the reaction was actually catalyzed by acid arising from hydrolysis of Zn(OTf)₂, two test reactions were conducted. With HOTf alone, there was only trace formation of the desired product. Conversely, with the inclusion of acid scavenger 2,6,-di-*t*-butylpyridine in the reaction with Zn(OTf)₂, the yield was actually slightly improved over the reaction with Zn(OTf)₂ alone, at 39%. This confirmed that zinc ion is responsible for catalysis of this rearrangement.

In an effort to improve the yield, the solvent was changed, due to the relative insolubility of **144** in anhydrous toluene. The starting material was soluble in (ClCH₂)₂, but in this solvent the yield was slightly decreased (23%) compared to the reaction in toluene. A 1:1 mixture of toluene and (ClCH₂)₂ was also employed, leading to a slight improvement in yield, 38%. Despite this slight increase, solvent effects were not studied any further.

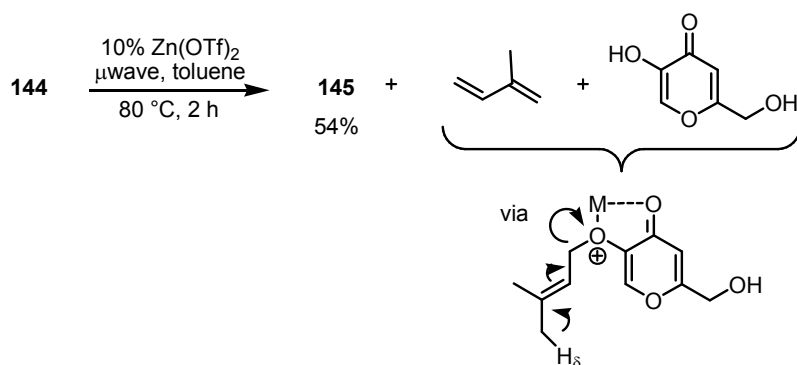
Under the standard conditions (Zn(OTf)₂, 100 °C, 1 h, toluene), full conversion of starting material **144** was always observed, but the yields could not be improved above 31%. Hypothesizing that the high temperature was causing degradation of the reaction

mixture, the temperature was decreased to 80 °C. Gratifyingly, the yield improved to 48%, though starting material was still remaining following the reaction. Full conversion was achieved by irradiating the reaction mixture at 80 °C for 2 h, which generated **145** in an improved, albeit moderate, yield of 54%.

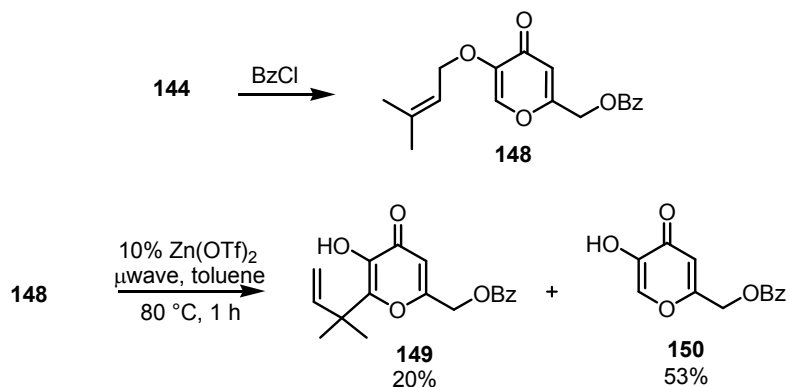
To support our earlier observation that the inclusion of PyBOX inhibits the Claisen rearrangement with our substrates, **145** was treated with Zn(OTf)₂ and PyBOX (10 mol% of each, 80 °C, 2 h). This reaction generated the product in the same yield (55%) as that obtained using Zn(OTf)₂ alone. This moderate yield was only achieved when the PyBOX reactions were conducted under an atmosphere of nitrogen. Conducting the Zn(OTf)₂-PyBOX reaction under air, as had been done for all of the reactions of the catalyst screen, furnished **145** in only 34% yield. Conversely, a nitrogen atmosphere was judged detrimental to the reaction catalyzed by Zn(OTf)₂ alone; the isolated yield decreased to 44%. Doubling the amount of PyBOX ligand had the same detrimental effect observed previously with the conversion of **142** to **143** (Table 4.3); the yield of **145** was only 18%. These results caused us to question Wender's brief report of success performing the asymmetric rearrangement of an *O*-allyl kojate, using the catalytic system of Zn(OTf)₂ and PyBOX (Scheme 4.3).^{100c}

Despite consistently high conversions, we were unable to obtain high yields, causing us to wonder if there was a divergent reaction pathway that was causing the formation of products we could not isolate. We hypothesized that, if the prenyl ether underwent elimination instead of the Claisen rearrangement, then this side reaction would yield volatile isoprene and kojic acid, which is polar and would not be recovered by

chromatography (Scheme 4.16). To test this hypothesis, benzoate **148** was synthesized to give an elimination product that could be isolated. When **148** was subjected to the catalyzed rearrangement conditions (10 mol% Zn(OTf)₂, 80 °C, 1 h), the desired product **149** was obtained in 20% yield, but the deprenylated product **150** was isolated in 53% yield (Scheme 4.17). These results indicate that the moderate yields with the unprotected substrate **144** are most likely due to an elimination side reaction from the presence of δ -protons.



Scheme 4.16 Possible explanation for consistent moderate yields in the Zn(OTf)₂-catalyzed rearrangement of *O*-prenyl kojate **144**.



Scheme 4.17 Evidence of a competing elimination reaction pathway.

To determine the rate acceleration for the $\text{Zn}(\text{OTf})_2$ -catalyzed rearrangement of **144** compared to the uncatalyzed version, kinetic studies were performed at 80 °C. Data for the catalyzed and uncatalyzed processes were collected at 3 time points (30, 120, 190 min), determining percent conversion at each time point from the ^1H integration of the vinylic protons of the crude reaction mixture. All reactions were performed in triplicate. The data for the percent conversion at each time point were fitted to a first-order kinetic equation. The rate constant for the catalyzed reaction was determined to be 0.035 s^{-1} (Figure 4.5) which, when compared to the rate constant for the uncatalyzed process (0.001 s^{-1} ; Figure 4.6), shows a 35-fold acceleration of the rate at 80 °C.

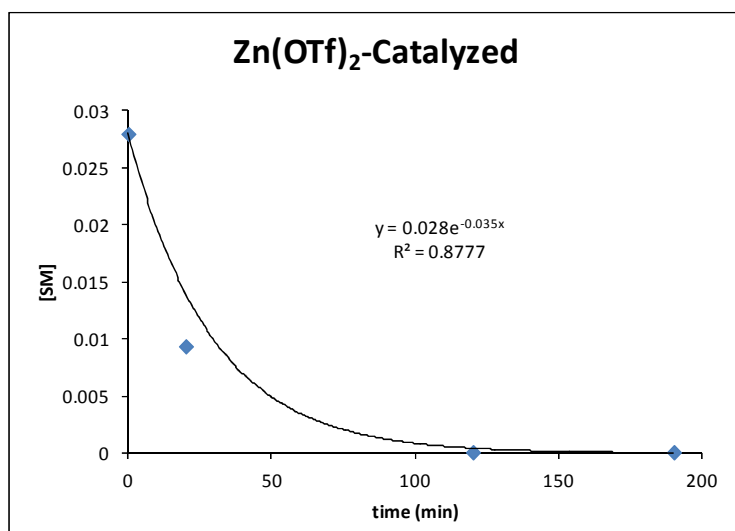


Figure 4.5 Kinetic rate plot for the $\text{Zn}(\text{OTf})_2$ -catalyzed Claisen rearrangement of **144**.

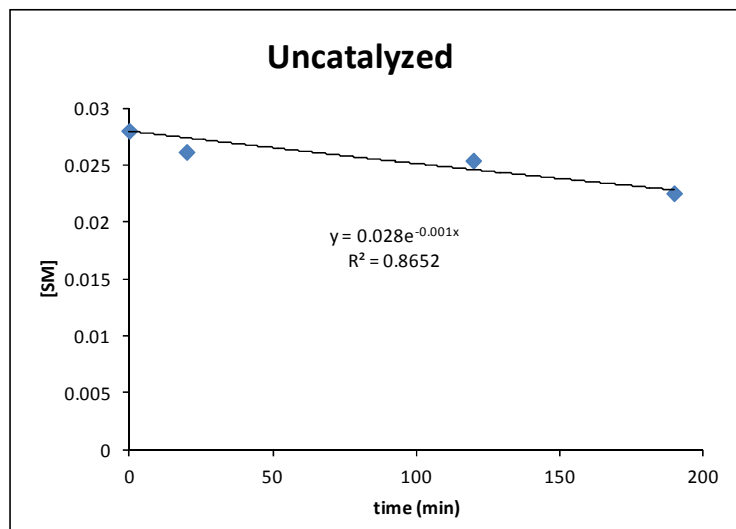
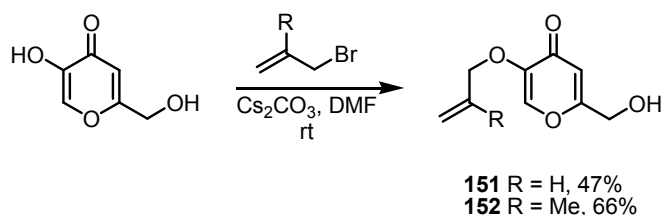


Figure 4.6 Kinetic rate plot for the uncatalyzed Claisen rearrangement of **144**.

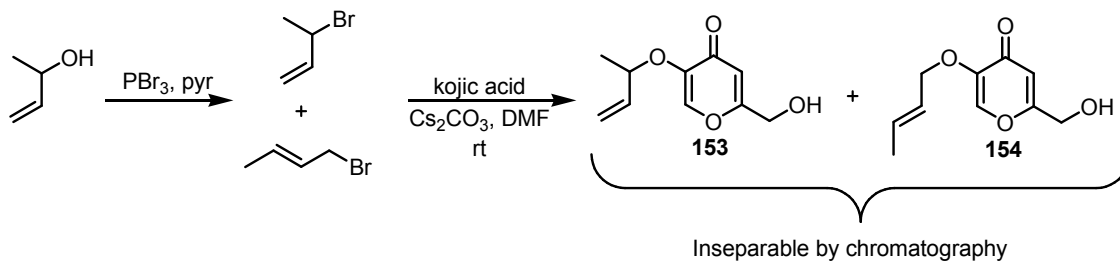
4.6 Synthesis of Other *O*-Allyl Kojates

In order to study the breadth of the $\text{Zn}(\text{OTf})_2$ -catalyzed reaction, a range of *O*-allyl kojates was synthesized. To begin, allyl kojate **151** and methallyl kojate **152** were easily synthesized by treating kojic acid with the corresponding allylic bromide (47% and 66% yield, respectively; Scheme 4.18). The brominated precursor for the allylic moiety of **153** is not commercially available, so a literature procedure was followed for the synthesis of 1-bromo-1-methyl-2-propene from 3-buten-2-ol.¹¹⁴ Unfortunately, the product isolated from this reaction was always a mixture of the desired bromide and *trans*-crotyl bromide, arising from allylic rearrangement (Scheme 4.19). This mixture was subjected to the typical coupling conditions with kojic acid, resulting in the formation of both of the expected products, **153** and **154**. Unfortunately, these two compounds are inseparable by chromatography, so a different route to **153** was devised. To circumvent these issues, the mesylate of 3-buten-2-ol was synthesized according to a

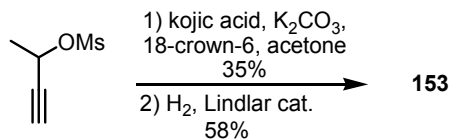
literature procedure¹¹⁵ and coupled to kojic acid in an unoptimized reaction (Scheme 4.20). Subsequent semihydrogenation yielded substrate **153** in moderate yield (58%).



Scheme 4.18 Facile synthesis of **151** and **152**.



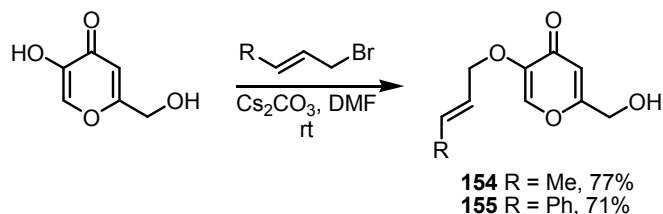
Scheme 4.19 Unsuccessful synthesis of **153**.



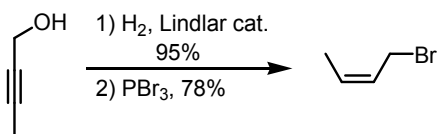
Scheme 4.20 Alternative route for the synthesis of **153**.

The *trans*-crotyl and *trans*-cinnamyl kojates, **154** and **155**, were synthesized under the typical conditions, treating kojic acid with the corresponding bromide (77% and 71%, respectively; Scheme 4.21). A synthetic pathway to *cis*-crotyl kojate **156** was also sought.

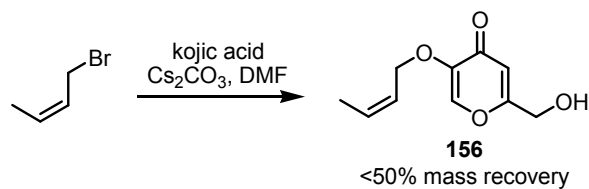
According to literature procedures, the internal alkyne of 2-butyn-1-ol was semihydrogenated to yield *cis*-2-buten-1-ol¹¹⁶ and the alcohol was treated with PBr₃ to yield the bromide (Scheme 4.22).¹¹⁷ With this material in hand, the *cis*-crotyl bromide was subjected to the coupling conditions with kojic acid, but the crude product always had low crude yields and the crude ¹H NMR spectra were always messy, indicating decomposition (Scheme 4.23). Due to the challenges in coupling *cis*-crotyl bromide to kojic acid, direct methylation of the terminal alkyne of **55** was attempted. Treatment of **55** with *n*-butyllithium or LDA, followed by methyl iodide did not yield the desired product though (Scheme 4.24). These synthetic issues prompted the abandonment of this route in favor of the development of an approach to the synthesis of *cis*-cinnamyl kojate **158**.



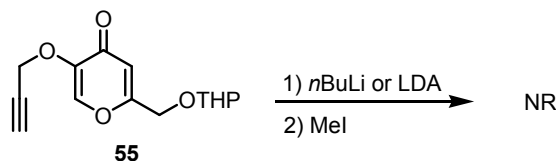
Scheme 4.21 Synthesis of *trans*-substituted allylic kojates.



Scheme 4.22 Literature synthesis of *cis*-crotyl bromide.

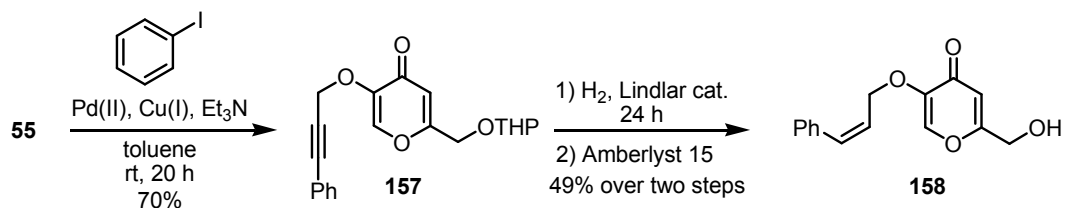


Scheme 4.23 Attempted coupling of kojic acid and *cis*-crotyl bromide.

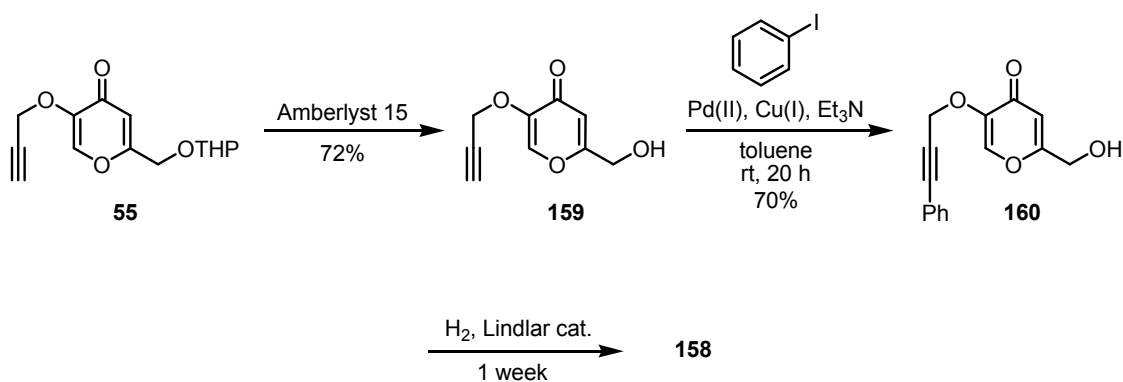


Scheme 4.24 Fruitless attempts to methylate **55**.

The *cis*-cinnamyl bromide needed to make **158** is not commercially available, so its synthesis was achieved in a three-step protocol by Sonogashira coupling of **55** with iodobenzene (70% yield of **157**), followed by Lindlar-catalyzed hydrogenation and THP removal to yield kojate **158** (49% yield over two steps; Scheme 4.25). An alternative route to **158** beginning with THP removal to obtain *O*-propargyl kojic acid **159** was also attempted to encourage the exploration of the direct synthesis of **159** from kojic acid, which would allow for the avoidance of THP protection altogether (Scheme 4.26). Unfortunately, the semihydrogenation step for unprotected kojate **160** was very difficult, requiring more than a week of reaction time under high H₂ pressure to obtain a product with low crude mass recovery, indicating THP protection is necessary for the successful semihydrogenation of this *cis*-cinnamate precursor.



Scheme 4.25 Efficient protocol for the formation of **158**.

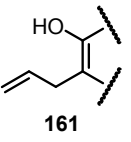
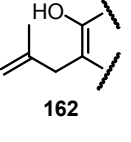
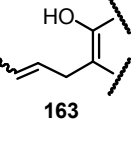
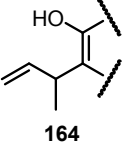
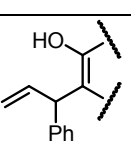
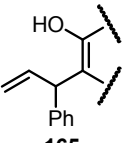
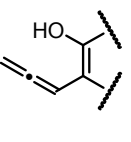


Scheme 4.26 Initial THP removal in the synthesis of **157**.

4.7 Reaction Scope

Results from the examination of the $\text{Zn}(\text{OTf})_2$ -catalyzed Claisen rearrangement of various *O*-allyl kojates are summarized in Table 4.5. Conducting the microwave-assisted rearrangement of **151** at 100 °C for 1 h led to a meager 26% conversion to desired product **161**. Doubling the time and increasing the temperature (120 °C, 120 min) improved the conversion of **151** to **161** (62% conversion), but extending the reaction time at a slightly lower temperature was not beneficial (58% conversion). Finally, full conversion was achieved by irradiating **151** at 120 °C for 200 min, though the isolated yield was moderate (49%).

Table 4.5 Catalyzed Claisen rearrangement of various *O*-allyl kojates, conducted with Zn(OTf)₂ (10 mol%).

Substrate	Product	Conditions	Yield (%)
151	 161	120 °C, 200 min	49
152	 162	120 °C, 200 min	33
153	 163	120 °C, 200 min	59
154	 164	80 °C, 120 min	46
155	 165	80 °C, 120 min	84
158	 165	120 °C, 60 min	41
159	 165	80° C, 120 min	NR

Ligand effects were also examined with this allylated substrate **151**. Conducting the reaction at 120 °C for 200 min in the presence of Zn(OTf)₂ (10 mol%) and PyBOX

(10 mol%) was detrimental to the reaction outcome, as evidenced by the isolated yield of only 20%. To ensure that the time or temperature were not detrimental to the catalyzed reaction, the time and temperature were both decreased (100 °C, 100 min) while maintaining the amount of Zn(OTf)₂ and PyBOX (10 mol% each). In this case, the yield decreased even further to only 12%, a result that again suggests that the inclusion of PyBOX ligand actually hinders catalysis.

The optimized conditions for the rearrangement of *O*-prenyl kojate **144** (80 °C, 2 h) were judged insufficient for the analogous reaction of **152** due to the low conversion to desired product **162** (25%). Extending the time and temperature to 200 min at 120 °C, just as with allyl kojate **151**, allowed for the full conversion of starting material and the isolation of **162** in 33% yield. Likewise, harsh conditions were essential to the rearrangement of **153** in order to produce **163** in a decent 59% yield. The additional time and temperature needed for acceptable conversion of allylic substrates **151-153** compared to prenylated kojate **144** is consistent with the fact that greater substitution on the end of the allyl chain facilitates the Claisen rearrangement. Hiersemann reported similar results with various allyl vinyl ethers, where the substrates required a higher catalyst loading (20 mol%) and longer reaction times (5 days).¹⁰⁵

In contrast to the allylic kojates **151-153**, *trans*-substituted kojic acid derivatives **154** and **155** were exceedingly reactive at lower temperatures. Rearrangement of *trans*-crotyl kojate **154** catalyzed by Zn(OTf)₂ at 80 °C for 2 h afforded **164** in 46% yield, a decent result on par with that of **144** under identical conditions. Astonishingly, the catalytic Claisen rearrangement of **155** generated **165** in excellent yield (84%). The high

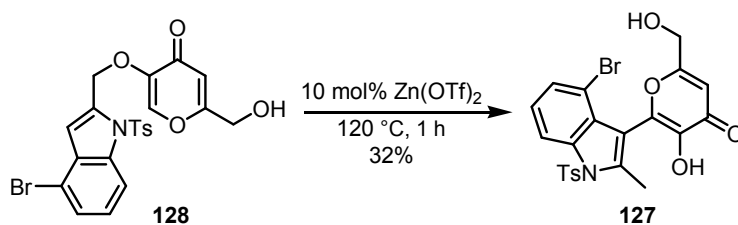
yield of the rearrangement of the *trans*-cinnamyl derivative **155** compared to the moderate yield of that with the *trans*-crotyl derivative **154** provides further support for our theory that compounds, such as prenyl (**142** and **144**) and crotyl kojates (**154**), with δ -protons have an elimination pathway available to them that diminishes the yields of the corresponding rearranged products.

Interestingly, *trans*-crotyl kojate **154** rearranges readily when stored at room temperature over time or when heat is used to remove solvent, so this precursor had to be handled with care. Indeed, when **154** was heated neat at only 45 °C for 3 days, there was an 8% conversion to the Claisen rearrangement product (by ^1H NMR). As a point of comparison, *trans*-cinnamyl kojate **155** was also heated neat for an extended period of time (45 °C, 3 days), but there was no conversion to product at all. Due to the facile uncatalyzed rearrangement of **154**, CH_2Cl_2 , instead of relatively high-boiling EtOAc, was used as the extraction solvent during the work-up following the coupling reaction to generate **154**, and this Claisen precursor was purified and used immediately in the catalyzed rearrangement step. These findings indicate that, though the *trans*-crotyl derivative **154** is a more reactive substrate for the Claisen rearrangement in general, under the catalyzed conditions, the *trans*-cinnamyl derivative **155** is far superior due to this compound lacking δ -protons.

Following the reaction of *cis*-cinnamyl kojate **158** for 2 h at 80 °C in the presence of $\text{Zn}(\text{OTf})_2$, only half of the product mixture was composed of the rearrangement product **165**. The similarity of starting material and product by TLC encouraged the development of conditions that would induce total conversion of **158** to **165**. This goal

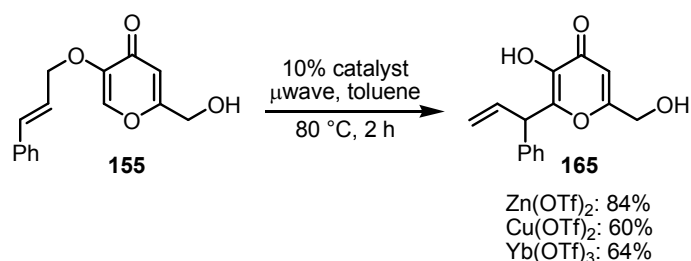
was achieved by increasing the reaction temperature (120 °C, 1 h), a change that afforded **165** in 41% isolated yield. This moderate result compared to that of *trans*-cinnamate derivative **155** suggested that, though the absence of δ -protons is integral to the avoidance of an elimination side reaction, the configuration of the vicinal-disubstituted alkene is integral to reactivity. These findings also suggest that Wender was fortunate to have used a *trans*-disubstituted allyl kojate precursor (Scheme 4.2),^{100c} as we have established that these compounds are excellent substrates for the Claisen rearrangement.

At 80 °C for 2 h, *O*-propargyl kojic acid **159** (Scheme 4.26) gave no reaction. Indolylkojate **128** (Scheme 4.27) was also subjected to the Zn(OTf)₂-catalyzed rearrangement conditions (80 °C, 2 h), but there was only 13% conversion to **127**. As was previously discussed (Section 3.2), complete conversion to product was essential for successful purification, making it necessary to modify the time and temperature parameters for this catalytic reaction. Through much trial and error, it was determined that conducting the catalyzed reaction at 120 °C for 1 h led to near total conversion to product and 32% yield. Heating for longer periods of time or at higher temperatures only resulted in decomposition of the reaction mixture.



Scheme 4.27 Indolylkojate used to examine the scope of the Zn(OTf)₂-catalyzed reaction.

In light of the findings that *trans*-cinnamyl kojate **155** is a better substrate for the Zn(OTf)₂-catalyzed rearrangement when compared to prenyl kojate **144** used in the initial catalyst screen, we sought to validate the superiority of Zn(OTf)₂ as the catalyst with this enhanced substrate. Two of the catalysts from the original screen, Yb(OTf)₃ and Cu(OTf)₂, were chosen for this study due to their established ability to fully convert **144** to product. Though the isolated yields for the rearrangement of **155** with Yb(OTf)₃ and Cu(OTf)₂ (64% and 60%, respectively) were a vast improvement over the original yields with **144**, these results indicate that Zn(OTf)₂ is indeed the optimal catalyst tested for the Claisen rearrangement of *O*-allyl kojates (Scheme 4.28).



Scheme 4.28 Establishment of the superiority of Zn(OTf)₂ as catalyst.

4.8 Conclusion

Conventional heating methods were found to be ineffective for the catalyzed Claisen rearrangement of indolylkojate **53**. By using a simpler substrate and microwave irradiation, a wide variety of catalysts, known to catalyze the Claisen rearrangement of allyl aryl ethers and (allyloxy)acrylates, were tested for their ability to catalyze the rearrangement of the kojate ether substrate **144**. Of those tested, only select metal

triflates, Yb(OTf)₃, Cu(OTf)₂, and Zn(OTf)₂, provided complete conversion to **145**, with Zn(OTf)₂ giving the highest yield of 31%. Through a few optimizations, the yield was improved to 54%. The inability to improve this moderate yield any further is most likely due to a competing elimination pathway. A 35-fold rate acceleration was calculated for this Zn(OTf)₂-catalyzed process, compared to the thermal rearrangement at 80 °C. This methodology was extended to a range of allylic kojate ethers, including indolylkojate **128**. Of the kojic acid derivatives tested, *trans*-cinnamyl kojate **155** afforded the best yield (84%), due to both the fact that this substrate does not have the elimination pathway available to it and the fact that *trans*-substituted alkenes work best under these conditions. PyBOX ligand was also observed to be an inhibitor of the Zn(OTf)₂-catalyzed rearrangement of *O*-allyl kojates, despite a report indicating otherwise.

Chapter 5. Experimental Details

General. All reagents were purchased from commercial sources and used without further purification. Anhydrous solvents and unstabilized solvents for column chromatography were obtained from a Glass Contour Solvent Purification System. Reactions were carried out in oven-dried glassware under a nitrogen atmosphere using standard syringe and septum techniques unless otherwise stated. Microwave reactions were carried out in an oven-dried microwave vessel sealed under air, unless otherwise stated. Microwave irradiation was performed in a CEM Discover™ microwave reactor (maximum 300 W and 250 psi). Temperature was monitored with the IR temperature monitoring function of the Discover™ reactor. Thin-layer chromatography (TLC) was carried out on aluminum-backed plates of silica gel 60 F₂₅₄. Visualization of the developed TLC plate was performed by UV light and staining with vanillin. Flash column chromatography was performed using silica gel 60, except in the case of Claisen rearrangement precursors that are acid-sensitive, where silica gel was neutralized by the addition of 1% Et₃N into the solvent used to equilibrate the column. All melting point data were measured on a Büchi Melting Point B-545 and are uncorrected. GC analysis was accomplished using an Agilent Technologies 6890N instrument with an HP-5 column (30 m × 0.32 mm) and using an injection temperature of 325 °C and detector temperature of 350 °C. HPLC analysis was conducted using an Agilent Technologies 1100 Series instrument with a Chiralpak AD column from Daicel Chemical Industries. IR spectra were recorded on a Perkin Elmer Spectrum One FT-IR spectrometer using the Universal ATR Sampling Accessory and are reported in absorption frequency (cm⁻¹). ¹H and ¹³C NMR spectra were

recorded on Varian Inova NMR spectrometers (300 MHz or 400 MHz) and were internally referenced to residual solvent proton signals. Data for ^1H NMR spectra are reported as follows: chemical shift (δ ppm), integration, multiplicity (s = singlet, br s = broad singlet, d = doublet, t = triplet, q = quartet, m = multiplet), and coupling constant (Hz). Data for ^{13}C NMR are reported in terms of chemical shift (δ ppm). Mass spectra were obtained on an Agilent Time-of-flight LCMS instrument.

1-Butyl-5-(prop-2-ynyloxy)-2-((tetrahydro-2H-pyran-2-yloxy)methyl)pyridin-4(1H)-one (77).

To a solution of 5-prop-2-ynyloxy-2-(tetrahydro-pyran-2-yloxymethyl)-pyran-4-one **55**⁵⁰ (1.37 g, 5.17 mmol) in 1:1 H_2O :EtOH (100 mL) was added 40% wt. solution *n*-butylamine in H_2O (1.85 mL, 10.1 mmol). The reaction mixture was stirred at 75 °C for 6 h and was concentrated. The residue was resubmitted to the reaction conditions, by dissolving the residue in 1:1 H_2O :EtOH (100 mL) and adding 40% *n*-butylamine in H_2O (1.85 mL, 10.1 mmol). The reaction mixture was heated at 70 °C for 4 h and concentrated. The residue was partitioned between H_2O and 4:1 CHCl_3 :*i*-PrOH. The aqueous phase was extracted twice with 4:1 CHCl_3 :*i*-PrOH. The combined organic phases were dried and concentrated. Purification of the crude product by flash column chromatography on silica gel, eluting with 12:1 CH_2Cl_2 :MeOH, gave the title compound (0.96 g, 58%) as a light brown oil. R_f = 0.25 (12:1 CH_2Cl_2 :MeOH). IR (neat) 3211, 2937, 2872, 2113, 1631, 1578, 1538, 1455, 1352, 1276, 1220, 1201, 1182, 1117, 1076, 1056, 1029, 968, 904, 870, 815, 7331, 698 cm^{-1} . ^1H NMR (300 MHz, CDCl_3) δ 7.19 (1H, s),

6.35 (1H, s), 4.72 (2H, d, $J = 2.3$ Hz), 4.56-4.54 (1H, m), 4.50 (1H, d, $J = 12.9$ Hz), 4.22 (1H, d, $J = 12.9$ Hz), 3.88-3.66 (3H, m), 3.45-3.39 (1H, m), 2.41 (1H, t, $J = 2.3$ Hz), 1.73-1.21 (10H, m), 0.83 (3H, t, $J = 7.3$ Hz). ^{13}C NMR (100 MHz, CDCl_3) δ 173.0, 146.4, 144.4, 130.0, 119.0, 98.1, 78.8, 76.0, 64.6, 62.5, 57.6, 52.6, 33.0, 30.2, 25.0, 19.6, 19.1, 13.6. HRMS calcd for $\text{C}_{18}\text{H}_{25}\text{NO}_4$ (M) $^+$ 319.1778, found 319.1775.

1-Allyl-5-(prop-2-ynyloxy)-2-((tetrahydro-2H-pyran-2-yloxy)methyl)pyridin-4(1H)-one (78).

The procedure for the synthesis of **77** was followed, except the reaction was conducted using allylamine at 45 °C for 14 h total. Purification of the crude product by flash column chromatography on silica gel, eluting with 12:1 CH_2Cl_2 :MeOH gave the title compound (0.51 g, 55%) as a light orange solid, mp 84.5-86.0 °C. $R_f = 0.58$ (12:1 CH_2Cl_2 :MeOH). IR (neat) 3138, 2947, 2871, 2106, 1631, 1563, 1536, 1451, 1414, 1391, 1352, 1321, 1308, 1288, 1256, 1227, 1202, 1183, 1130, 1075, 1050, 1033, 997, 968, 918, 906, 887, 864, 815, 750, 716 cm^{-1} . ^1H NMR (300 MHz, CDCl_3) δ 7.26 (1H, s), 6.51 (1H, s), 5.99-5.87 (1H, m), 5.29 (1H, d, $J = 10.0$ Hz), 5.07 (1H, dd, $J = 1.2$ Hz, 17.0 Hz), 4.88 (2H, m), 4.64-4.46 (3H, m), 4.31 (1H, d, $J = 12.9$ Hz), 3.84-3.72 (1H, m), 3.54-3.51 (1H, m), 2.47 (1H, t, $J = 2.3$ Hz), 1.83-1.52 (7H, m). ^{13}C NMR (100 MHz, CDCl_3) δ 173.6, 146.8, 144.9, 132.4, 130.6, 119.5, 118.6, 98.4, 79.0, 76.2, 64.9, 62.9, 58.0, 54.8, 30.5, 25.3, 19.5. HRMS calcd for $\text{C}_{17}\text{H}_{21}\text{NO}_4$ (M) $^+$ 303.1465, found 303.1472.

1-Isopropyl-5-(prop-2-ynyloxy)-2-((tetrahydro-2H-pyran-2-yloxy)methyl)pyridin-4(1H)-one (79).

To a stirring mixture of 5-prop-2-ynyloxy-2-(tetrahydro-pyran-2-yloxymethyl)-pyran-4-one **55** (0.514 g, 1.94 mmol) in EtOH (40 mL) was added isopropylamine (1.6 mL, 19 mmol). The reaction mixture was stirred at 45 °C and monitored by TLC. Every 6-18 h, another portion of isopropylamine (1.6 mL, 19 mmol) was added until the reaction was judged complete by TLC (139 h). In total, 6 portions of isopropylamine were added. The reaction mixture was concentrated. Purification of the crude product by flash column chromatography on silica gel, eluting with 25% hexanes in THF (unstabilized) gave the title compound (0.51 g, 87%) as an off-white solid, mp 110.9-111.7 °C. $R_f = 0.32$ (12:1 CH₂Cl₂:MeOH). IR (neat) 3243, 2941, 2872, 2113, 1629, 1571, 1532, 1463, 1388, 1351, 1262, 1191, 1163, 1115, 1079, 1027, 968, 904, 869, 815 cm⁻¹. ¹H NMR (400 MHz, CDCl₃) δ 7.42 (1H, s), 6.44 (1H, s), 4.85 (2H, d, $J = 2.3$ Hz), 4.66-4.60 (3H, m), 4.34 (1H, d, $J = 12.5$ Hz), 3.82-3.76 (1H, m), 3.54-3.51 (1H, m), 2.48 (1H, t, $J = 2.3$ Hz), 1.83-1.46 (6H, m), 1.42 (6H, d, $J = 6.3$ Hz). ¹³C NMR (100 MHz, CDCl₃) δ 173.2, 147.0, 144.2, 125.9, 120.0, 98.3, 79.2, 76.0, 65.3, 62.8, 58.1, 52.0, 30.5, 25.3, 22.9, 19.4. HRMS calcd for C₁₇H₂₃NO₄ (M)⁺ 305.1622, found 305.1626.

2-Amino-3-iodophenyl *tert*-butyl carbonate (102).

A suspension of 2-amino-3-iodophenol (0.219 g, 0.940 mmol) and di-*tert*-butyl dicarbonate (0.309 g, 1.41 mmol) in EtOH (4 mL) was stirred at room temperature for 5.5 h and the product mixture was concentrated. Purification of the crude product by flash

column chromatography on silica gel, eluting with 5% EtOAc in hexanes, gave the title compound (0.18 g, 57%) as a red-orange oil. $R_f = 0.44$ (silica gel, 9:1 hexanes:EtOAc). IR (neat) 3475, 3376, 2980, 2933, 2291, 1756, 1613, 1569, 1469, 1395, 1370, 1271, 1252, 1191, 1131, 1069, 1044, 1010, 904, 883, 842, 817, 778, 756, 737, 709 cm^{-1} . ^1H NMR (300 MHz, CDCl_3) δ 7.49 (1H, dd, $J = 1.2$ Hz, 8.2 Hz), 7.09 (1H, dd, $J = 1.2$ Hz, 8.2 Hz), 6.51 (1H, t, $J = 8.2$ Hz), 4.11 (2H, brs), 1.57 (9H, s). ^{13}C NMR (100 MHz, CDCl_3) δ 151.4, 139.8, 137.3, 136.2, 122.6, 119.5, 84.5, 84.3, 27.9. HRMS calcd for $\text{C}_{11}\text{H}_{14}^{127}\text{INO}_3\text{H} (\text{M}+\text{H})^+$ 336.0091, found 336.0081.

***tert*-Butyl 2-hydroxy-6-iodophenylcarbamate (104).**

A suspension of 2-amino-3-iodophenol (59 mg, 0.25 mmol) and di-*tert*-butyl dicarbonate (59 mg, 0.27 mmol) in anhydrous DCE (2 mL) was stirred at 85 °C for 42 h and concentrated. The crude residue was purified by flash column chromatography on silica gel equilibrated with hexanes. The crude material, dissolved in CH_2Cl_2 , was added to the column, followed by an additional portion of hexanes to elute the CH_2Cl_2 . Elution with 5% EtOAc in hexanes gave the title compound (39 mg, 45%) as a red oil. $R_f = 0.41$ (silica gel, 15% EtOAc in hexanes). IR (neat) 3377, 2979, 2931, 1683, 1571, 1512, 1463, 1393, 1368, 1292, 1248, 1152, 1078, 1052, 1026, 908, 864, 830, 812, 769, 731, 708 cm^{-1} . ^1H NMR (300 MHz, CDCl_3) δ 8.69 (1H, br s), 7.39 (1H, dd, $J = 1.2$ Hz, 7.6 Hz), 7.02 (1H, dd, $J = 1.2$ Hz, 8.2 Hz), 6.83 (1H, dd, $J = 7.6$ Hz, 8.2 Hz), 6.68 (1H, br s), 1.57 (9H, s). ^{13}C NMR (100 MHz, CDCl_3) δ 155.8, 149.7, 131.3, 128.2, 127.0, 120.9, 83.4, 28.4.

***tert*-Butyl 2-(benzyloxy)-6-iodophenylcarbamate (101).**

A suspension of **104** (17 mg, 0.049 mmol), benzyl bromide (8.0 μ L, 0.067 mmol), and K_2CO_3 (10 mg, 0.070 mmol) in anhydrous DMF (1 mL) under N_2 was stirred at room temperature for 15 h. Water was added and the reaction mixture was extracted with EtOAc twice. The combined organic phases were washed with brine, dried ($MgSO_4$), and concentrated. The crude product was purified by flash column chromatography on silica gel equilibrated with hexanes. The crude material, dissolved in CH_2Cl_2 , was added to the column, followed by an additional portion of hexanes to elute the CH_2Cl_2 . Elution with 19:1 hexanes:EtOAc gave the title compound (13 mg, 63%) as an off-white solid, mp 67.1-67.8 $^{\circ}C$. $R_f = 0.39$ (silica gel, 15% EtOAc in hexanes). IR (neat) 3388, 2957, 2921, 2851, 1705, 1570, 1487, 1454, 1439, 1366, 1245, 1157, 1080, 1021, 910, 862, 838, 820, 763, 732, 695 cm^{-1} . 1H NMR (400 MHz, $CDCl_3$) δ 7.47-7.33 (6H, m), 6.96-6.90 (2H, m), 6.01 (1H, br s), 5.10 (2H, s), 1.49 (9H, s). ^{13}C NMR (100 MHz, $CDCl_3$) δ 154.9, 153.6, 136.7, 131.3, 129.3, 128.7, 128.2, 127.5, 113.3, 100.8, 80.6, 71.0, 29.9, 28.5. HRMS calcd for $C_{18}H_{20}^{127}INO_3Na$ ($M+Na$) $^+$ 448.0380, found 448.0399.

***tert*-Butyl 7-(benzyloxy)-2-((4-oxo-6-((tetrahydro-2H-pyran-2-yloxy)methyl)-4H-pyran-3-yloxy)methyl)-1H-indole-1-carboxylate (107).**

To a degassed suspension of **101** (61 mg, 0.14 mmol), $Pd(PPh_3)Cl_2$ (10 mg, 0.015 mmol), and CuI (3 mg, 0.015 mmol) in anhydrous toluene (1.4 mL) under Ar was added anhydrous DIPEA (0.29 mL). An initial portion of **55**⁵⁰ (89 mg, 0.33 mmol) in anhydrous toluene (2.4 mL) was added in a dropwise manner over 20 min. Reaction progress was

monitored by TLC and additional portions of **55** in toluene were added as needed. In total, 3 portions of **55** (0.211 g total, 0.799 mmol) were added over 32 h. When **101** was judged by TLC to be consumed, the product mixture was filtered through Celite, washing with CH₂Cl₂. The filtrate was washed with water and brine. The organic phase was dried (MgSO₄) and concentrated. The crude residue was placed under a N₂ atmosphere and anhydrous THF (8 mL) was added. TBAF (1.0 M in THF, 1.6 mL, 1.6 mmol) was added in a dropwise manner to the solution and the reaction mixture was stirred at room temperature for 2 h and concentrated. The residue was partitioned between CH₂Cl₂ and water. The aqueous phase was extracted with CH₂Cl₂ twice and the combined organic extracts were dried (MgSO₄) and concentrated. The crude product was purified by flash column chromatography on silica gel equilibrated with hexanes/1% Et₃N. The crude material, dissolved in CH₂Cl₂, was added to the column, followed by an additional portion of hexanes/1% Et₃N to elute the CH₂Cl₂. Elution with 30% EtOAc in hexanes gave the title compound (28 mg, 35%) as a light orange oil. $R_f = 0.39$ (silica gel, 1:1 EtOAc:hexanes). IR (neat) 2920, 2851, 1746, 1653, 1626, 1591, 1492, 1455, 1431, 1369, 1349, 1317, 1236, 1199, 1152, 1103, 1076, 1035, 971, 943, 905, 870, 844, 815, 765, 728, 696 cm⁻¹. ¹H NMR (300 MHz, CDCl₃) δ 7.52 (1H, s), 7.50 (2H, d, $J = 6.4$ Hz), 7.41-7.29 (4H, m), 7.15-7.08 (2H, m), 6.85 (1H, dd, $J = 2.3$ Hz, 6.4 Hz), 6.51 (1H, s), 6.50 (1H, s), 5.41 (2H, s), 5.20 (2H, s), 4.71-4.68 (1H, m), 4.46 (1H, d, $J = 14.7$), 4.27 (1H, d, $J = 14.7$), 3.84-3.76 (1H, m), 3.56-3.39 (1H, m), 2.05-1.51 (6 H, m), 1.48 (9H, s). ¹³C NMR (75 MHz, CDCl₃) δ 175.4, 164.8, 150.1, 147.2, 146.0, 145.3, 137.1, 134.6, 130.7, 128.6, 128.1, 126.8, 123.2, 114.0, 113.9, 109.5, 107.5, 105.0, 98.4, 84.6, 71.0, 65.4, 64.3, 62.2,

30.3, 29.9, 27.7, 25.4, 19.0. HRMS calcd for C₃₂H₃₄NO₈Na (M+Na)+[-H] 583.2177, found 583.2205.

***tert*-Butyl 7-(benzyloxy)-2-((1-methyl-4-oxo-6-((tetrahydro-2*H*-pyran-2-yloxy)methyl)-1,4-dihydropyridin-3-yloxy)methyl)-1*H*-indole-1-carboxylate (108).**

The procedure for the synthesis of **107** was followed, except alkyne **67**⁵⁰ was added as a solution in anhydrous THF in the Sonogashira coupling step. The crude product was purified by flash column chromatography on silica gel equilibrated with hexanes/1% Et₃N. The crude material, dissolved in CH₂Cl₂, was added to the column, followed by an additional portion of hexanes/1% Et₃N to elute the CH₂Cl₂. Elution with 40% hexanes in THF (unstabilized) gave the title compound (18 mg, 35%) as a light brown oil. *R*_f = 0.19 (silica gel, 3:1 THF:hexanes). IR (neat) 2933, 2872, 2216, 1746, 1630, 1575, 1492, 1455, 1369, 1315, 1278, 1177, 1153, 1129, 1103, 1076, 1030, 968, 906, 846, 815, 727, 697 cm⁻¹. ¹H NMR (300 MHz, CDCl₃) δ 7.51 (2H, d, *J* = 7.0 Hz), 7.41-7.29 (3H, m), 7.12-7.06 (2H, m), 6.91 (1H, s), 6.84 (1H, dd, *J* = 3.2 Hz, 5.6 Hz), 6.52 (1H, s), 6.46 (1H, s), 5.53 (2H, s), 5.30 (2H, s), 4.65-4.63 (1H, m), 4.54 (1H, d, *J* = 13.5 Hz), 4.28 (1H, d, *J* = 12.9 Hz), 3.83-3.75 (1H, m), 3.55-3.53 (1H, m), 3.49 (3H, s), 1.88-1.58 (6H, m), 1.52 (9H, s). ¹³C NMR (100 MHz, CDCl₃) δ 174.0, 150.3, 147.1, 146.6, 144.9, 137.1, 135.7, 133.2, 130.8, 128.6, 128.1, 126.8, 123.0, 119.6, 113.9, 109.1, 107.2, 105.0, 98.4, 85.5, 71.0, 65.2, 64.8, 62.8, 59.4, 40.6, 30.5, 27.7, 25.3, 24.4, 20.0, 19.4, 13.9. HRMS calcd for C₃₃H₃₈N₂O₇ (M) 574.2674, found 574.2693.

***tert*-Butyl 7-(benzyloxy)-2-((1-butyl-4-oxo-6-((tetrahydro-2*H*-pyran-2-yloxy)methyl)-1,4-dihydropyridin-3-yloxy)methyl)-1*H*-indole-1-carboxylate (109).**

The procedure for the synthesis of **107** was followed, except alkyne **77** was added as a solution in anhydrous THF in the Sonogashira coupling step. The crude product was purified by flash column chromatography on silica gel equilibrated with hexanes/1% Et₃N. The crude material, dissolved in CH₂Cl₂, was added to the column, followed by an additional portion of hexanes/1% Et₃N to elute the CH₂Cl₂. Elution with 40% hexanes in THF (unstabilized) gave the title compound (15 mg, 18%) as a light brown oil. *R_f* = 0.34 (silica gel, 25% hexanes in THF). IR (neat) 2928, 2871, 2212, 1747, 1631, 1575, 1533, 1492, 1455, 1436, 1369, 1350, 1318, 1232, 1177, 1153, 1118, 1102, 1075, 1029, 966, 905, 870, 845, 814, 766, 728, 695 cm⁻¹. ¹H NMR (300 MHz, CDCl₃) δ 7.51 (2H, d, *J* = 7.6 Hz), 7.40-7.31 (3H, m), 7.07 (2H, d, *J* = 4.7 Hz), 6.88 (1H, s), 6.83 (1H, t, *J* = 4.7 Hz), 6.52 (1H, s), 6.40 (1H, s), 5.49 (2H, s), 5.20 (2H, s), 4.63-4.62 (1H, m), 4.53 (1H, d, *J* = 12.9 Hz), 4.26 (1H, d, *J* = 12.9 Hz), 3.98-3.51 (5H, m), 1.87-0.85 (25H, m), 0.68 (3H, t, *J* = 7.0 Hz). ¹³C NMR (100 MHz, CDCl₃) δ 174.1, 150.3, 147.1, 146.2, 144.6, 137.3, 137.1, 135.5, 133.1, 130.7, 130.0, 128.6, 128.0, 123.0, 119.9, 113.87, 109.5, 108.1, 107.3, 98.3, 84.6, 70.9, 67.9, 65.1, 64.9, 62.8, 52.62, 33.02, 30.5, 29.9, 29.3, 27.7, 25.4, 24.1, 19.7, 19.4, 13.6. HRMS calcd for C₃₆H₄₄N₂O₇Na (M+Na)⁺ 639.3041, found 639.3055.

***tert*-Butyl 7-(benzyloxy)-2-((1-isopropyl-4-oxo-6-((tetrahydro-2*H*-pyran-2-yloxy)methyl)-1,4-dihydropyridin-3-yloxy)methyl)-1*H*-indole-1-carboxylate (110).**

The procedure for the synthesis of **107** was followed, except alkyne **79** was added as a solution in anhydrous THF in the Sonogashira coupling step. The crude product was purified by flash column chromatography on silica gel equilibrated with hexanes/1% Et₃N. The crude material, dissolved in CH₂Cl₂, was added to the column, followed by an additional portion of hexanes/1% Et₃N to elute the CH₂Cl₂. Elution with 35% hexanes in THF (unstabilized) gave the title compound (32 mg, 23%) as a yellow oil. $R_f = 0.18$ (silica gel, 25% hexanes in THF). IR (neat) 2933, 2874, 1744, 1632, 1575, 1492, 1456, 1370, 1348, 1319, 1239, 1189, 1154, 1103, 1076, 1033, 967, 905, 845, 815, 729, 697 cm⁻¹. ¹H NMR (300 MHz, CDCl₃) δ 7.52 (2H, d, $J = 6.4$ Hz), 7.40-7.30 (3H, m), 7.05-7.03 (3H, m), 6.80 (1H, dd, $J = 4.1$ Hz, 4.7 Hz), 6.48 (1H, s), 6.38 (1H, s), 5.46 (2H, s), 5.21 (2H, s), 4.61-4.60 (1H, m), 4.55 (1H, d, $J = 12.9$ Hz), 4.38 (1H, qq, $J = 6.4$ Hz, 6.7 Hz), 4.29 (1H, d, $J = 12.9$ Hz), 3.83-3.75 (1H, m), 3.56-3.51 (1H, m), 2.12-1.26 (6H, m), 1.56 (9H, s), 1.05 (3H, d, $J = 5.3$ Hz), 1.03 (3H, d, $J = 7.0$ Hz). ¹³C NMR (100 MHz, CDCl₃) δ 178.1, 150.4, 147.0, 146.4, 144.1, 137.2, 135.5, 130.6, 129.1, 128.6, 128.1, 128.0, 123.0, 120.1, 113.8, 109.9, 107.4, 98.1, 84.7, 71.0, 65.5, 65.2, 63.0, 59.3, 51.9, 48.3, 30.6, 29.9, 27.8, 25.4, 24.3, 22.5, 20.0, 19.5, 13.9. HRMS calcd for C₃₅H₄₂N₂O₇ (M) 602.2987, found 602.3000.

2-(7-(Benzyloxy)-2-methyl-1*H*-indol-3-yl)-3-hydroxy-6-(hydroxymethyl)-4*H*-pyran-4-one (111).

A glass sample vial was charged with **107** (51 mg, 0.091 mmol) and heated neat in an oil bath at 155-160 °C open to the air for 49 h and cooled. The residue was purified by flash column chromatography, eluting with 20:1 CH₂Cl₂:MeOH to give the title compound (5 mg, 14%) as a light brown solid, mp 174.6 °C (dec.). *R_f* = 0.21 (silica gel, 20:1 CH₂Cl₂:MeOH). IR (neat) 3211, 2919, 2850, 1646, 1567, 1451, 1374, 1259, 1196, 1079, 1040, 857, 748, 723, 697 cm⁻¹. ¹H NMR (400 MHz, CD₃OD) δ 7.56 (2H, d, *J* = 7.0 Hz), 7.40 (2H, dd, *J* = 7.0 Hz, 7.8 Hz), 7.34 (1H, d, *J* = 7.0 Hz), 7.20 (1H, d, *J* = 7.8 Hz), 6.97 (1H, d, *J* = 7.8 Hz), 6.75 (1H, d, *J* = 7.8 Hz), 6.57 (1H, s), 5.26 (2H, s), 4.52 (2H, s), 2.49 (3H, s). ¹³C NMR (100 MHz, acetone-d₆) δ 193.9, 174.8, 169.0, 145.9, 145.7, 138.6, 138.4, 137.8, 129.3, 128.7, 128.6, 121.4, 113.7, 108.5, 104.2, 70.7, 61.4, 32.7, 23.4, 23.1, 14.4, 13.6. HRMS calcd for C₂₂H₂₀NO₅ (M+H)⁺ 378.1336, found 378.1347.

(*Z*)-Methyl 2-azido-3-(2-bromophenyl)acrylate (117).

Sodium metal (prewashed with petroleum ether, 0.401 g, 17.5 mmol) was added to anhydrous MeOH (17 mL) in a 3-neck round bottom flask under N₂. The reaction mixture was stirred at -40 °C for 20 min. A solution of methyl azidoacetate (2.70 g, 23.4 mmol) and 2-bromobenzaldehyde (0.54 mL, 4.6 mmol) in anhydrous MeOH (4.2 mL) under N₂ was added in a dropwise manner over a 40 min period. The reaction mixture was stirred at -40 °C for an additional 5.5 h and at 4 °C for 18.5 h. Water was added and the product mixture was concentrated. The product was extracted twice from the residue

using EtOAc and the combined organic extracts were washed with water and brine. The organic phase was dried (MgSO_4) and concentrated to give the title compound (1.1 g, 85%) as an orange solid. The resulting solid product needed no further purification and matched all literature data.⁹⁶

Methyl 4-bromo-1-tosyl-1*H*-indole-2-carboxylate (122).

Anhydrous CH_2Cl_2 (12 mL) was added to methyl 4-bromo-1*H*-indole-2-carboxylate **118**⁹⁶ (409 mg, 1.61 mmol), *p*-toluenesulfonyl chloride (342 mg, 1.79 mmol), triethylbenzylammonium chloride (37 mg, 0.16 mmol), and sodium hydroxide (104 mg, 2.61 mmol) under N_2 . The reaction mixture was stirred at room temperature for 2.5 h, filtered, and concentrated. Purification of the crude product by flash column chromatography on silica gel, eluting with hexanes:EtOAc (9:1), gave the title compound (0.56 g, 85%) as a white solid, mp 143.4-143.9 °C. $R_f = 0.31$ (silica gel, 25:1 hexanes:EtOAc). IR (neat) 2920, 2851, 1736, 1597, 1464, 1418, 1378, 1340, 1263, 1172, 1120, 1090, 1033, 969, 912, 814, 757, 702, 675, 660 cm^{-1} . ^1H NMR (300 MHz, CDCl_3) δ 8.10 (1H, d, $J = 8.7$ Hz), 7.94 (2H, d, $J = 8.4$ Hz), 7.45 (1H, d, $J = 7.8$ Hz), 7.29 (3H, m), 7.23 (1H, s), 3.96 (3H, s), 2.39 (3H, s). ^{13}C NMR (75 MHz, CDCl_3) δ 161.6, 145.6, 138.4, 135.7, 132.0, 130.0, 129.1, 128.1, 127.7, 127.2, 116.3, 116.1, 114.6, 53.2, 21.9. HRMS calcd for $\text{C}_{17}\text{H}_{14}^{79}\text{BrNO}_4\text{SNa}^+$ ($\text{M}+\text{Na}$)⁺ 431.9700, found 431.9690.

(4-Bromo-1-tosyl-1*H*-indol-2-yl)methanol (123).

To a solution of **122** (239 mg, 0.586 mmol) in anhydrous THF (6 mL) under N₂ at 50 °C was added LiBH₄ (2.0M in THF, 1.05 mL, 2.10 mmol) dropwise. The reaction was stirred at 50 °C under N₂ for 6.5 h and cooled to room temperature. The reaction mixture was diluted with CH₂Cl₂, washed with brine twice, dried (MgSO₄), and concentrated. Purification of the crude product by flash column chromatography on silica gel, eluting with hexanes:EtOAc (3:1), gave the title compound (145 mg, 65%) as a white oil. *R*_f = 0.43 (silica gel, 3:1 hexanes:EtOAc). IR (neat) 3567, 3369, 3111, 2921, 1910, 1652, 1596, 1559, 1493, 1471, 1452, 1421, 1370, 1341 1307, 1271, 1254, 1225, 1188, 1166, 1150, 1085, 1064, 1048, 1015, 959, 932, 826, 815, 808, 773, 766, 754, 700, 673 cm⁻¹. ¹H NMR (300 MHz, CDCl₃) δ 8.02 (1H, d, *J* = 9.0 Hz), 7.72 (2H, d, *J* = 8.4 Hz), 7.39 (1H, d, *J* = 8.4 Hz), 7.18 (3H, m), 6.74 (1H, s), 4.94 (2H, s), 3.01 (1H, br s), 2.34 (3H, s). ¹³C NMR (75 MHz, CDCl₃) δ 145.7, 141.1, 137.3, 135.4, 130.3, 130.0, 126.8, 126.7, 126.0, 115.1, 113.6, 110.9, 58.7, 21.8. HRMS calcd for C₁₆H₁₄⁷⁹BrNO₃SNa⁺ (M+Na)⁺ 401.9770, found 401.9761.

4-Bromo-2-(chloromethyl)-1-tosyl-1*H*-indole (124).

To a solution of **123** (0.141 g, 0.370 mmol) and Et₃N (0.11 mL, 0.79 mmol) in anhydrous CH₂Cl₂ (11.2 mL) under N₂ was added methanesulfonyl chloride (0.06 mL, 0.8 mmol) dropwise. The reaction mixture was stirred at room temperature under N₂ for 24 h and poured into sat aq NH₄Cl. The product was extracted twice with CH₂Cl₂ and the combined organic extracts were washed with brine, dried (MgSO₄), and concentrated.

Purification of the crude product by flash column chromatography on silica gel, eluting with hexanes:EtOAc (9:1), gave the title compound (110 mg, 72%) as a white solid, mp 110.0-111.9 °C. R_f = 0.58 (silica gel, 9:1 hexanes:EtOAc). IR (neat) 2924, 1697, 1597, 1556, 1494, 1473, 1419, 1370, 1324, 1309, 1294, 1261, 1211, 1190, 1174, 1150, 1122, 1089, 1062, 1049, 1018, 948, 902, 839, 809, 777, 764, 748, 728, 696 cm^{-1} . ^1H NMR (300 MHz, CDCl_3) δ 8.05 (1H, d, J = 8.1 Hz), 7.78 (2H, d, J = 8.7 Hz), 7.41 (1H, d, J = 7.5 Hz), 7.21 (3H, m), 6.88 (1H, s), 5.08 (2H, s), 2.35 (3H, s). ^{13}C NMR (75 MHz, CDCl_3) δ 145.7, 137.4, 137.2, 135.3, 130.1, 129.4, 126.9, 126.8, 126.4, 115.1, 113.8, 112.6, 53.6, 38.7, 21.7. HRMS calcd for $\text{C}_{16}\text{H}_{13}^{79}\text{Br}^{35}\text{ClNO}_2\text{SH}^+$ (M+H) $^+$ 399.9590, found 399.9601.

5-((4-Bromo-1-tosyl-1*H*-indol-2-yl)methoxy)-2-(hydroxymethyl)-4*H*-pyran-4-one (128).

To a stirring solution of kojic acid (45 mg, 0.32 mmol) and **124** (0.164 g, 0.410 mmol) in acetone (10 mL) was added K_2CO_3 (52 mg, 0.38 mmol) and tetrabutylammonium bromide (10 mg, 0.030 mmol). The reaction mixture was heated at reflux for 96 h, cooled, and concentrated. The residue was partitioned between H_2O and EtOAc. The aqueous phase was extracted with EtOAc. The combined organic phases were washed with brine, dried (MgSO_4), and concentrated. The crude material was purified by flash column chromatography on silica gel equilibrated with hexanes/1% Et_3N . The crude material, dissolved in CH_2Cl_2 , was added to the column, followed by an additional portion of hexanes/1% Et_3N to elute the CH_2Cl_2 . Elution with 20% hexanes in EtOAc gave the title compound (0.13 g, 83%) as a white solid, mp 158.4-159.0 °C. R_f = 0.36

(silica gel, 3:1 EtOAc:hexanes). IR (neat) 3369, 3100, 2930, 1646, 1631, 1608, 1591, 1558, 1447, 1418, 1401, 1370, 1351, 1333, 1303, 1295, 1260, 1230, 1201, 1193, 1153, 1087, 1065, 1048, 986, 945, 883, 874, 858, 840, 811, 778, 750, 739, 702, 673 cm^{-1} . ^1H NMR (300 MHz, CDCl_3) δ 8.00 (1H, d, $J = 8.2$ Hz), 7.91 (2H, d, $J = 8.8$ Hz), 7.64 (1H, s), 7.36 (1H, d, $J = 7.0$ Hz), 7.23 (2H, d, $J = 8.2$ Hz), 7.16 (1H, t, $J = 8.2$ Hz), 6.83 (1H, s), 6.56 (1H, s), 5.34 (2H, s), 4.43 (2H, s), 2.30 (3H, s). ^{13}C NMR (75 MHz, CDCl_3) δ 175.1, 168.2, 147.0, 145.8, 141.6, 137.1, 135.4, 135.1, 130.2, 129.6, 127.4, 126.7, 126.3, 115.2, 113.6, 112.9, 112.3, 64.9, 60.8, 21.7. HRMS calcd for $\text{C}_{22}\text{H}_{18}^{79}\text{BrNO}_6\text{SH}^+$ ($\text{M}+\text{H}$) $^+$ 506.0093, found 506.0111.

2-(4-Bromo-2-methyl-1-tosyl-1*H*-indol-3-yl)-3-hydroxy-6-(hydroxymethyl)-4*H*-pyran-4-one (127).

A glass sample vial was charged with **128** (24 mg, 0.048 mmol) and heated neat in an oil bath at 150 °C open to the air for 7 h and cooled. The crude material was purified by flash column chromatography on silica gel equilibrated with hexanes/1% Et_3N . The crude material, dissolved in CH_2Cl_2 , was added to the column, followed by an additional portion of hexanes/1% Et_3N to elute the CH_2Cl_2 . Elution with 20% hexanes in EtOAc gave the title compound (24 mg, 96%) as a white solid, mp 99 °C (dec.). $R_f = 0.32$ (silica gel, 4:1 EtOAc:hexanes). IR (neat) 3263, 2921, 2851, 1713, 1626, 1594, 1561, 1455, 1423, 1363, 1305, 1248, 1192, 1168, 1104, 1090, 1019, 997, 971, 939, 861, 842, 812, 776, 746, 703, 666 cm^{-1} . ^1H NMR (400 MHz, CDCl_3) δ 8.23 (1H, d, $J = 8.6$ Hz), 7.74 (2H, d, $J = 8.6$ Hz), 7.41 (1H, d, $J = 7.8$ Hz), 7.28 (2H, d, $J = 8.6$ Hz), 7.17 (1H, dd, $J =$

7.8 Hz, 8.6 Hz), 6.69 (1H, s), 4.55 (2H, d, $J = 10.1$ Hz), 2.57 (3H, s), 2.39 (3H, s). ^{13}C NMR (100 MHz, CDCl_3) δ 175.5, 168.2, 145.9, 144.4, 140.4, 140.1, 137.4, 135.8, 130.5, 128.5, 127.2, 126.8, 125.6, 113.9, 113.1, 110.1, 109.0, 61.6, 58.1, 29.9, 21.9, 14.2. HRMS calcd for $\text{C}_{22}\text{H}_{18}^{79}\text{BrNO}_6\text{SH}^+$ ($\text{M}+\text{H}$) $^+$ 504.0111, found 504.0118.

5-((4-Bromo-1-tosyl-1*H*-indol-2-yl)methoxy)-2-(hydroxymethyl)-1-methylpyridin-4(1*H*)-one (130).

To a solution of **128** (0.100 g, 0.198 mmol) in EtOH (7 mL) was added methylamine (40% solution in H_2O , 0.15 mL, 1.9 mmol). The reaction mixture was heated at reflux for 5.5 h and a second portion of methylamine was added (0.18 mL, 2.3 mmol). The reaction mixture was heated at reflux for an additional 16.5 h, cooled, and concentrated. The crude material was purified by flash column chromatography on silica gel equilibrated with hexanes/1% Et_3N . The crude oil was added to the column dissolved in CH_2Cl_2 :MeOH (20:1). Elution with CH_2Cl_2 :MeOH (20:1) gave the title compound (73 mg, 71%) as an off-white solid, mp 181.2-182.3 °C. $R_f = 0.10$ (silica gel, 20:1 CH_2Cl_2 :MeOH). IR (neat) 3095, 1709, 1631, 1560, 1528, 1451, 1418, 1370, 1331, 1295, 1264, 1232, 1190, 1165, 1152, 1133, 1087, 1064, 1050, 990, 941, 863, 853, 811, 768, 731, 700, 670 cm^{-1} . ^1H NMR (400 MHz, CDCl_3) δ 8.02 (1H, d, $J = 8.6$ Hz), 7.89 (2H, d, $J = 8.6$ Hz), 7.37 (1H, d, $J = 7.8$ Hz), 7.24 (2H, d, $J = 7.8$ Hz), 7.16 (1H, t, $J = 7.8$ Hz), 7.15 (1H, s), 6.82 (1H, s), 6.50 (1H, s), 5.45 (2H, s), 4.49 (2H, s), 3.69 (3H, s), 2.30 (3H, s). ^{13}C NMR (100 MHz, CDCl_3) δ 172.7, 149.3, 147.3, 145.7, 137.2, 136.5, 135.3, 130.5,

130.3, 129.8, 127.3, 126.8, 126.1, 117.9, 115.2, 113.7, 112.6, 65.3, 61.3, 41.0, 21.8.

HRMS calcd for $C_{23}H_{21}^{79}BrN_2O_5SH^+$ (M+H)⁺ 517.0427, found 517.0439.

2-(Hydroxymethyl)-5-(3-methylbut-2-enyloxy)-4H-pyran-4-one (144).

General procedure for the synthesis of *O*-allyl kojates: To a stirring solution of kojic acid (57 mg, 0.40 mmol) and Cs_2CO_3 (0.149 g, 0.457 mmol) in anhydrous DMF (1.21 mL) under N_2 at room temperature was added 3,3-dimethylallyl bromide (0.05 mL, 0.4 mmol). The reaction mixture was stirred at room temperature for 95 h and EtOAc was added, followed by H_2O . The aqueous phase was extracted with EtOAc. The combined organic phases were washed with brine, dried ($MgSO_4$), and concentrated. The crude oil was purified by flash column chromatography on silica gel equilibrated with hexanes/1% Et_3N . The crude material, dissolved in CH_2Cl_2 , was added to the column, followed by an additional portion of hexanes/1% Et_3N to elute the CH_2Cl_2 . Elution with unstabilized THF:hexanes (1:1) gave the title compound (70 mg, 84%) as a white solid, mp 88.7-89.8 °C. R_f = 0.32 (silica gel, 1:1 THF:hexanes). IR (neat) 3348, 3070, 2943, 1721, 1643, 1606, 1586, 1447, 1380, 1356, 1260, 1196, 1147, 1085, 1045, 966, 949, 877, 862, 781, 744, 667 cm^{-1} . 1H NMR (300 MHz, $CDCl_3$) δ 7.67 (1H, s), 6.52 (1H, s), 5.42 (1H, t, J = 7.0 Hz), 4.48 (2H, s), 4.45 (2 H, d, J = 7.0 Hz), 1.76 (3H, s), 1.70 (3H, s). ^{13}C NMR (75 MHz, $CDCl_3$) δ 175.4, 168.4, 147.1, 139.8, 139.3, 118.7, 111.4, 66.3, 60.5, 25.7, 18.2. HRMS calcd for $C_{11}H_{14}O_4Na^+$ (M+Na)⁺ 233.0784, found 233.0788.

3-Hydroxy-6-(hydroxymethyl)-2-(2-methylbut-3-en-2-yl)-4H-pyran-4-one (145).

Claisen procedure A: To a solution of **144** (35 mg, 0.17 mmol) in anhydrous toluene (6 mL, 0.028 M) in a microwave vessel was added Zn(OTf)₂ (6 mg, 0.02 mmol) and the vessel was sealed under air. The reaction was irradiated at 80 °C for 2 h (300 W, 4 min ramp time, 250 psi max, with stirring on). The product was filtered and concentrated. The crude material was purified by flash column chromatography on silica gel equilibrated with hexanes/1% Et₃N. The crude material, dissolved in CH₂Cl₂, was added to the column, followed by an additional portion of hexanes/1% Et₃N to elute the CH₂Cl₂. Elution with EtOAc:hexanes (3:1) gave the title compound (19 mg, 54%) as a light brown oil. *R*_f = 0.57 (silica gel, 3:1 EtOAc:hexanes). IR (neat) 3287, 2927, 1728, 1620, 1571, 1453, 1364, 1312, 1204, 1140, 1082, 1044, 988, 915, 860, 785, 764, 695 cm⁻¹. ¹H NMR (300 MHz, CDCl₃) δ 6.56 (1H, s), 6.11 (1H, dd, *J* = 10.6, 17.3 Hz), 5.00 (1H, d, *J* = 17.0 Hz), 5.00 (1H, d, *J* = 11.1 Hz), 4.51 (2H, s), 1.49 (6H, s). ¹³C NMR (75 MHz, CDCl₃) δ 175.0, 168.0, 154.0, 142.8, 141.9, 112.4, 107.8, 61.0, 42.0, 29.9, 25.0. HRMS calcd for C₁₁H₁₄O₄H⁺ (M+H)⁺ 211.0965, found 211.0975.

(5-(3-Methylbut-2-enyloxy)-4-oxo-4H-pyran-2-yl)methyl benzoate (148).

To a solution of **144** (89 mg, 0.42 mmol) in CH₂Cl₂ (2.3 mL) at 0 °C was successively added benzoyl chloride (0.10 mL, 0.86 mmol), 4-dimethylaminopyridine (5 mg, 0.04 mmol), and Et₃N (0.15 mL, 1.1 mmol). The reaction mixture was stirred at 0 °C for 5.5 h and poured into sat aq NH₄Cl. The product was extracted with CH₂Cl₂ twice and the combined organic phases were dried (MgSO₄) and concentrated. The crude oil was

purified by flash column chromatography on silica gel equilibrated with 3% acetone in CH₂Cl₂/1% Et₃N. Elution with 3% acetone in CH₂Cl₂ gave the title compound (0.13 g, 98%) as a white solid. Recrystallization of the product (29 mg) from hexanes gave the title compound (9 mg, 31%) as a white solid, mp 105.0-106.5 °C. *R_f* = 0.19 (silica gel, 3% acetone in CH₂Cl₂). IR (neat) 3095, 2924, 22855, 1982, 1719, 1647, 1624, 1599, 1467, 1449, 1375, 1316, 1276, 1257, 1212, 1179, 1158, 1112, 1098, 1072, 1028, 1010, 994, 955, 866, 839, 787, 766, 754, 708, 684, 675 cm⁻¹. ¹H NMR (300 MHz, CDCl₃) δ 8.08 (2H, dd, *J* = 1.6 Hz, 7.0 Hz), 7.65-7.59 (2H, m), 7.48 (2H, t, *J* = 7.6 Hz), 6.54 (1H, s), 5.45 (1H, t, *J* = 7.0 Hz), 5.15 (2H, s), 4.48 (2H, d, *J* = 7.0 Hz), 1.78 (3H, s), 1.71 (3H, s). ¹³C NMR (75 MHz, CDCl₃) δ 174.5, 165.7, 161.7, 147.9, 140.0, 139.6, 134.0, 130.1, 128.8, 119.0, 113.9, 66.6, 61.7, 26.0, 18.4. HRMS calcd for C₁₈H₁₈O₅H⁺ (M+H)⁺ 315.1227, found 315.1235.

(5-Hydroxy-6-(2-methylbut-3-en-2-yl)-4-oxo-4H-pyran-2-yl)methyl benzoate (149) and (5-Hydroxy-4-oxo-4H-pyran-2-yl)methyl benzoate (150).

To a solution of **148** (40 mg, 0.13 mmol) in anhydrous toluene (4.5 mL) in a microwave vessel was added Zn(OTf)₂ (5 mg, 0.01 mmol) and the vessel was sealed under air. The reaction was irradiated at 80 °C for 1 h (300 W, 4 min ramp time, 250 psi max, with stirring on). The product was filtered and concentrated. The crude material was purified by flash column chromatography on silica gel equilibrated with hexanes/1% Et₃N. The crude material, dissolved in CH₂Cl₂, was added to the column, followed by an additional portion of hexanes/1% Et₃N to elute the CH₂Cl₂. Elution with 3:1 hexanes: THF

(unstabilized) gave **149** and further elution of the column with acetone gave **150**. Compound **149** (8 mg, 20%) was isolated as an off-white solid, mp 108.8-110.6 °C. $R_f = 0.37$ (silica gel, 3% acetone in CH₂Cl₂). IR (neat) 3268, 2928, 2853, 1730, 1650, 1623, 1590, 1477, 1450, 1400, 1379, 1365, 1328, 1316, 1265, 1206, 1178, 1149, 1118, 1096, 1070, 1055, 1019, 989, 912, 858, 852, 801, 768, 705, 684 cm⁻¹. ¹H NMR (300 MHz, CDCl₃) δ 8.09 (2H, dd, $J = 1.8$ Hz, 7.0 Hz), 7.63 (1H, t, $J = 7.3$ Hz), 7.49 (2H, t, $J = 7.6$ Hz), 6.55 (1H, s), 6.11 (1H, dd, $J = 10.5, 17.6$ Hz), 5.20 (2H, s), 5.08 (1H, d, $J = 17.0$ Hz), 5.06 (1H, d, $J = 10.0$ Hz), 1.49 (6H, s). ¹³C NMR (100 MHz, CDCl₃) δ 174.3, 165.7, 161.7, 153.7, 142.8, 142.2, 134.0, 130.0, 129.1, 128.8, 112.6, 109.5, 61.9, 42.0, 25.1. HRMS calcd for C₁₉H₁₈O₅H⁺ (M+H)⁺ 315.1227, found 315.1238.

Compound **150** (16 mg, 53%) was isolated as an off-white solid, mp 140.9-142.0 °C. $R_f = 0.08$ (silica gel, 3% acetone in CH₂Cl₂). IR (neat) 3255, 3091, 2922, 2852, 1719, 1615, 1593, 1448, 1404, 1359, 1314, 1244, 1209, 1144, 1115, 1098, 1071, 1029, 1000, 952, 859, 849, 809, 770, 705, 688, 676 cm⁻¹; ¹H NMR (300 MHz, CDCl₃) δ 8.08 (2H, dd, $J = 7.0, 1.1$ Hz), 7.89 (1H, s), 7.63 (1H, tt, $J = 7.0$ Hz, 1.2 Hz), 7.49 (2H, tt, $J = 7.0, 1.2$ Hz), 6.61 (1H, s), 5.19 (2H, s); ¹³C NMR (100 MHz, CDCl₃) δ 174.1, 165.7, 163.3, 146.1, 138.1, 134.0, 130.1, 128.9, 121.4, 111.3, 61.9, 46.9; HRMS calcd for C₁₃H₁₀O₅H⁺ (M+H)⁺ 247.0601, found 247.0601.

5-(Allyloxy)-2-(hydroxymethyl)-4H-pyran-4-one (151).

The general procedure for the synthesis of *O*-allyl kojates was followed, using allyl bromide. The crude material was purified by flash column chromatography on silica gel

equilibrated with hexanes/1% Et₃N. The crude material, dissolved in CH₂Cl₂, was added to the column, followed by an additional portion of hexanes/1% Et₃N to elute the CH₂Cl₂. Elution with unstabilized Et₂O (~120 mL), EtOAc (~200 mL), and acetone (~200 mL) gave the title compound (37 mg, 47%) as a light yellow solid, mp 60.1-64.5 °C (Lit.⁹⁹ mp 61-64 °C). *R_f* = 0.10 (silica gel, Et₂O). IR (neat) 3335, 3090, 2921, 1640, 1601, 1442, 1347, 1261, 1198, 1147, 1079, 983, 941, 863, 748 cm⁻¹. ¹H NMR (300 MHz, CDCl₃) δ 7.61 (1H, s), 6.51 (1H, s), 6.03-5.90 (1H, m), 5.36 (1H, d, *J* = 17.6 Hz), 5.29 (1H, d, *J* = 10.6 Hz), 4.46-4.44 (4H, m). ¹³C NMR (75 MHz, CDCl₃) δ 175.3, 168.6, 147.0, 140.5, 132.1, 119.2, 111.6, 70.6, 60.6. HRMS calcd for C₉H₉O₄ (M-H) 181.0495, found 181.0504.

2-(Hydroxymethyl)-5-(2-methylallyloxy)-4*H*-pyran-4-one (152).

The general procedure for the synthesis of *O*-allyl kojates was followed, using 3-bromo-2-methylpropene. The crude material was purified by flash column chromatography on silica gel equilibrated with 1% Et₃N in hexanes. The crude material, dissolved in CH₂Cl₂, was added to the column, followed by an additional portion of hexanes/1% Et₃N to elute the CH₂Cl₂. Elution with EtOAc:hexanes (3:1) gave the title compound (48 mg, 66%) as a white oil. *R_f* = 0.21 (silica gel, 3:1 EtOAc:hexanes). IR (neat) 3337, 3087, 2920, 1642, 1603, 1445, 1377, 1258, 1196, 1148, 1080, 1037, 993, 945, 912, 863, 779, 747 cm⁻¹. ¹H NMR (300 MHz, CDCl₃) δ 7.61 (1H, s), 6.51 (1H, s), 5.03 (1H, s), 4.99 (1H, s), 4.46 (2H, s), 4.37 (2H, s), 1.77 (3H, s). ¹³C NMR (75 MHz, CDCl₃) δ 175.3, 168.2, 147.3,

140.4, 139.9, 114.4, 111.9, 73.7, 60.8, 19.3. HRMS calcd for C₁₀H₁₁O₄ (M-H) 195.0652, found 195.0658.

5-(But-3-yn-2-yloxy)-2-(hydroxymethyl)-4*H*-pyran-4-one.

A suspension of kojic acid (348 mg, 2.45 mmol), but-3-yn-2-yl methanesulfonate¹¹⁵ (436 mg, 2.94 mmol), K₂CO₃ (407 mg, 2.95 mmol), 18-crown-6 (259 mg, 0.981 mmol) in acetone (40 mL) was heated at reflux for 16 h and the reaction mixture was concentrated. The residue was partitioned between H₂O and EtOAc. The aqueous phase was extracted with EtOAc. The combined organic phases were washed with brine, dried (MgSO₄), and concentrated. The crude material was purified by flash column chromatography on silica gel equilibrated with hexanes. The crude material, dissolved in CH₂Cl₂, was added to the column, followed by an additional portion of hexanes to elute the CH₂Cl₂. Elution with 15% hexanes in Et₂O (unstabilized) gave the title compound (167 mg, 35%) as a white solid, mp 95.1-96.1 °C. *R_f* = 0.26 (silica gel, Et₂O). IR (neat) 3304, 3206, 3104, 2992, 2928, 2824, 2108, 1648, 1613, 1591, 1454, 1375, 1317, 1252, 1205, 1190, 1147, 1126, 1093, 1081, 1028, 942, 923, 864, 817, 754, 727 cm⁻¹. ¹H NMR (300 MHz, CDCl₃) δ 7.83 (1H, s), 6.53 (1H, s), 5.07 (1H, dq, *J* = 2.3 Hz, 6.4 Hz), 4.51 (2H, s), 2.52 (1H, d, *J* = 2.3 Hz), 1.67 (3H, d, *J* = 6.4 Hz). ¹³C NMR (100 MHz, CDCl₃) δ 175.8, 168.3, 145.6, 145.0, 112.7, 81.8, 75.7, 66.1, 60.8, 22.1. HRMS calcd for C₁₀H₁₀O₄H⁺ (M+H)⁺ 195.0652, found 195.0658.

5-(But-3-en-2-yloxy)-2-(hydroxymethyl)-4H-pyran-4-one (153).

A suspension of 5-(but-3-yn-2-yloxy)-2-(hydroxymethyl)-4H-pyran-4-one (104 mg, 0.533 mmol) and Lindlar catalyst (104 mg) in MeOH (8 mL) was hydrogenated, stirring the reaction at room temperature under H₂ (1 atm) until it was judged complete by NMR. The crude material was purified by flash column chromatography on silica gel equilibrated with 1% Et₃N in hexanes. The crude material, dissolved in CH₂Cl₂, was added to the column, followed by an additional portion of hexanes/1% Et₃N to elute the CH₂Cl₂. Elution with Et₂O (unstabilized):hexanes (9:1) gave the title compound (61 mg, 58%) as a white oil. *R*_f = 0.18 (silica gel, Et₂O). IR (neat) 3331, 3087, 2979, 2924, 2854, 1643, 1607, 1445, 1423, 1375, 1327, 1253, 1200, 1149, 1081, 1047, 989, 920, 863, 784, 739 cm⁻¹. ¹H NMR (300 MHz, CDCl₃) δ 7.59 (1H, s), 6.48 (1H, s), 5.76 (1H, ddd, *J* = 7.0 Hz, 10.4 Hz, 17.3 Hz), 5.17 (1H, d, *J* = 18.8 Hz), 5.16 (1H, d, *J* = 10.5 Hz), 4.64 (1H, m), 4.43 (2H, s), 1.45 (3H, d, *J* = 6.4 Hz). ¹³C NMR (75 MHz, CDCl₃) δ 176.0, 168.2, 146.2, 143.6, 138.0, 117.6, 112.1, 77.5, 60.6, 21.3. HRMS calcd for C₁₀H₁₂O₄Na⁺ (M+Na)⁺ 219.0628, found 219.0626.

(*E*)-5-(But-2-enyloxy)-2-(hydroxymethyl)-4H-pyran-4-one (154).

The general procedure for the synthesis of *O*-allyl kojates was followed, using *trans*-crotyl bromide and using CH₂Cl₂ for product extraction following the reaction. The crude material was purified by flash column chromatography on silica gel equilibrated with 1% Et₃N in hexanes. The crude material, dissolved in CH₂Cl₂, was added to the column, followed by an additional portion of hexanes/1% Et₃N to elute the CH₂Cl₂. Elution with

EtOAc:hexanes (3:1) gave the title compound (50 mg, 77%) as a white oil. $R_f = 0.13$ (silica gel, 3:1 EtOAc:hexanes). IR (neat) 3342, 3092, 3028, 2919, 2856, 2244, 1642, 1606, 1441, 1377, 1347, 1258, 1195, 1148, 1078, 966, 946, 913, 863, 729, 645, 626, 582, 535, 528 cm^{-1} . ^1H NMR (400 MHz, CDCl_3) δ 7.58 (1H, s), 6.49 (1H, s), 5.83-5.69 (1H, m), 5.66- 5.56 (1H, m), 4.44 (2H, s), 4.33 (2H, d, $J = 6.2$ Hz), 1.70 (3H, d, $J = 6.2$ Hz). ^{13}C NMR (100 MHz, CDCl_3) δ 175.4, 168.4, 147.2, 140.2, 132.2, 125.1, 111.6, 70.5, 60.7, 17.9. HRMS calcd for $\text{C}_{10}\text{H}_{12}\text{O}_4$ (M) 196.0730, found 196.0738.

(E)-5-(Cinnamyloxy)-2-(hydroxymethyl)-4H-pyran-4-one (155).

The general procedure for the synthesis of *O*-allyl kojates was followed, using *trans*-3-bromo-1-phenyl-1-propene. The CH_2Cl_2 -soluble impurities were removed from the crude solid following work-up by adding a few mL of CH_2Cl_2 and filtering. The CH_2Cl_2 -insoluble crystals were collected to give the title compound (73 mg, 71%) as a white solid, mp 141.6-142.2 $^\circ\text{C}$. $R_f = 0.05$ (silica gel, 3:1 EtOAc:hexanes). IR (neat) 3242, 3108, 3055, 2940, 2878, 2842, 1968, 1643, 1589, 1603, 1497, 1453, 1384, 1318, 1253, 1192, 1153, 1083, 1010, 983, 950, 968, 868, 848, 832, 783, 753, 738, 692 cm^{-1} . ^1H NMR (300 MHz, CDCl_3) δ 7.65 (1H, s), 7.42-7.25 (5H, m), 6.69 (1H, d, $J = 15.8$ Hz), 6.53 (1H, s), 6.37 (1H, dt, $J = 6.4$ Hz, 15.8 Hz), 4.68 (2H, d, $J = 6.4$ Hz), 4.49 (2H, s). ^{13}C NMR (100 MHz, CDCl_3) δ 175.4, 167.8, 147.3, 140.9, 136.1, 134.7, 128.8, 128.4, 126.9, 123.3, 112.1, 70.7, 60.9, 50.9, 31.1. HRMS calcd for $\text{C}_{15}\text{H}_{14}\text{O}_4\text{H}^+$ (M+H) $^+$ 257.0808, found 257.0804.

5-(3-Phenylprop-2-ynyloxy)-2-((tetrahydro-2H-pyran-2-yloxy)methyl)-4H-pyran-4-one (157).

To a mixture of **55**⁵⁰ (66 mg, 0.25 mmol), CuI (3 mg, 0.02 mmol), and Pd(PPh₃)₂Cl₂ (13 mg, 20 μmol) under N₂ was sequentially added iodobenzene (0.02 mL, 0.2 mmol), anhydrous toluene (1 mL), and Et₃N (0.36 mL). The reaction mixture was stirred at room temperature under N₂ for 20 h and filtered through Celite. The filter cake was washed with EtOAc. The filtrate was washed with H₂O twice, washed with brine, dried (MgSO₄), and concentrated. The crude material was purified by flash column chromatography on silica gel, eluting with 40% EtOAc in hexanes to obtain the title compound (43 mg, 70%) as a yellow oil. *R*_f = 0.20 (silica gel, 40% EtOAc in hexanes). IR (neat) 3082, 2941, 2870, 2234, 1712, 1652, 1626, 1596, 1490, 1442, 1353, 1260, 1196, 1153, 1121, 1077, 1033, 993, 974, 943, 904, 869, 816, 756, 691 cm⁻¹. ¹H NMR (400 MHz, CDCl₃) δ 7.86 (1H, s), 7.43-7.40 (2H, m), 7.34-7.30 (3H, m), 6.53 (1H, s), 4.97 (2H, s), 4.72 (1H, t, *J* = 3.2 Hz), 4.53 (1H, d, *J* = 14.7 Hz), 4.34 (1H, d, *J* = 14.7 Hz), 3.86-3.78 (1H, m), 3.58-3.51 (1H, m), 1.82-1.53 (6H, m). ¹³C NMR (75 MHz, CDCl₃) δ 174.8, 164.8, 146.2, 142.9, 131.9, 129.0, 128.4, 122.0, 113.7, 98.3, 88.7, 82.8, 64.3, 62.1, 58.7, 30.2, 25.3, 18.9. HRMS calcd for C₂₀H₂₀O₅Na⁺ (M+Na)⁺ 364.1237, found 364.1241.

(Z)-2-(Hydroxymethyl)-5-(3-phenylallyloxy)-4H-pyran-4-one (158).

A suspension of **158** (55 mg, 0.16 mmol) and Lindlar catalyst (55 mg) in MeOH (2 mL) was hydrogenated, stirring the reaction at room temperature under H₂ (1 atm) until it was judged complete by NMR. The reaction mixture was filtered and concentrated. To the

residue was added Amberlyst® 15 (135 mg) and MeOH (1.3 mL). The reaction mixture was stirred at room temperature for 2 h, filtered, and concentrated. The crude material was purified by flash column chromatography on silica gel equilibrated with 1% Et₃N in hexanes. The crude material, dissolved in CH₂Cl₂, was added to the column, followed by an additional portion of hexanes/1% Et₃N to elute the CH₂Cl₂. Elution with unstabilized THF:hexanes (1:1) gave a white solid. The solid was recrystallized, by adding a few mL of room temperature CH₂Cl₂ and filtering to collect the solid, to give the title compound (20 mg, 49% over two steps) as a white solid, mp 139.2-140.4 °C. *R_f* = 0.15 (silica gel, 1:1 THF:hexanes). IR (neat) 3331, 3085, 3026, 2924, 1645, 1610, 1495, 1447, 1345, 1261, 1202, 1150, 1081, 987, 947, 920, 865, 774, 749, 701 cm⁻¹. ¹H NMR (300 MHz, CDCl₃) δ 7.41-7.25 (5H, m), 7.20 (2H, d, *J* = 6.4 Hz) 6.74 (1H, d, *J* = 11.7 Hz), 6.51 (1H, s), 5.92 (1H, dt, *J* = 6.4, 11.7 Hz), 4.77 (2H, d, *J* = 6.4 Hz), 4.47 (2H, s). ¹³C NMR (100 MHz, CDCl₃) δ 174.9, 167.2, 147.3, 140.1, 136.1, 133.7, 128.9, 128.7, 128.0, 126.5, 112.2, 66.5, 61.2, 32.1. HRMS calcd for C₁₅H₁₃O₄ (M-H) 257.0808, found 257.0808.

2-(Hydroxymethyl)-5-(prop-2-ynyloxy)-4H-pyran-4-one (159).

A suspension of **55**⁵⁰ (0.193 g, 0.728 mmol) and Amberlyst® 15 (0.731 g) in MeOH (7 mL) was stirred at room temperature for 1.5 h, filtered, and concentrated. The crude material was purified by adding the oil, dissolved in CH₂Cl₂, to a plug of silica gel, wet with hexanes/1% Et₃N. More hexanes/1% Et₃N was run through the plug of silica gel to elute the CH₂Cl₂. Elution with 1% hexanes in EtOAc gave the title compound (95 mg, 72%) as a yellow solid, mp 88.5-90.1 °C. *R_f* = 0.14 (silica gel, 3:1 EtOAc:hexanes). IR

(neat) 3279, 3089, 2921, 2130, 1646, 1605, 1542, 1492, 1436, 1385, 1372, 1333, 1253, 1206, 1150, 1082, 1001, 978, 942, 905, 875, 853, 789, 761, 694 cm^{-1} . ^1H NMR (300 MHz, CDCl_3) δ 7.82 (1H, s), 6.53 (1H, s), 4.71 (2H, s), 4.48 (2H, s), 2.59 (1H, s). ^{13}C NMR (100 MHz, CDCl_3) δ 175.4, 168.2, 145.9, 143.5, 143.4, 112.6, 77.4, 60.9, 58.1. HRMS calcd for $\text{C}_9\text{H}_8\text{O}_4$ (M) 180.0417, found 180.0409.

2-Allyl-3-hydroxy-6-(hydroxymethyl)-4H-pyran-4-one (161).

Claisen procedure B: To a solution of **151** (35 mg, 0.19 mmol) in anhydrous toluene (6.8 mL, 0.028 M) in a microwave vessel was added $\text{Zn}(\text{OTf})_2$ (7 mg, 0.02 mmol) and the vessel was sealed under air. The reaction was irradiated at 120 °C for 200 min (300 W, 4 min ramp time, 250 psi max, with stirring on). The product was filtered and concentrated. The crude material was purified by flash column chromatography on silica gel equilibrated with hexanes/1% Et_3N . The crude material, dissolved in CH_2Cl_2 , was added to the column, followed by an additional portion of hexanes/1% Et_3N to elute the CH_2Cl_2 . Elution with unstabilized Et_2O gave the title compound (17 mg, 49%) as a light yellow solid, mp 113.5-114.9 °C. Recrystallization of the product (32 mg) from hexanes gave the title compound (4 mg, 13%) as a white solid, mp 115.2-116.2 °C (Lit.⁹⁹ mp 124.2-125.2 °C). R_f = 0.28 (silica gel, Et_2O). IR (neat) 3084, 2920, 1664, 1633, 1584, 1445, 1463, 1312, 1233, 1212, 1185, 1081, 1012, 968, 994, 917, 880, 853, 762 cm^{-1} . ^1H NMR (400 MHz, CDCl_3) δ 6.53 (1H, s), 5.96-5.86 (1H, m), 5.22 (1H, d, J = 17.1 Hz), 5.19 (1H, d, J = 8.6 Hz), 4.52 (2H, s), 3.48 (2H, d, J = 6.2 Hz). ^{13}C NMR (100 MHz, CDCl_3) δ 174.2,

167.3, 149.0, 141.9, 131.4, 118.6, 108.8, 61.4, 32.8. HRMS calcd for C₉H₁₀O₄H⁺ (M+H)⁺ 183.0652, found 183.0652.

3-Hydroxy-6-(hydroxymethyl)-2-(2-methylallyl)-4H-pyran-4-one (162).

Claisen procedure B was followed [**152** (31 mg, 0.16 mmol), Zn(OTf)₂ (6 mg, 0.02 mmol), anhydrous toluene (5.7 mL)]. The crude material was purified by flash column chromatography on silica gel equilibrated with hexanes/1% Et₃N. The crude material, dissolved in CH₂Cl₂, was added to the column, followed by an additional portion of hexanes/1% Et₃N to elute the CH₂Cl₂. Elution with unstabilized Et₂O gave the title compound (10 mg, 33%) as an orange oil. *R*_f = 0.41 (silica gel, Et₂O). IR (neat) 3296, 3080, 2921, 2853, 1723, 1666, 1652, 1623, 1576, 1463, 1378, 1316, 1271, 1227, 1171, 1157, 1095, 1046, 1033, 1003, 986, 975, 958, 888, 860, 853, 773, 764, 744 cm⁻¹. ¹H NMR (300 MHz, CDCl₃) δ 6.53 (1H, s), 4.89 (1H, s), 4.81 (1H, s), 4.51 (2H, s), 3.42 (2H, s), 1.79 (3H, s). ¹³C NMR (75 MHz, CDCl₃) δ 174.3, 167.8, 149.2, 142.5, 113.7, 108.8, 61.3, 36.7, 29.9, 22.5. HRMS calcd for C₁₀H₁₁O₄ (M-H) 195.0652, found 195.0643.

2-(But-2-enyl)-3-hydroxy-6-(hydroxymethyl)-4H-pyran-4-one (163).

Claisen procedure B was followed [**153** (17 mg, 90 μmol), Zn(OTf)₂ (4 mg, 0.01 mmol), anhydrous toluene (3.6 mL)]. The crude material was purified by flash column chromatography on silica gel equilibrated with hexanes/1% Et₃N. The crude material, dissolved in CH₂Cl₂, was added to the column, followed by an additional portion of

hexanes/1% Et₃N to elute the CH₂Cl₂. Elution with EtOAc:hexanes:Et₃N (11:8:1) gave the title compound (10 mg, 59%) as an off-white oil. $R_f = 0.28$ (silica gel, 4:1 EtOAc:hexanes). IR (neat) 3114, 3027, 2962, 2919, 2854, 1731, 1662, 1632, 1619, 1586, 1461, 1444, 1418, 1379, 1321, 1305, 1269, 1231, 1211, 1177, 1161, 1083, 1054, 1013, 991, 963, 881, 855, 763, 686 cm⁻¹. ¹H NMR (300 MHz, CDCl₃) δ 6.52 (1H, s), 5.70-5.46 (2H, m), 4.51 (2H, s), 3.39 (2H, d, $J = 5.9$ Hz), 1.70 (3H, dd, $J = 1.2$ Hz, 6.4 Hz). ¹³C NMR (75 MHz, CDCl₃) δ 174.1, 167.2, 149.7, 141.6, 129.4, 123.9, 108.7, 61.4, 31.7, 18.1. HRMS calcd for C₁₀H₁₂O₄H (M+H)⁺ 197.0808, found 197.0808.

2-(But-3-en-2-yl)-3-hydroxy-6-(hydroxymethyl)-4H-pyran-4-one (164).

Claisen procedure A was followed [**154** (39 mg, 0.20 mmol), Zn(OTf)₂ (8 mg, 0.02 mmol), anhydrous toluene (7.2 mL)]. The crude material was purified by flash column chromatography on silica gel equilibrated with hexanes/1% Et₃N. The crude material, dissolved in CH₂Cl₂, was added to the column, followed by an additional portion of hexanes/1% Et₃N to elute the CH₂Cl₂. Elution with unstabilized Et₂O gave the title compound (18 mg, 46%) as an orange oil. $R_f = 0.40$ (silica gel, Et₂O). IR (neat) 3263, 2978, 2926, 1651, 1618, 1574, 1454, 1414, 1358, 1308, 1259, 1201, 1095, 1036, 989, 920, 860, 785, 764, 735 cm⁻¹. ¹H NMR (400 MHz, CDCl₃) δ 6.55 (1H, s), 6.00-5.91 (1H, ddd, $J = 7.0$ Hz, 10.1 Hz, 17.2 Hz), 5.19 (1H, d, $J = 17.0$ Hz), 5.13 (1H, d, $J = 10.0$ Hz), 4.52 (2H, s), 3.89 (1H, dq, $J = 7.0$ Hz, 7.0 Hz), 1.38 (3H, d, $J = 7.0$ Hz). ¹³C NMR (100 MHz, CDCl₃) δ 174.4, 167.4, 152.5, 141.0, 137.6, 116.1, 108.6, 61.3, 36.8, 17.1. HRMS calcd for C₁₀H₁₁O₄ (M-H) 195.0652, found 195.0661.

3-Hydroxy-6-(hydroxymethyl)-2-(1-phenylallyl)-4H-pyran-4-one (165).

Using *trans*-cinnamyl kojate **155**: Claisen procedure A was followed [**155** (38 mg, 0.15 mmol), Zn(OTf)₂ (5 mg, 0.02 mmol), anhydrous toluene (5.2 mL)]. The crude material was purified by flash column chromatography on silica gel equilibrated with hexanes/1% Et₃N. The crude material, dissolved in CH₂Cl₂, was added to the column, followed by an additional portion of hexanes/1% Et₃N to elute the CH₂Cl₂. Elution with EtOAc:hexanes (3:1) gave the title compound (32 mg, 84%) as an orange oil. $R_f = 0.36$ (silica gel, 3:1 EtOAc:hexanes). IR (neat) 3265, 3086, 3030, 2923, 1720, 1651, 1620, 1575, 1495, 1451, 1361, 1306, 1200, 1089, 1031, 986, 924, 860, 836, 788, 762, 729, 698 cm⁻¹. ¹H NMR (300 MHz, CDCl₃) δ 7.32-7.20 (5H, m), 6.53 (1H, s), 6.23 (1H, ddd, $J = 7.0$ Hz, 10.0 Hz, 17.3 Hz), 5.26 (1H, d, $J = 10.5$ Hz), 5.18 (1H, d, $J = 17.0$ Hz), 5.05 (1H, d, $J = 7.0$ Hz), 4.42 (2H, s). ¹³C NMR (75 MHz, CDCl₃) δ 174.7, 168.1, 151.1, 141.6, 139.1, 135.3, 128.9, 128.2, 127.4, 118.5, 108.7, 61.0, 47.8, 29.9. HRMS calcd for C₁₅H₁₄O₄Na⁺ (M+Na)⁺ 281.0784, found 281.0773.

Claisen procedure C: To a solution of *cis*-cinnamyl kojate **158** (21 mg, 79 μ mol) in anhydrous toluene (2.7 mL, 0.028 M) in a microwave vessel was added Zn(OTf)₂ (3 mg, 8 μ mol) and the vessel was sealed under air. The reaction was irradiated at 120 °C for 1 h (300 W, 4 min ramp time, 250 psi max, with stirring on). The product was filtered and concentrated. The crude material was purified by flash column chromatography on silica gel equilibrated with hexanes/1% Et₃N. The crude material, dissolved in CH₂Cl₂, was added to the column, followed by an additional portion of hexanes/1% Et₃N to elute the

CH₂Cl₂. Elution with EtOAc:hexanes (3:1) gave the title compound (9 mg, 41%), with all characterization data identical to above.

References

- 1) Stretton, A. O. W. The First Sequence: Fred Sanger and Insulin. *Genetics* **2002**, *162*, 527-532.
- 2) Chang, S. G.; Choi, K. D.; Jang, S. H.; Shin, H. C. Role of Disulfide Bonds in the Structure and Activity of Human Insulin. *Mol. Cells* **2003**, *16*, 323-330.
- 3) Tirosh, A.; Shai, I.; Tekes-Manova, D.; Israeli, E.; Pereg, D.; Shochat, T.; Kochba, I.; Rudich, A. Normal Fasting Plasma Glucose Levels and Type 2 Diabetes in Young Men. *N. Engl. J. Med.* **2005**, *353*, 1454-1462.
- 4) Beta Cell Biology Consortium. Retrieved July 3, 2013 from http://www.betacell.org/content/articlepanelview/article_id/1/panel_id/2.
- 5) Horton, R. A. et al. *Principles of Biochemistry*, 4th ed. **2006**, Upper Saddle River, NJ: Pearson Prentice Hall.
- 6) Menting, J. G.; Whittaker, J.; Margetts, M. B.; Whittaker, L. J.; Kong, G. K.-W.; Smith, B. J.; Watson, C. J.; Žáková, L.; Kletvíková, E.; Jiráček, J.; Chan, S. J.; Steiner, D. F.; Dodson, G. G.; Brzozowski, A. M.; Weiss, M. A.; Ward, C. W.; Lawrence, M. C. How Insulin Engages Its Primary Binding Site on the Insulin Receptor. *Nature* **2013**, *493*, 241-245.
- 7) Ward, C. W.; Lawrence, M. C. Landmarks in Insulin Research. *Front. Endocrinol.* **2011**, *2*, 76.
- 8) Hubbard, S. R. Insulin Meets Its Receptor. *Nature* **2013**, *493*, 171-172.
- 9) Stöckli, J.; Fazakerley, D. J.; James, D. E. GLUT4 Exocytosis. *J. Cell Sci.* **2011**, *124*, 4147-4159.
- 10) Barcala Tabarozzi, A. E.; Castro, C. N.; Dewey, R. A.; Sogayar, M. C.; Labriola, L.; Perone, M. J. Cell-based Interventions to Halt Autoimmunity in Type 1 Diabetes Mellitus. *Clin. Exp. Immunol.* **2013**, *171*, 135-146.
- 11) Weir, G. C.; Bonner-Weir, S. Islet β Cell Mass in Diabetes and How it Relates to Function, Birth, and Death. *Ann. N. Y. Acad. Sci.* **2013**, *1281*, 92-105.
- 12) Dang, M. N.; Buzzetti, R.; Pozzilli, P. Epigenetics in Autoimmune Diseases with Focus on Type 1 Diabetes. *Diabetes Metab. Res. Rev.* **2013**, *29*, 8-18.
- 13) Roivainen, M.; Klingel, K. Virus Infections and Type 1 Diabetes Risk. *Curr. Diab. Rep.* **2010**, *10*, 350-356.

- 14) Lazar, M. A. How Obesity Causes Diabetes: Not a Tall Tale. *Science* **2005**, *307*, 373-375.
- 15) Hivert, M.-F.; Jablonski, K. A.; Perreault, L.; Saxena, R.; McAteer, J. B.; Franks, P. W.; Hamman, R. F.; Kahn, S. E.; Haffner, S.; Meigs, J. B.; Altshuler, D.; Knowler, W. C.; Florez, J. C. Updated Genetic Score Based on 34 Confirmed Type 2 Diabetes Loci is Associated with Diabetes Incidence and Regression to Normoglycemia in the Diabetes Prevention Program. *Diabetes*, **2011**, *60*, 1340-1348.
- 16) Rhodes, C. J. Type 2 Diabetes- a Matter of β -Cell Life and Death. *Science*, **2005**, *307*, 380-384.
- 17) Kolterman, O. G.; Gray, R. S.; Griffin, J.; Burstein, P.; Insel, J. Receptor and Postreceptor Defects Contribute to the Insulin Resistance in Noninsulin-dependent Diabetes Mellitus. *J. Clin. Invest.* **1981**, *68*, 957-969.
- 18) (a) Goodyear, L. J.; Giorgino, F.; Sherman, L. A.; Carey, J.; Smith, R. J.; Dohm, G. L. Insulin Receptor Phosphorylation, Insulin Receptor Substrate-1 Phosphorylation, and Phosphatidylinositol 3-Kinase Activity Are Decreased in Intact Skeletal Muscle Strips from Obese Subjects. *J. Clin. Invest.* **1995**, *95*, 2195-2204. (b) Caro, J. F.; Sinha, M. K.; Raju, S. M.; Ittoop, O.; Pories, W. J.; Flickinger, E. G.; Meelheim, D.; Dohm, G. L. Insulin Receptor Kinase in Human Skeletal Muscle from Obese Subjects with and Without Noninsulin Dependent Diabetes. *J. Clin. Invest.* **1987**, *79*, 1330-1337.
- 19) Olokoba, A. B.; Obateru, O. A.; Olokoba, L. B. Type 2 Diabetes Mellitus: A Review of Current Trends. *Oman Med. J.* **2012**, *27*, 269-273.
- 20) Vaidyanathan, J.; Choe, S.; Sahajwalla, C. G. Type 2 Diabetes in Pediatrics and Adults: Thoughts from a Clinical Pharmacology Perspective. *J. Pharm. Sci.* **2012**, *101*, 1659-1671.
- 21) Rosenfeld, L. Insulin: Discovery and Controversy. *Clin. Chem.* **2002**, *48*, 2270-2288.
- 22) Cochran Jr., H. A.; Marble, A.; Galloway, J. A. Factor in the Survival of Patients with Insulin-requiring Diabetes for 50 Years. *Diabetes Care* **1979**, *2*, 363-368.
- 23) Valla, V. Therapeutics of Diabetes Mellitus: Focus on Insulin Analogues and Insulin Pumps. *Exp. Diabetes Res.* **2010**, Article ID 178372.

- 24) Rabi, D. M.; Edwards, A. L.; Southern, D. A.; Svenson, L. W.; Sargious, P. M.; Norton, P.; Larsen, E. T.; Ghali, W. A. Association of Socio-economic Status with Diabetes Prevalence and Utilization of Diabetes Care Services. *BMC Health Serv. Rev.* **2006**, *6*, 124.
- 25) Zhang, B.; Salituro, G.; Szalkowski, D.; Li, Z.; Zhang, Y.; Royo, I.; Vilella, D.; Díez, M. T.; Pelaez, F.; Ruby, C.; Kendall, R. L.; Mao, X.; Griffin, P.; Calaycay, J.; Zierath, J. R.; Heck, J. V.; Smith, R. G.; Moller, D. E. Discovery of a Small Molecule Insulin Mimetic with Antidiabetic Activity in Mice. *Science*, **1999**, *284*, 974-977.
- 26) Salituro, G. M.; Pelaez, F.; Zhang, B. B. Discovery of a Small Molecule Insulin Receptor Activator. *Recent Prog. Horm. Res.* **2001**, *56*, 107-126.
- 27) Air, E. L.; Strowski, M. Z.; Benoit, S. C.; Conarello, S. L.; Salituro, G. M.; Guan, X.-M.; Liu, K.; Woods, S. C.; Zhang, B. B. Small Molecule Insulin Mimetics Reduce Food Intake and Body Weight and Prevent Development of Obesity. *Nat. Med.* **2002**, *8*, 179-183.
- 28) Webster, N. J. G.; Park, K.; Pirrung, M. C. Signaling Effects of Demethylasterriquinone B1, a Selective Insulin Receptor Modulator. *ChemBioChem* **2003**, *4*, 379-385.
- 29) Kim, H.; Deng, L.; Xiong, X.; Hunter, W. D.; Long, M. C.; Pirrung, M. C. Glyceraldehyde 3-Phosphate Dehydrogenase is a Cellular Target of the Insulin Mimic Demethylasterriquinone B1. *J. Med. Chem.* **2007**, *50*, 3423-3426.
- 30) Xu, G. G.; Gao, Z.-Y.; Borge Jr., P. D.; Jegier, P. A.; Young, R. A.; Wolf, B. A. Insulin Regulation of β -Cell Function Involves a Feedback Loop on SERCA Gene Expression, Ca^{2+} Homeostasis, and Insulin Expression and Secretion. *Biochemistry* **2000**, *39*, 14912-14919.
- 31) Roper, M. G.; Qian, W.-J.; Zhang, B. B.; Kulkarni, R. N.; Kahn, R.; Kennedy, R. T. Effect of the Insulin Mimetic L-783,281 on Intracellular $[\text{Ca}^{2+}]$ and Insulin Secretion from Pancreatic β -Cells. *Diabetes* **2002**, *51* (Suppl. 1), S43-S49.
- 32) Liu, K.; Wood, H. B.; Jones, A. B. Total Synthesis of Asterriquinone B1. *Tet. Lett.* **1999**, *40*, 5119-5122.
- 33) Tatsuta, K.; Mukai, H.; Mitsumoto, K. Short and Convergent Synthesis of Asterriquinone B1 and Demethylasterriquinone B1. *J. Antibiot.* **2001**, *54*, 105-108.

- 34) Wood Jr., H. B.; Black, R.; Salituro, G.; Szalkowski, D.; Li, Z.; Zhang, Y.; Moller, D. E.; Zhang, B.; Jones, A. B. The Basal SAR of a Novel Insulin Receptor Activator. *Bioorg. Med. Chem. Lett.* **2000**, *10*, 1189-1192.
- 35) Liu, K.; Xu, L.; Szalkowski, D.; Li, Z.; Ding, V.; Kwei, G.; Huskey, S.; Moller, D. E.; Heck, J. V.; Zhang, B. B.; Jones, A. B. Discovery of a Potent, Highly Selective, and Orally Efficacious Small-Molecule Activator of the Insulin Receptor. *J. Med. Chem.* **2000**, *43*, 3487-3494.
- 36) Quereshi, S. A.; Ding, V.; Li, Z.; Szalkowski, D.; Biazzo-Ashnault, D. E.; Xie, D.; Saperstein, R.; Brady, E.; Huskey, S.; Shen, X.; Liu, K.; Xu, L.; Salituro, G. M.; Heck, J. V.; Moller, D. E.; Jones, A. B. Activation of Insulin Signal Transduction Pathway and Anti-diabetic Activity of Small Molecule Insulin Receptor Activators. *J. Biol. Chem.* **2000**, *275*, 36590-36595.
- 37) Strowski, M. Z.; Li, Z.; Szalkowski, D.; Shen, X.; Guan, X.-M.; Jüttner, S.; Moller, D. M.; Zhang, B. B. Small-Molecule Insulin Mimetic Reduces Hyperglycemia and Obesity in a Nongenetic Mouse Model of Type 2 Diabetes. *Endocrinology* **2004**, *145*, 5259-5268.
- 38) Pirrung, M. C.; Li, Z.; Park, K.; Zhu, J. Total Syntheses of Demethylasterriquinone B1, an Orally Active Insulin Mimetic, and Demethylasterriquinone A1. *J. Org. Chem.* **2002**, *67*, 7919-7926.
- 39) (a) Pirrung, M. C.; Park, K.; Li, Z. Synthesis of 3-Indolyl-2,5-dihydroxybenzoquinones. *Org. Lett.* **2001**, *3*, 365-367. (b) Pirrung, M. C.; Deng, L.; Li, Z.; Park, K. Synthesis of 2,5-dihydroxy-3-(indol-3-yl)benzoquinones by Acid-Catalyzed Condensation of Indoles with 2,5-Dichlorobenzoquinone. *J. Org. Chem.* **2002**, *67*, 8374-8388.
- 40) Pirrung, M. C.; Liu, Y.; Deng, L.; Halstead, D. K.; Li, Z.; May, J. F.; Wedel, M.; Austin, D. A.; Webster, N. J. G. Methyl Scanning: Total Synthesis of Demethylasterriquinone B1 and Derivatives for Identification of Sites of Interaction with and Isolation of Its Receptor(s). *J. Am. Chem. Soc.* **2005**, *127*, 4609-4624.
- 41) (a) Kaji, A.; Saito, R.; Shinbo, Y.; Kiriya, N. Transformation of Asterriquinone Diacetate to Asterriquinone Monoalkyl Ether via Its Monoacetal. *Chem. Pharm. Bull.* **1996**, *44*, 2340-2341. (b) Kaji, A.; Saito, R.; Hata (née Shinbo), Y.; Kiriya, N. Preparation and Route of Asterriquinone Monoalkyl Ether from Asterriquinone Diacetate by Treatment with a Mixture of Alcohol and Alkali, Followed by Acidification. *Chem. Pharm. Bull.* **1999**, *47*, 77-82.

- 42) Pirrung, M. C.; Li, Z.; Hensley, E.; Liu, Y.; Tanksale, A.; Lin, B.; Pai, A.; Webster, N. J. G. Parallel Synthesis of Indolylquinones and Their Cell-Based Insulin Mimicry. *J. Comb. Chem.* **2007**, *9*, 844-854.
- 43) Lin, B.; Li, Z.; Park, K.; Deng, L.; Pai, A.; Zhong, L.; Pirrung, M. C.; Webster, N. J. G. Identification of Novel Orally Available Small Molecule Insulin Mimetics. *J. Pharmacol. Exp. Ther.* **2007**, *323*, 579-585.
- 44) Monks, T. J.; Hanzlik, R. P.; Cohen, G. M.; Ross, D.; Graham, D. G. Quinone Chemistry and Toxicity. *Toxicol. Appl. Pharmacol.* **1992**, *112*, 2-16.
- 45) Pirrung, M. C.; Deng, L.; Lin, B.; Webster, N. J. G. Quinone Replacements for Small Molecule Insulin Mimics. *ChemBioChem* **2008**, *9*, 360-362.
- 46) Massoud, T. Synthesis of Indolylquinones as a Potential Therapy for Diabetes and as Candidates for Neuroprotection. Ph.D. Dissertation, University of California, Riverside, 2010.
- 47) Burdock, G. A.; Soni, M. G.; Carabin, I. G. Evaluation of Health Aspects of Kojic Acid in Food. *Regul. Toxicol. Pharm.* **2001**, *33*, 80-101.
- 48) Yabuta, T. A New Organic Acid (Kojic Acid) Formed by *Aspergillus Oryzae*. *Nippon Kagaku Kaishi* **1916**, *37*, 1185-1269.
- 49) Tolentino, L.; Kagan, J. On the Nuclear Bromination in the Kojic Acid Series. *J. Org. Chem.* **1974**, *39*, 2308-2309.
- 50) Xiong, X.; Pirrung, M. C. Modular Synthesis of Candidate Indole-based Insulin Mimics by Claisen Rearrangement. *Org. Lett.* **2008**, *10*, 1151-1154.
- 51) Nagarathnam, D. A Simple Synthesis of 2-Substituted Indoles. *Synthesis* **1992**, 743-745.
- 52) Miyano, M.; Deason, J. R.; Nakao, A.; Stealey, M. A.; Villamil, C. I.; Sohn, D. D.; Mueller, R. A. (Acyloxy)benzophenones and (Acyloxy)-4-pyrones. A New Class of Inhibitors of Human Neutrophil Elastase. *J. Med. Chem.* **1988**, *31*, 1052-1061.
- 53) Yasuhara, A.; Kanamori, Y.; Kaneko, M.; Numata, A.; Kondo, Y.; Sakamoto, T. Convenient Synthesis of 2-Substituted Indoles from 2-Ethynylanilines with Tetrabutylammonium Fluoride. *J. Chem. Soc., Perkin Trans.* **1999**, 529-534.
- 54) Abe, D.; Saito, T.; Sekiya, K. Sennidin Stimulates Glucose Incorporation in Rat Adipocytes. *Life Sci.* **2006**, *79*, 1027-1033.

- 55) He, K.; Chan, C.-B.; Liu, X.; Jia, Y.; Luo, H. R.; France, S. A.; Liu, Y.; Wilson, W. D.; Ye, K. Identification of a Molecular Activator for Insulin Receptor with Potent Anti-Diabetic Effects. *J. Biol. Chem.* **2011**, *286*, 37379-37388.
- 56) (a) Tsai, H. J.; Chou, S.-Y. A Novel Hydroxyfuroic Acid Compound as an Insulin Receptor Activator and Structure Activity Relationship of a Prenyl Moiety to Insulin Receptor Activation. *J. Biomed. Sci.* **2009**, *16*, 68. (b) Chou, S.-Y.; Chen, S.-S. T.; Chen, C.-H.; Chang, L.-S. Regioselective Synthesis of 3-Aryl-5-(1*H*-indole-3-carbonyl)-4-hydroxyfuroic Acids as Potential Insulin Receptor Activators. *Tetrahedron Lett.* **2006**, *47*, 7579-7582.
- 57) (a) Manchem, V. P.; Goldfine, I. D.; Kohanski, R. A.; Cristobal, C. P.; Lum, R. T.; Schow, S. R.; Shi, S.; Spevak, W. R.; Laborde, E.; Toavs, D. K.; Villar, H. O.; Wick, M. M.; Kozlowski, M. R. A Novel Small Molecule That Directly Sensitizes the Insulin Receptor In Vitro and In Vivo. *Diabetes* **2001**, *50*, 824-830. (b) Cheng, M.; Chen, S.; Schow, S. R.; Manchem, V. P.; Spevak, W. R.; Cristobal, C. P.; Shi, S.; Macsata, R. W.; Lum, R. T.; Goldfine, I. D.; Keck, J. G. In Vitro and In Vivo Prevention of HIV Protease Inhibitor-Induced Insulin Resistance by a Novel Small Molecule Insulin Receptor Activator. *J. Cell. Biochem.* **2004**, *92*, 1234-1245. (c) Lum, R. T.; Cheng, M.; Cristobal, C. P.; Goldfine, I. D.; Evan, J. L.; Keck, J. G.; Macsata, R. W.; Manchem, V. P.; Matsumoto, Y.; Park, S. J.; Rao, S. S.; Robinson, L.; Shi, S.; Spevak, W. R.; Schow, S. R. Design, Synthesis, and Structure-Activity Relationships of Novel Insulin Receptor Tyrosine Kinase Activators. *J. Med. Chem.* **2008**, *51*, 6173-6187.
- 58) Shen, Y.; Fukushima, M.; Ito, Y.; Muraki, E.; Hosono, T.; Seki, T.; Ariga, T. Verification of the Antidiabetic Effects of Cinnamon (*Cinnamomum zeylanicum*) Using Insulin-Uncontrolled Type 1 Diabetic Rats and Cultured Adipocytes. *Biosci. Biotechnol. Biochem.* **2010**, *74*, 2418-2425.
- 59) Jung, S. H.; Ha, Y. J.; Shim, E. K.; Choi, S. Y.; Jin, J. L.; Yun-Cho, H. S.; Lee, J. R. Insulin-Mimetic and Insulin-Sensitizing Activities of a Pentacyclic Triterpenoid Insulin Receptor Activator. *Biochem. J.* **2007**, *403*, 243-250.
- 60) (a) Li, Y.; Kim, J.; Li, J.; Liu, F.; Liu, X.; Himmeldirk, K.; Ren, Y.; Wagner, T. E.; Chen, X. Natural Anti-Diabetic Compound 1,2,3,4,6-penta-*O*-galloyl-*D*-glucopyranose Binds to Insulin Receptor and Activates Insulin-Mediated Glucose Transport Signaling Pathway. *Biochem. Biophys. Res. Commun.* **2005**, *336*, 430-437. (b) Ren, Y.; Himmeldirk, K.; Chen, X. *J. Med. Chem.* **2006**, *49*, 2829-2837.

- 61) Yamasaki, K.; Hishiki, R.; Kato, E.; Kawabata, J. Study of Kaempferol Glycoside as an Insulin Mimic Reveals Glycon to be the Key Active Structure. *ACS Med. Chem. Lett.* **2011**, *2*, 17-21.
- 62) Yamasaki, K.; Hishiki, R.; Kato, E.; Kawabata, J. Screening and Identification of Disaccharides with Insulin Mimetic Activity against L6 Cells. *Biosci. Biotechnol. Biochem.* **2012**, *76*, 841-842.
- 63) Dang, N. T.; Mukai, R.; Yoshida, K.-I.; Ashida, H. D-Pinitol and *myo*-Inositol Stimulate Translocation of Glucose Transporter 4 in Skeletal Muscle of C57BL/6 Mice. *Biosci. Biotechnol. Biochem.* **2010**, *74*, 1062-1067.
- 64) Armit, J. W.; Nolan, T. J. Derivatives of Kojic Acid. *J. Chem. Soc.* **1931**, 3023-3031.
- 65) (a) Molenda, J. J.; Jones, M. M.; Basinger, M. A. Enhancement of Iron Excretion via Monoanionic 3-Hydroxypyrid-4-ones. *J. Med. Chem.* **1994**, *37*, 93-98. (b) Molenda, J. J.; Basinger, M. A.; Hanusa, T. P.; Jones, M. M. Synthesis and Iron(III) Binding Properties of 3-Hydroxypyrid-4-ones Derived from Kojic Acid. *J. Inorg. Biochem.* **1994**, *55*, 131-146.
- 66) Garratt, S. The Mechanism of the Reaction Between Dehydroacetic Acid and Alkylamines. *J. Org. Chem.* **1963**, *28*, 1886-1888.
- 67) Kim, K. S. et al. Discovery of Pyrrolopyridine-Pyridone Based Inhibitors of Met Kinase: Synthesis, X-ray Crystallographic Analysis, and Biological Activities. *J. Med. Chem.* **2008**, *51*, 5330-5341.
- 68) (a) Tam, T. F.; Leung-Toung, R.; Wang, Y.; Zhao, Y. (Apotex Technologies Inc., Can). Preparation of Fluorinated Derivatives of Deferiprone as Iron Chelators for Treating Iron-Overload Diseases Including Neurodegenerative Disorders. WO 2008116301, October 2, 2008. (b) Tam, T. F.; Spino, M.; Li, W.; Wang, Y.; Zhao, Y.; Shah, B. H. (Apotex Technologies Inc., Can). Preparation of Cycloalkyl Derivatives of 3-Hydroxy-4-pyridinones as Therapeutic Iron Chelating Agents. WO 2005049609, June 2, 2005. (c) Shin, K. J.; Roh, E. J.; Chung, M. K.; Cha, H. J.; Seo, S. H. (Korea Institute of Science and Technology, S. Korea; SNU R&DB Foundation). Preparation of 3-Phenoxy-4-pyrone, 3-Phenoxy-4-pyridone or 4-Pyridone Derivatives as FabI (Enoyl-ACP Reductase) Inhibitors. WO 2011014008, February 3, 2011.
- 69) Wang, Y.; Agostino, S. V.; Tam, T. F.; Zhao, Y.; Li, W.; Shah, B. K.; Leung-Toung, R. (Apotex Technologies Inc., Can). Process for the Preparation of 3-Hydroxy-1-cycloalkyl-6-alkyl-4-oxo-1,4-dihydropyridine-2-carboxamides by

Treatment of the Corresponding Acids with Acid Chloride Formation Reagents and Amines. WO 2006053429, May 26, 2006.

- 70) Teitei, T. Chemistry of Kojic Acid: One-Step Syntheses of Benzothiazoles and Other Fused Heterocycles from Kojic Acid Derivatives. *Aust. J. Chem.* **1983**, *36*, 2307-2315.
- 71) Ogino, H.; Iwamatsu, K.; Katano, K.; Nakabayashi, S.; Yoshida, T.; Shibahara, S.; Tsuruoka, T.; Inouye, S.; Kondo, S. New Aminothiazolylglycylcephalosporins with a 1,5-Dihydroxy-4-pyridone-2-carbonyl Group. II. Synthesis and Antibacterial Activity of MT0703 and Its Diastereomers. *J. Antibiot.* **1990**, *43*, 189-198.
- 72) (a) Tang, J.; Park, J. G.; Millard, C. B.; Schmidt, J. J.; Pang, Y.-P. Computer-Aided Lead Optimization: Improved Small-Molecule Inhibitor of the Zinc Endopeptidase of Botulinum Neurotoxin Serotype A. *PLoS One* **2007**, *2*, e761.
(b) Hiroya, K.; Itoh, S.; Sakamoto, T. Development of an Efficient Procedure for Indole Ring Synthesis from 2-Ethynylaniline Derivatives Catalyzed by Cu(II) Salts and Its Application to Natural Product Synthesis. *J. Org. Chem.* **2004**, *69*, 1126-1136.
- 73) Kim, J. S.; Han, J. H.; Lee, J. J.; Jun, Y. M.; Lee, B. M.; Kim, B. H. Indium-HI-mediated One-Pot Reaction of 1-(2-Arylethynyl)-2-nitroarenes to 2-arylindoles. *Tetrahedron Lett.* **2008**, *49*, 3733-3738.
- 74) Mitsumori, S.; Tsuru, T.; Honma, T.; Hiramatsu, Y.; Okada, T.; Hashizume, H.; Inagaki, M.; Arimura, A.; Yasui, K.; Asanuma, F.; Kishino, J.; Ohtani, M. Synthesis and Biological Activity of Various Derivatives of a Novel Class of Potent, Selective, and Orally Active Prostaglandin D₂ Receptor Antagonists. 1. Bicyclo[2.2.1]heptanes Derivatives. *J. Med. Chem.* **2003**, *46*, 2436-2445.
- 75) Liu, Y.; Lu, Y.; Prashad, M.; Repič, O.; Blacklock, T. J. A Practical and Chemoselective Reduction of Nitroarenes to Anilines Using Activated Iron. *Adv. Synth. Catal.* **2005**, *347*, 217-219.
- 76) DeRoy, P. L.; Surprenant, S.; Bertrand-Laperle, M.; Yoakim, C. Efficient Nucleophilic Aromatic Substitution Between Aryl Nitrofluorides and Alkynes. *Org. Lett.* **2007**, *9*, 2741-2743.
- 77) Ueno, M.; Hori, C.; Suzawa, K.; Ebisawa, M.; Kondo, Y. Catalytic Activation of Silylated Nucleophiles Using *t*Bu-P4 as a Base. *Eur. J. Org. Chem.* **2005**, 1965-1968.

- 78) Thorand, S.; Krause, N. Improved Procedures for the Palladium-Catalyzed Coupling of Terminal Alkynes with Aryl Bromides (Sonogashira Coupling). *J. Org. Chem.* **1998**, *63*, 8551-8553.
- 79) Kosynkin, D. V.; Tour, J. M. Phenylene Ethylene Diazonium Salts as Potential Self-Assembling Molecular Devices. *Org. Lett.* **2001**, *3*, 993-995.
- 80) Sonogashira, K. Development of Pd-Cu Catalyzed Cross-Coupling of Terminal Acetylenes with sp^2 -Carbon Halides. *J. Organomet. Chem.* **2002**, *653*, 46-49.
- 81) Chinchilla, R.; Nájera, C. The Sonogashira Reaction: A Booming Methodology in Synthetic Organic Chemistry. *Chem. Rev.* **2007**, *107*, 874-922.
- 82) Darses, S.; Michaud, G.; Genêt, J.-P. Potassium Organotrifluoroborates: New Partners in Palladium-Catalyzed Cross-Coupling Reactions. *Eur. J. Org. Chem.* **1999**, 1875-1883.
- 83) Vilaivan, T. A Rate Enhancement of *tert*-Butoxycarbonylation of Aromatic Amines with Boc_2O in Alcoholic Solvents. *Tetrahedron Lett.* **2006**, *47*, 6739-6742.
- 84) Powell, N. A.; Rychnovsky, S. D. Iodide Acceleration in the Pd-Catalyzed Coupling of Aromatic 1,2-Ditriflates with Alkynes: Synthesis of Eneidyne. *Tetrahedron Lett.* **1996**, *37*, 7901-7904.
- 85) (a) Dai, W.-M.; Guo, D.-S.; Sun, L.-P. Chemistry of Aminophenols. Part 1: Remarkable Additive Effect on Sonogashira Cross-Coupling of 2-Carboxamidoaryl Triflates and Application to Novel Synthesis of Indoles. *Tetrahedron Lett.* **2001**, *42*, 5275-5278. (b) Dai, W.-M.; Sun, L.-P.; Guo, D.-S. Chemistry of Aminophenols. Part 2: A General and Efficient Synthesis of Indoles Possessing a Nitrogen Substituent at the C4, C5, and C7 Positions. *Tetrahedron Lett.* **2002**, *43*, 7699-7702. (c) Sun, L.-P.; Huang, X.-H.; Dai, W.-M. Stepwise and One-Pot Cross-Coupling-Heteroannulation Approaches Toward 2-Substituted C5-, C6-, and C7-Nitroindoles. *Tetrahedron* **2004**, *60*, 10983-10992. (d) Chiou, C.-T.; Chen, G. S.; Chen, M.-L.; Li, H.; Shi, L.; Huang, X.-H.; Dai, W.-M.; Chern, J.-W. Synthesis of Anti-Microtubule *N*-(2-Arylindol-7-yl)-benzenesulfonamide Derivatives and Their Antitumor Mechanisms. *ChemMedChem* **2010**, *5*, 1489-1497.
- 86) Dubash, N. P.; Mangu, N. K.; Satyam, A. Synthesis of 7-Alkoxy/Hydroxy- α -methyltryptamines. *Synth. Commun.* **2004**, *34*, 1791-1799.
- 87) (a) Jia, X.; Huang, Q.; Li, J.; Li, S.; Yang, Q. Environmentally Benign *N*-Boc Protection Under Solvent- and Catalyst-Free Conditions. *Synlett* **2007**, 806-808.

- (b) Chankeshwara, S. V.; Chakraborti, A. K. Catalyst-Free Chemoselective *N*-*tert*-Butyloxycarbonylation of Amines in Water. *Org. Lett.* **2006**, *8*, 3259-3262.
- (c) Van Otterlo, W. A. L.; Morgans, G. L.; Khanye, S. D.; Aderibigbe, B. A. A.; Michael, J. P.; Billing, D. G. Isomerization and Ring-Closing Metathesis for the Synthesis of 6-, 7-, and 8-Membered Benzo- and Pyrido-Fused *N,N*-, *N,O*- and *N,S*-Heterocycles. *Tetrahedron Lett.* **2004**, *45*, 9171-9175.
- (d) Chacun-Lefèvre, L.; Buon, C.; Bouyssou, P.; Coudert, G. Synthesis of 3-Substituted-4*H*-1,4-benzoxazines. *Tetrahedron Lett.* **1998**, *39*, 5763-5764.
- (e) Buon, C.; Chacun-Lefèvre, L.; Rabot, R.; Bouyssou, P.; Coudert, G. Synthesis of 3-Substituted and 2,3-Disubstituted-4*H*-1,4-benzoxazines. *Tetrahedron* **2000**, *56*, 605-614.
- 88) Pirrung, M. C.; Zhang, F.; Ambadi, S.; Ibarra-Rivera, T. R. Reactive Esters in Amide Ligation with β -Hydroxyamines. *Eur. J. Org. Chem.* **2012**, 4283-4286.
- 89) Dighe, S. N.; Jadhav, H. R. Microwave Assisted Mild, Rapid, Solvent-Less, and Catalyst-Free Chemoselective *N*-*tert*-Butyloxycarbonylation of Amines. *Tetrahedron Lett.* **2012**, *53*, 5803-5806.
- 90) Clayden, J.; Moran, W. J.; Edwards, P. J.; LaPlante, S. R. The Challenge of Atropisomerism in Drug Discovery. *Angew. Chem. Int. Ed.* **2009**, *48*, 6398-6401.
- 91) FDA's Policy Statement for the Development of New Stereoisomeric Drugs. *Chirality* **1992**, *4*, 338-340.
- 92) Bringman, G.; Price Mortimer, A. J.; Keller, P. A.; Gresser, M. J.; Garner, J.; Breuning, M. Atroposelective Synthesis of Axially Chiral Biaryl Compounds. **2005**, *44*, 5384-5427.
- 93) Oki, K. Recent Advances in Atropisomerism. *Topics in Stereochemistry* **1983**, Wiley Interscience, NY; pp. 1-76.
- 94) (a) Shi, Y. Huang, M.-H.; Macor, J. E.; Hughes, D. E. Characterization of the In Vitro Atropisomeric Interconversion Rates of an Endothelin A Antagonist by Enantioselective Liquid Chromatography. *J. Chromatogr. A.* **2005**, *1078*, 67-73.
- (b) Zhou, Y. S.; Tay, L. K.; Hughes, D.; Donahue, S. Stimulation of the Impact of Atropisomer Interconversion on Plasma Exposure of Atropisomers of an Endothelin Receptor Antagonist. *J. Clin. Pharmacol.* **2004**, *44*, 680-688.
- 95) Deng, L. Synthesis of Analogues of DAQ B1 as Potential Anti-Diabetic Drugs. Ph.D. Dissertation, Duke University, 2005.

- 96) Fryatt, T.; Pettersson, H. I.; Gardipee, W. T.; Bray, K. C.; Green, S. J.; Slawin, A. M. Z.; Beall, H. D.; Moody, C. J. Novel Quinolinequinone Antitumor Agents: Structure-Metabolism Studies with NAD(P)H:Quinone Oxidoreductase (NQO1). *Bioorg. Med. Chem.* **2004**, *12*, 1667-1687.
- 97) Hui, X.; Yangyang, W. An Efficient Synthesis of *N*-Arylsulfonylindoles from Indoles and Arylsulfonyl Chlorides in the Presence of Triethylbenzylammonium Chloride (TEBA) and NaOH. *Chin. J. Chem.* **2010**, *28*, 125-127.
- 98) Claisen, L. Rearrangement of Phenyl Allyl Ethers into *C*-Allylphenols. *Chem. Ber.* **1912**, *45*, 3157-3166.
- 99) McLamore, W. M.; Gelblum, E.; Bavley, A. The Preparation and Rearrangement of Allyl Kojate. *J. Am. Chem. Soc.* **1956**, *78*, 2816-2818.
- 100) (a) Wender, P. A.; McDonald, F. E. Studies on Tumor Promoters. 9. A Second-Generation Synthesis of Phorbol. *J. Am. Chem. Soc.* **1990**, *112*, 4956-4958. (b) Wender, P. A.; Mascareñas, J. L. Studies on Tumor Promoters. 11. A New [5 + 2] Cycloaddition Method and Its Application to the Synthesis of BC Ring Precursors of Phorboids. *J. Org. Chem.* **1991**, *56*, 6267-6269. (c) Wender, P. A.; D'Angelo, N.; Elitzin, V. I.; Ernst, M.; Jackson-Ugueto, E. E.; Kowalski, J. A.; McKendry, S.; Rehfeuter, M.; Sun, R., Voigtlaender, D. Function-Oriented Synthesis: Studies Aimed at the Synthesis and Mode of Action of 1 α -Alkyldaphnane Analogues. *Org. Lett.* **2007**, *9*, 1829-1832. (d) Wender, P. A.; Buschmann, N.; Cardin, N. B.; Jones, L. R.; Kan, C.; Kee, J.-M.; Kowalski, J. A.; Longcore, K. E. Gateway Synthesis of Daphnane Congeners and Their Protein Kinase C Affinities and Cell-Growth Activities. *Nat. Chem.* **2011**, *3*, 615-619.
- 101) (a) Kaeobamrung, J.; Mahatthananchai, J.; Zheng, P.; Bode, J. W. An Enantioselective Claisen Rearrangement Catalyzed by *N*-Heterocyclic Carbenes. *J. Am. Chem. Soc.* **2010**, *132*, 8810-8812. (b) Mahatthananchai, J.; Kaeobamrung, J.; Bode, J. W. Chiral *N*-Heterocyclic Carbene-Catalyzed Annulations of Enals and Ynals with Stable Enols: A Highly Enantioselective Coates-Claisen Rearrangement. *ACS Catal.* **2012**, *2*, 494-503.
- 102) Burgstahler, A. W.; Gibbons, L. K.; Nordin, I. C. Thermal Rearrangement of Arylmethyl Vinyl Ethers. *J. Chem. Soc.* **1963**, 4986-4989.
- 103) Sharma, G. V. M.; Ilangovan, A.; Sreenivas, P.; Mahalingam, A. K. Alternative Lewis Acids to Effect Claisen Rearrangement. *Synlett* **2000**, 615-618.

- 104) Hiersemann, M.; Abraham, L. The Cu(OTf)₂- and Yb(OTf)₃-Catalyzed Claisen Rearrangement of 2-Alkoxy carbonyl-Substituted Allyl Vinyl Ethers. *Org. Lett.* **2001**, *3*, 49-52.
- 105) (a) Abraham, L.; Czerwonka, R.; Hiersemann, M. The Catalytic Enantioselective Claisen Rearrangement of an Allyl Vinyl Ether. *Angew. Chem. Int. Ed.* **2001**, *40*, 4700-4703. (b) Abraham, L.; Körner, M.; Hiersemann, M. Highly Enantioselective Catalytic Asymmetric Claisen Rearrangement of 2-Alkoxy carbonyl-Substituted Allyl Vinyl Ethers. *Tetrahedron Lett.* **2004**, *45*, 3647-3650.
- 106) (a) Uyeda, C.; Jacobsen, E. N. Enantioselective Claisen Rearrangements with a Hydrogen-Bond Donor Catalyst. *J. Am. Chem. Soc.* **2008**, *130*, 9228-9229. (b) Uyeda, C.; Jacobsen, E. N. Transition-State Charge Stabilization through Multiple Non-Covalent Interactions in the Guanidinium-Catalyzed Enantioselective Claisen Rearrangement. *J. Am. Chem. Soc.* **2011**, *133*, 5062-5075.
- 107) Hiersemann, M. The Pd(II)-Catalyzed and the Thermal Claisen Rearrangement of 2-Alkoxy carbonyl-Substituted Allyl Vinyl Ethers. *Synlett* **1999**, 1823-1825.
- 108) Reich, N. W.; Yang, C.-G.; Shi, Z.; He, C. Gold(I)-Catalyzed Synthesis of Dihydrobenzofurans from Aryl Allyl Ethers. *Synlett* **2006**, 1278-1280.
- 109) Cairns, N.; Harwood, L. M.; Astles, D. P. Application of the Lewis Acid-Catalyzed Claisen Rearrangement of 4'-(1,1-Dimethylallyloxy)coumarates to the Synthesis of Demethylsuberosin. *J. Chem. Soc., Chem. Commun.* **1986**, *10*, 750-751.
- 110) Trost, B. M.; Toste, F. D. Asymmetric *O*- and *C*-Alkylation of Phenols. *J. Am. Chem. Soc.* **1998**, *120*, 815-816.
- 111) (a) Gester, S.; Metz, P.; Zierau, O.; Vollmer, G. An Efficient Synthesis of the Potent Phytoestrogens 8-Prenylnaringenin and 6-(1,1-Dimethylallyl)naringenin by Europium(III)-Catalyzed Claisen Rearrangement. *Tetrahedron* **2001**, *57*, 1015-1018. (b) Tischer, S.; Metz, P. Selective C-6 Prenylation of Flavonoids via Europium(III)-Catalyzed Claisen Rearrangement and Cross-Metathesis. *Adv. Synth. Catal.* **2007**, *349*, 147-151. (c) Poerwono, H.; Sasaki, S.; Hattori, Y.; Higashiyama, K. Efficient Microwave-Assisted Prenylation of Pinostrobin and Biological Evaluation of its Derivatives as Antitumor Agents. *Bioorg. Med. Chem. Lett.* **2010**, *20*, 2086-2089.

- 112) Zou, Y. Preparation of 1-Substituted Cyclopropenes as Ethylene Antagonists and Elucidation of the Mechanism of Ethylene Binding in the Ethylene Receptor. Ph.D. dissertation, Duke University, 2006.
- 113) Park, Y. J.; Jung, K.-H. Hydrophobic Effects of *o*-Phenanthroline and 2,2'-Bipyridine on Adsorption of Metal(II) Ions onto Silica Gel Surface. *J. Colloid Interface Sci.* **1993**, *160*, 324-331.
- 114) Stella, L.; Raynier, B.; Surzer, J. M. Homolytic Synthesis of Potential Analgesics: 2-Substituted 4-Arylpiperidines and Benzomorphans. *Tetrahedron* **1981**, *37*, 2843-2854.
- 115) Grishina, A. A.; Polyakova, S. M.; Kunetskiy, R. A.; Císařová, I.; Lyapkalo, I. M. 4,5-Disubstituted *N,N'*-di-*tert*-alkyl Imidazolium Salts: New Synthesis and Structural Features. *Chem. Eur. J.* **2011**, *17*, 96-100.
- 116) Balduzzi, S.; Brook, M. A.; McGlinchey, M. J. Diastereoselective Addition of Allyl- and Crotylstannanes to Dicobalt-Complexed Acetylenic Aldehydes. *Organometallics*, **2005**, *24*, 2617-2627.
- 117) Herve Du Penhoat, C.; Julia, M. Synthesis with Sulfones XLIV. Stereoselective Preparation of *EE* 1,3-Dienes by Elimination of Benzenesulfinic Acid from *E* Homoallylic Sulfones. *Tetrahedron*, **1986**, *42*, 4807-4816.